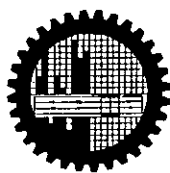# PREPARATION AND CHARACTERIZATION OF NICKEL DISPERSED POLYANILINE MATRIX

BY

MD. SAIFUL ISLAM

SUBMITTED IN PARTIAL FULFILMENT OF THE REQUIREMENT FOR THE DEGREE OF M.PHIL IN CHEMISTRY

DEPARTMENT OF CHEMISTRY

BANGLADESH UNIVERSITY OF ENGINEERING AND

TECHNOLOGY (BUET)
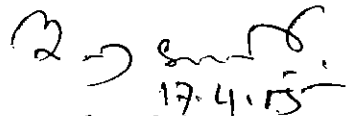
DHAKA-1000, BANGLADESH

APRIL, 2005

DECLARATION

This thesis work has been done by the candidate himself and does not cotain any material extracted from elsewhere or from a work published by anybody else. The work for this thesis has not been presented elsewhere by the author for any degree or diploma.

Saiful 17/04/05

Md. Saiful Islam
(Candidate)
M. Phil Student
Roll No. 040203201F
Department of Chemistry
BUET, Dhaka
Bangladesh

CERTIFICATE

This is to certify that the research work embodying in this thesis has been carried out under my supervision. The work presented herein is original. This thesis has not been submitted elsewhere for the award of any other degree or diploma in any University or institution.

17.4.15

Dr. Al-Nakib Chowdhury
(Supervisor)
Associate Professor
Department of Chemistry
BUET, Dhaka
Bangladesh

Dedicated

TO

My Beloved Parents

ACKNOWLEDGEMENT

I would like to extent my thanks to Aminul Islam, Kamrul Haque, Mohammad Salim, Tareque Chowdhury and other friends who shared with me to solve all the problems confronted in the whole thesis period. Special thanks to Md. Mamaun-Or-Rashid, Chemistry department, BUET, for his assistance in composing the thesis.

I would like to express my deep gratitude to my beloved parents, brothers and sisters for their sacrifice and continuous encouragement throughout the research work.

Above all, all thanks are due to almighty Allah for making things situation congenial and favorable for me for the task undertaken.

Md. Saiful Islam
Author

Bangladesh University of Engineering and Technology
Dhaka
Department of Chemistry
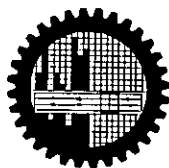
Certification of Thesis

A thesis on
"PREPARATION AND CHARACTERIZATION OF NICKEL DISPERSED POLYANILINE MATRIX"
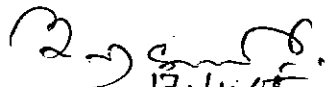
BY

MD. SAIFUL ISLAM
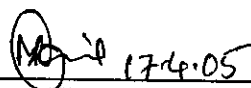
has been accepted as satisfactory in partial fulfillment of the requirements for the degree of Master of Philosophy (M.Phil) in Chemistry and certify that the student has demonstrated a satisfactory knowledge of the field covered by this thesis in an oral examination held on April 17, 2005.

Board of Examiners
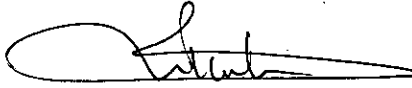
1. **Dr. Al-Nakib Chowdhury**
   Associate Professor
   Department of Chemistry
   BUET, Dhaka

   _____
   17.4.05
   Supervisor & Chairman
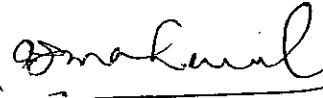
2. **Dr. Md. Abdur Rashid**
   Professor & Head
   Department of Chemistry
   BUET, Dhaka.

   _____
   17-4-05
   Member (Ex-officio)

3. **Dr. Md. Rafique Ullah**
   Professor
   Department of Chemistry
   BUET, Dhaka

   _____
   Member

4. **Dr. Abu Jafar Mahmood**
   Professor
   Department of Chemistry
   Dhaka University, Dhaka.

   _____
   Member (External)

Contents

Chapter 2: Experimental

Chapter 3: Results and Discussion

Abstract

Electronically conducting polyaniline was made magnetic in nature by incorporating magnetic metals into its matrix. In this connection, metallic Ni particles were successfully dispersed onto polyaniline matrix by a simple one step electrochemical method. Ni particles as deposited onto the polymer (PANI/Ni) seem to have much smaller size compared to that deposited on the bare Pt. Size of the Ni deposits was found to be influenced by the electrolytic bath compositions and potential sweep rate. Polyaniline/Ni matrix thus prepared was further characterized by a wide range of experimental techniques including optical microscopy, scanning electron microscopy, IR spectroscopy, X-ray diffraction, solid-state d.c. conductance and magnetic susceptibility measurements. Polyaniline/Ni film matrix as prepared was found to have excellent electroactivity. The stability and durability of PANI/Ni film in repeated oxidation/reduction cycle and its degradation at high positive potential were also examined. The result based on cyclic voltammogram suggests a better electrochemical stability of the polyaniline/Ni film electrode relative to the bulk polyaniline film.

Deposition of Ni both on a bare Pt and polyaniline surfaces were performed by varying the electrolytic bath composition and potential sweep rate. The bath composition employed are: (i) 0.1M Ni-II salt solution, (ii) 0.1M Ni-II salt + 0.1M boric acid and (iii) 0.1M Ni-II salt + 0.1M boric acid + 10^{-4} H_2SO_4 solutions. Sweeping potential rates of 50 and 200 mV sec^{-1} were employed. Under all the experimental conditions employed, Ni was found to be casted both on Pt and polyaniline substrates. An energy dispersed X-ray analysis showed a Ni content of approximately 4.26% in the polyaniline matrix.

Surface morphology obtained by optical microscope and SEM provides very interesting results. The optical micrographs of the matrices showed clear deposition of Ni both on the Pt and polymer. The Ni deposits randomly distributed onto matrix surfaces and have definite size and shape with sharp edges. The SEM study also shows clear differences in the surfaces morphologies of polyaniline dispersed with and without Ni.

The electrical conductivity measurements showed the conductivity of PANI and PANI/Ni in the order of 10^{-3} and 10^{-7} Scm^{-1}. The Ni particles that incorporated into the polymer matrix may create blockage in the conductance for the PANI/Ni matrix. Magnetic susceptibility measurement also showed a clear differences in the magnetic property of PANI and PANI/Ni samples. The gram susceptibility for the samples PANI and PANI/Ni were found to be -3.68×10^{-7} and 9.025×10^{-5}, respectively. The sign of the susceptibility values clearly indicates that PANI is diamagnetic in nature whereas PANI/Ni is paramagnetic one.

The PANI and PANI/Ni films thus synthesized were found to be electoactive both in aqueous and non-aqueous electrolytic solvents. The redox activity of both the film electrodes was examined by following the redox process, $Fe^{+2} \rightarrow Fe^{+3} + e^{-}$, on their surface. Both the films were seen to be capable of performing the redox process efficiently. The electrochemical stability of the film electrodes were also examined. In the repeated oxidation/reduction cycles both films gradually deactivated but the rate of deactivation seems to be less in the PANI/Ni matrix. Compared to PANI, PANI/Ni film electrode was also found to provide a superior stability on its degradation at highly positive potential.

Chapter 1

INTRODUCTION

1.1 Fundamentals of Electrochemical Technique

A.   Design of Electrochemical experiments

The study of spontaneous oxidation-reduction reactions that generate an electrical current and the study of non-spontaneous oxidation-reduction reactions that are forced to occur by the passage of an electrical current are the types of electrochemical experiment. In both cases, the conversion between chemical and electrical energy carried out. Such experiments need special arrangement to be occurred and thus electrochemical cell is deigned to perform electrochemical experiments.

i) Electrochemical cell: An electrochemical cell provides room for reaction. It consists primarily of electrodes and the electrolyte compacted together in a glass container. Commonly, a glass frit separator or membrane may be incorporated to isolate the anolyte from the catholyte. Three electrodes are commonly employed: a working electrode which defines the interface under study, a reference electrode which maintains a constant reference potential and a counter (or secondary) electrode which supplies the current. The cell must be designed so that the experimental data are determined by the properties of the reaction at the working electrode.

ii) Working electrode: Designs of working electrodes are diverse. Most commonly the working electrode is a small sphere, small disc or a short wire, but it could also be metal foil, a single crystal of semiconductor or metal, an evaporated thin film, or a powder as pressed discs or pellets. An essential features is that the electrode should not react chemically with the solvent or solution components. In principle, the electrodes can be large or

3

small, but there are commonly experimental reasons why the electrode area should be relatively small (<0.25 cm^2). Moreover it should preferably be smooth, as the geometry and mass transport are then better defined. A wide range of solid materials are used as electrodes but the most common 'inert' solid electrodes are lead, vitreous carbon, gold and platinum. In order to obtain consistent results with solid electrodes it is important to establish a satisfactory electrode pretreatment procedure which ensures a reproducible state of oxidation, surface morphology and freedom from adsorbed impurities. Electrodes are polished on cloth pads impregnated with diamond particles down to 1 μm and then with alumina of fixed grain size down to 0.05 μm.

iii) Counter electrode: The purpose of the counter electrode is to supply the current required by the working electrode without in any way limiting the measured response of the cell. It is essential that the electrode process is decomposition of the electrolyte medium or oxidation/reduction of a component of the electrolyte so that current flows readily without the need for a large overpotential.

The counter electrode should not impose any characteristics on the measured data and in consequence it should have a large area compared to the working electrode. Moreover, as also noted above, its shape and position are important science these determine whether the working electrode is an equipotential surface, and consequently it is preferable to avoid a separator in the cell.

4

iv) Reference electrodes: The role of the reference electrode is to provide a fixed potehtial which does not vary during the experiment (e.g. it should be independent of current density). In most cases, it will be necessary to relate the potential of the reference electrode to other scales, for example to the normal hydrogen electrode, the agreed standard for thermodynamic calculations.

In potentiostatic experiments the potential between the working electrode and reference electrode is controlled by a potentiostat and as the reference half cell maintains a fixed potential, any change in applied potential to the cell appears directly across the working electrode-solution interface. The reference electrode serves the dual purpose of providing a thermodynamic reference and also isolates the working electrode as the system under study. In practice, however, any measuring device must draw current to perform the measurement, so a good reference electrode should be able to maintain a constant potential even if a few microamperes are passed through its surface.

In practice, the main requirement of a reference electrode is that it has a stable potential and that it is not substantially polarized during the experiment. Hence, it is common to use the highly convenient aqueous saturated calomel electrode (SCE) in many experiments in all solvents. Even so, a very wide range of reference electrodes have been used in non-aqueous solvents. Potential of some common reference electrodes are listed in Table 1.1.1.

Table-1.1.1 Potential of some typical reference electrodes in aqueous solutions at 298K.

Common name	Electrode	Potential / V *vs* NHE
SCE	Hg/Hg_2Cl_2, sat KCl	+0.241
Calomel	Hg/Hg_2Cl_2, 1 mol dm^{-3} KCl	+0.280
Mercurous sulphate	Hg/Hg_2SO_4, sat K_2SO_4	+0.640
	Hg/Hg_2SO_4, 0.5 mol dm^{-3} H_2SO_4	+0.680
Mercurous oxide	Hg/HgO, 1 mol dm^{-3} NaOH	+0.098
Silver chloride	$Ag/AgCl$, sat KCl	+0.197

A great deal of modern electrochemistry is carried out in non-aqueous solvent media and often aqueous reference electrodes can be used at the expense of an unknown aqueous-non aqueous junction potential.

v) The electrolytic solution: The electrolytic solution is the medium between the electrodes in the cell and it consists of a solvent and a high concentration of an ionised salt as well as the electroactive species; it may also contain other materials, complexing agents, buffer, etc. The supporting electrolyte is present (a) to increase the conductivity of the solution and hence to reduce the resistance between the working and counter electrodes (to avoid undue Joule heating, to help maintain a uniform current and potential distribution and to reduce the power requirement on the potentiostat) and also to minimize the potential error due to the uncompen sated solution resistance. With appropriate precautions, electrochemical experiments are possible in almost any medium.

Some common solvents and media for electrochemical experiments are below:

1. Water

   Aqueous solutions of many salts and/or copmlexing agents at various pH. Buffered and unbuffered media.

2. Other protonic solvents

   e.g. acetic acid, ethanol, methanol, liquid HF.

3. Aprotic solvents

   e.g. acetonitrile, dimethylfomamide, dimethylsulphoxide, sulphur dioxide, ammonia, propylene carbonate, tetrahydrofuran. Many studies use as electrolytes $R_4N^+ X^-$, R=CH_3, C_2H_5 or C_4H_9, X= ClO_4^-, BF_4, PF_6, or halide ion. Media difficult to buffer.

4. Mixed solvents Particularly mixtures of water with ethanol, acetronitrile, etc. Again, these media may be buffered or unbuffered, contain many electrolytes, etc.

5. Molten salts

   e.g. NaCl, KCl/NaCl/LiCl eutectics etc.

6. Low temperature molten salts

   e.g.

   $AlCl_3$, KF_2HF
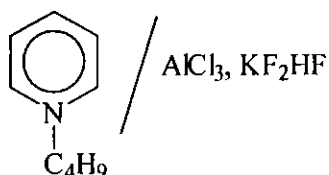
Electrode reactions can be extremely sensitive to impurities in the solution; for example, organic species arte often strongly adsorbed even at 10^{-4} mol dm^{-3} bulk concentration from aqueous solutions. Hence salts should be of

the highest available purity and/or recrystallised, solvents should be carefully purified, and solutions must be carefully deoxygenated. Purification and drying of non-aqueous solvents have been described elsewhere [1, 2] in some detail.

vi) Instrumentation: The electrochemist's armoury is based on electronic apparatus designed to control/measure the charge passed (coulostat/ integrator), current (galvanostat/current follower) and potential (potentiostat/high impedance voltmeter) in an electrochemical cell.

Potentiostat : The potentiostat is a device for controlling the potential between the working electrode and the reference electrode at a fixed and selected potential (also programme this potential with time).

Galvanostat : The simplest way to obtain a constant current is to apply a voltage from a low output impedance voltage source across a large resistor in series with the cell. The current will be given by the ratio E_{in}/R (provided resistance R is very large compared with the impedance of the cell.

B.   Processes at electrode surface

A solid conducting materials must be present to provide the site for each electrochemical reaction. These materials are called electrodes. The electrodes at which oxidation occurs is termed as the anode. The other electrode, the cathode, is the site of the reduction process.

8

i) Electrode reactions: An electrode reaction is a heterogeneous chemical process involving the transfer of electrons to or from a surface, generally a metal or a semiconductor. The electrode reaction may be an anodic process whereby a species is oxidised by the loss of electrons to the electrode, e.g.

$$2 H_2O - 4e^- \rightarrow O_2 + 4H^+ \qquad 1.1.1$$

$$Ce^{3+} - e^- \rightarrow Ce^{4+} \qquad 1.1.2$$

$$2Cl^- - 2e^- \rightarrow Cl_2 \qquad 1.1.3$$

$$Pb + SO_4^- - 2e^- \rightarrow PbSO_4 \qquad 1.1.4$$

$$2Al + 3H_2O - 6e^- \rightarrow Al_2O_3 + 6H^+ \qquad 1.1.5$$
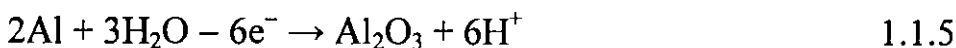
By convention [3], the current density, I, for an anodic process is a positive quantity. Conversely, the charge transfer may be a cathodic reaction in which a species is reduced by the gain of electrons from the electrode, e.g.

$$Fe^{3+} + e^- \rightarrow Fe^{2+} \qquad 1.1.6$$

$$Cu^{2+} + 2e^- \rightarrow Cu \qquad 1.1.7$$

$$2H_2O + 2e^- \rightarrow H_2 + 2OH^- \qquad 1.1.8$$

$$PbO_2 + 4H^+ + SO_4^{--} + 2e^- \rightarrow PbSO4 + 2H_2O \qquad 1.1.9$$

$$2CH2 = CHCN + 2H_2O + 2e^- \rightarrow (CH_2CH_2CN)_2 + 2OH^- \qquad 1.1.10$$
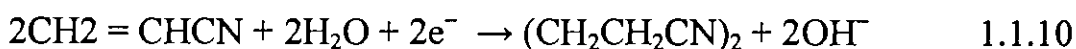
and the current density for a cathodic process is a quantity. The diversity of electrode reactions can already be seen from Equation (1.1.1.–1.1.10): the electroactive species may be organic or inorganic, neutral or charged, a species dissolved in solution, the solvent itself a film in the electrode surface, or indeed, the electrode materials itself. Moreover, the product may be dissolve in solution in a gas or a new phase on the electrode surface. The many type of electrodes reactions are also illustrated pictorially in Fig. 1.1.1.
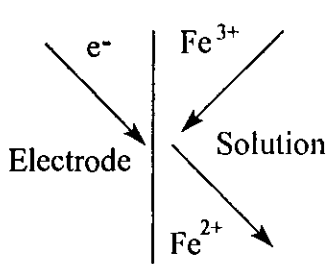
(a) simple electron transfer
$Fe^{3+} + e^- \longrightarrow Fe^{2+}$
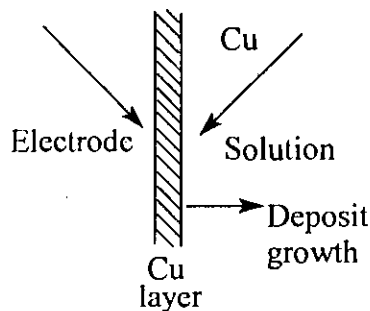
(b) metal deposition
e.g. $Cu^{2+} + 2e^- \longrightarrow Cu$
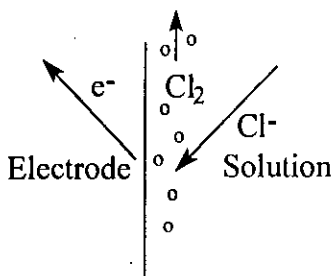
(c) gas evolution
e.g. $2Cl^- - 2e^- \longrightarrow Cl_2$
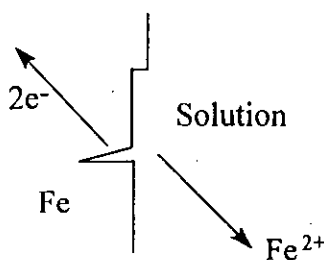
(d) corrosion
e.g. $Fe - 2e^- \longrightarrow Fe^{2+}$
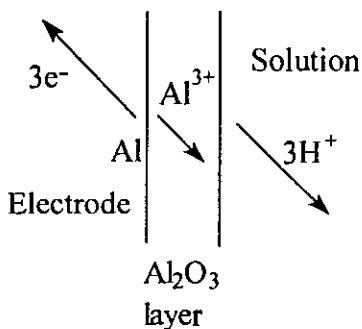
(e) oxide film formation
$2Al + 3 H_2O - 6e^- \longrightarrow Al_2O_3 + 6H^+$
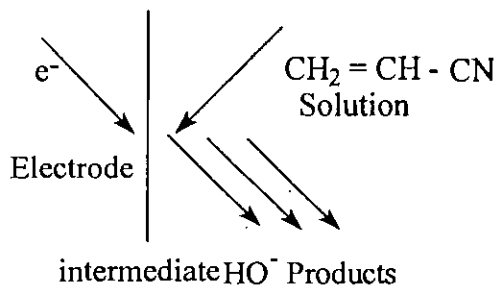
(f) electron transfer with coupled chemis
$2CH_2 = CH - CN + 2H_2O + 2e^-$
$\longrightarrow (CH_2 - CH_2 - CN)_2 + 2OH^-$

Fig. 1.1.1: Schematic view of some types of electrode reactions met in applied and fundamental electrochemistry.

Electrolysis is only possible in a cell with both an anode and a cathode, and because of the need to maintain an over all charge balance, the amount of reduction at the cathode and oxidation at the anode must be equal.

ii) Mass transport:

In general, in electrochemical systems, it is necessary to consider three modes of mass transport; namely,

(a) Diffusion: Diffusion is the moment of a species down a concentration gradient, and it must occur whenever there is a chemical change at surface. An electrode reaction converts starting material to product (O→R) and hence close to the electrode surface there is always a boundary layer (up to 10^{-2} cm thick) in which the concentrations of O and R are a function of distance from the electrode surface. The concentration of O is lower at the surface than in the bulk while opposite is the case for R, and hence O will diffuse towards and R away from the electrode.

(b) Migration: Migration is the moment of charged species due to a potential gradient and it is the mechanism by which charge passes through the electrolyte; the current of electrons through the external circuit must be balanced by the passage of ions through the solution between the electrode (both cations to the cathode and anions to the anode). It is however, not necessarily an important form of mass transport for the electroactive species even if it is charged. The forces leading to migration are purely electrostatic and hence the charge can be carried by any ionic species in the solution. As a result, if the electrolysis is carried out with a large excess of an inert electrolyte in the solution, this carries most of the charged and little of the electroactive species is transported by migration.

(c) Convection: Convection is the moment of a species due to mechanical forces. It can be eliminated, at least on a short timescale (it is difficult to eliminate natural convection arising from density difference on a longer time, i.e.> 10s by carrying out the electrolysis in a thermostat in the absence of stirring or vibrations. In industrial practice, it is much more common to stir or agitate the electrolyte or to flow the electrolyte through the cell. These are all forms of forced convection and, when present, they have a very large influence on the current density.

1.2　Some Important Electrode Materials

A.　Metals

Metals are crystalline solid materials consist of metal atoms distributed in a definite pattern resulting from their close packing. The types of close packing arrangement depends upon the size and electronic configuration of the atoms involved in the formation of crystal lattice. Since the metal atoms are all in direct contact with one another in the lattice and their valence electrons are in identical energy states, it is believed that the electrons are free to migrate between atoms. Metal atoms have an excess of low energy orbital vacancies. These vacancies enable valence electrons to move from near a certain nucleus to near any other nucleus where their position remains indistinguishable from the first. Thus, metals may be pictured as a collection of positive atomic cores embedded in a fluid of electrons or sea of electrons. For this fluid of electrons, metals are good conductors of electricity and heat. Metals have metallic luster; they are malleable, ductile and high melting points.

Metals have simple crystal lattices since metallic bonding envisages closest packing of atoms-one layer above another. Metals may have any system of seven common crystal system. Fe, Cu, Ni, Al, etc. are the most common metals which are very useful to us.

B.   Semiconductors

Semiconductors are special kind of materials which have the properties of semiconductivity. Semiconductivity is an electrical property of materials. A relatively small group of elements and compounds has an important electrical property, semiconduction in which they are neither good electrical conductors nor good electrical insulators. Instead, their ability to conduct electricity is intermediate. Si, Ge, impure ZnO, impure NiO are some examples of semiconductors.

The magnitude of conductivity in the simple semiconductors fall within the range 10^{-6} to 10^{-1} Ω^{-1} cm^{-1}. This intermediate range corresponds to band gaps of less then 2e V. Both conduction electrons and electron holes are charge carriers in a simple semiconductor.

In a semiconductor element, the energies of the valence electrons which bind the crystal together lie in the highest filled energy band, called the valence band. The empty band above, called the conduction band, is separated from the valence band by an energy gap. The magnitude of the energy gap or the width of the forbidden energy zone is characteristic of the lattice alone and varies widely for different crystals.

The transfer of an electron from the valence band to the conduction band requires high excitation energy to overcome the potential barrier of the forbidden energy zone. Consequently, such elements behave like an insulator at low temperatures. The application of heat or light energy may give enough energy to some electrons in the valence band to excite them across the forbidden zone into the conduction band. These electrons in the conduction band are now free to move and can carry electricity (Fig. 1.2.1).

Semiconductors are of two kinds such as

(i)   Intrinsic semiconductor

(ii)   Extrinsic semiconductor

(i) Intrinsic semiconductors :   If a pure, elemental substance shows the semiconducting properties, it is called intrinsic semiconductor. Pure Si, Ge shows these semiconducting properties. For this semiconduction results from the thermal promotion of electrons from a filled valence band to an empty conduction band . There, the electrons are negative charge carriers. The removal of electrons from the valence band produces electron holes which are positive charge carrier and identical to the conduction electrons (Fig. 1.2.1(a). This overall conduction scheme is possible because of the relatively small energy band gap between the valence and conduction bands in silicon. If δ is the conductivity of semiconductor then for intrinsic semiconductor, we can write.

$$\delta = nq \, (\mu_c + \mu_n) \qquad\qquad 1.2.1$$

Where, $n \rightarrow$ density of conduction electron

$q \rightarrow$ charge of single carrier

$\mu_e \rightarrow$ carrier mobility of electron

$\mu_n \rightarrow$ carrier mobility of hole

(ii) Extrinsic semiconductors: Extrinsic semiconduction results from impurity additions known as dopants and the process of adding these components is called doping. These types of semiconductors are extrinsic semiconductors. At room temperature, the conductivity of semiconductors results from electrons and holes introduced by impurities in the crystal. The presence of an impurity lowers considerably the activation energy necessary to transfer an electron from the valence band to the conduction band. This indicates that the ground state energies of such easily excited electrons must lie in the forbidden energy region. Two such discreate energy levels, known as donor levels and acceptor levels, may be introduced into the forbidden energy zone at a small interval of energy below the conduction band or above the valance band Fig.1.2.1(b). Donor levels give rise to electrons in the conduction band, whereas acceptor levels lead to the formation of holes in the valence band. Impurity of Si, with B, P, NiO, ZnO, are the examples of extrinsic semiconductors. Extrinsic semiconductors are of two kinds such as p-type extrinsic semiconductor and n-type extrinsic semiconductor.

p-type extrinsic semiconductors : The p-type semiconductor is obtained when the impurity atoms have fewer valence electrons than the silicon or germanium atoms of the original crystal. When a trivalent element such as B, Al, Ga, In is substituted for Si atom, the structure will be locally incomplete and the impurity atom will acquire an extra electron from a nearly bond in the lattice to approximate the terahedral cloude distribution of the lattice. This creates a positive hole localized near the impurity, which
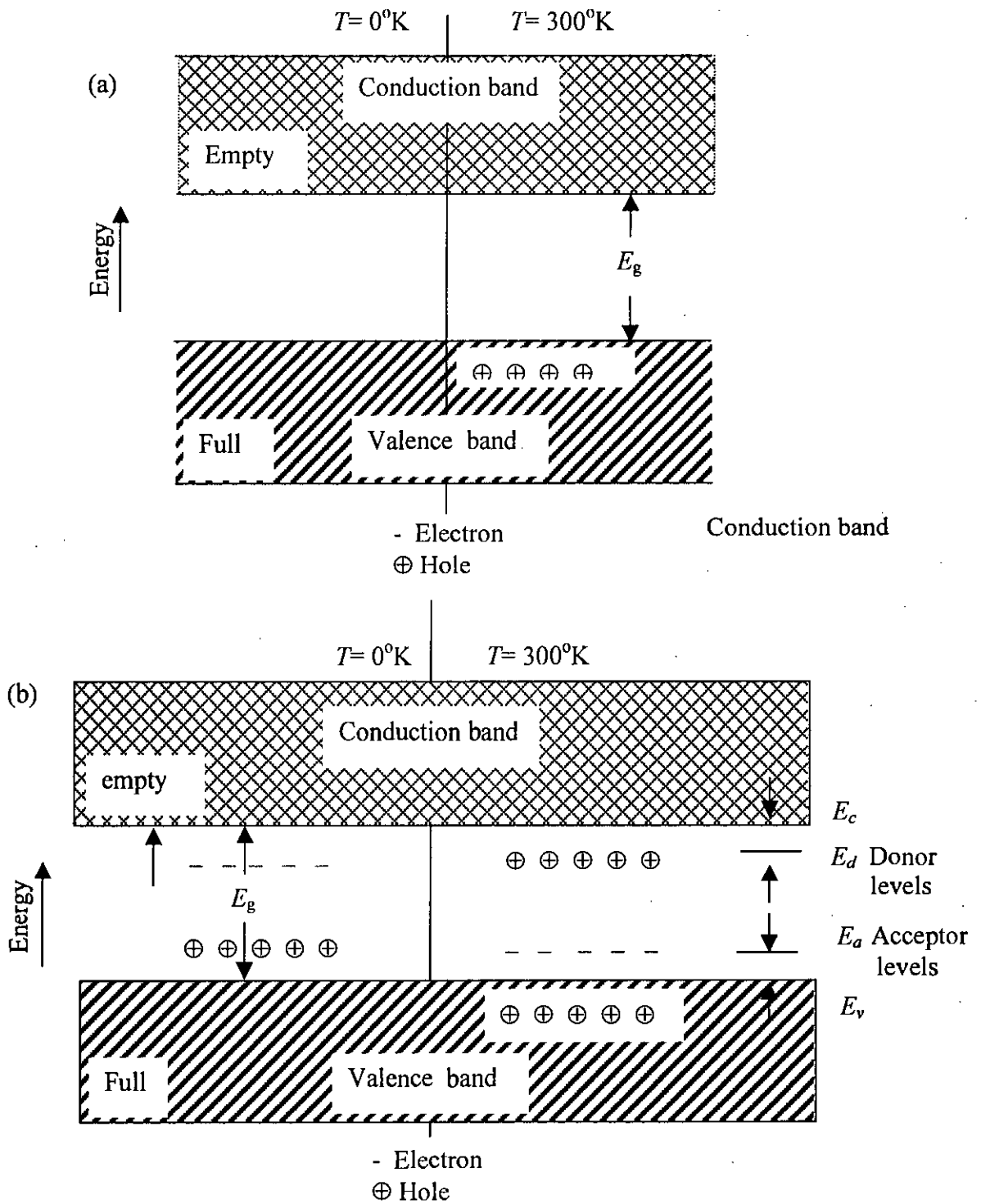
Fig. 1.2.1: A pictorial representation of an (a) intrinsic and
(b) extrensic semiconductor.

will attempt to neutralize itself by taking an electron from another neighboring bond. Then again a hole is formed in place of this electron and it will neutralize itself by taking another electron from the next neighboring bond. Such way the positive holes carry electricity in the extrinsic semiconductor. So it is called p (i.e. positive) type semiconductor (Fig. 1.2.2b) Cu_2O also p-type semiconductor.

n-type semiconductors : They n-type semiconductor arises from substitution of impurity atoms having more valence electrons than Si or Ge atoms. Elements such as P, As, Sb, and Bi have five valence electrons. When such an element is substituted for a silicon atom, four of its five electrons will enter the inter-atomic bonds, but the fifth electron will be only slightly attracted by the excess of the positive charge on the nucleus. Thermal agitation even at room temperature is sufficient to transfer this electron to the conduction band. Since conductivity is due to the motion of electrons in the conduction band, this semiconductor is called n-type and the impurity is called the donor. (Fig.1.2.2a). Titanium dioxide or titania is a non-stoichiometric transition metal oxide and behaves as n-type semiconductor [4].

There are three naturally occurring crystal phases of titanium dioxide: rutile, anatase, and brookhite. Most of the electrochemical and photocatalytic work to date have been performed on rutile or anatase, or a mixture of the two. Both rutile and anatase have tetragonal unit cells and both structures contain slightly distorted TiO_6 octahedral. Rutile is thermodynamically more stable than anatase at room temperature; the free energy change for antatase to rutile is -5.4 kJ/mol [5].

17

(a)

Si   Si   Si
Si
P +5
Si   Si   Si
Si   Si

P +5 Phosphorus

(b)

Si   Si   Si
B +3   Si
Si   Si   Si
Si   Si

B +3 — Boron
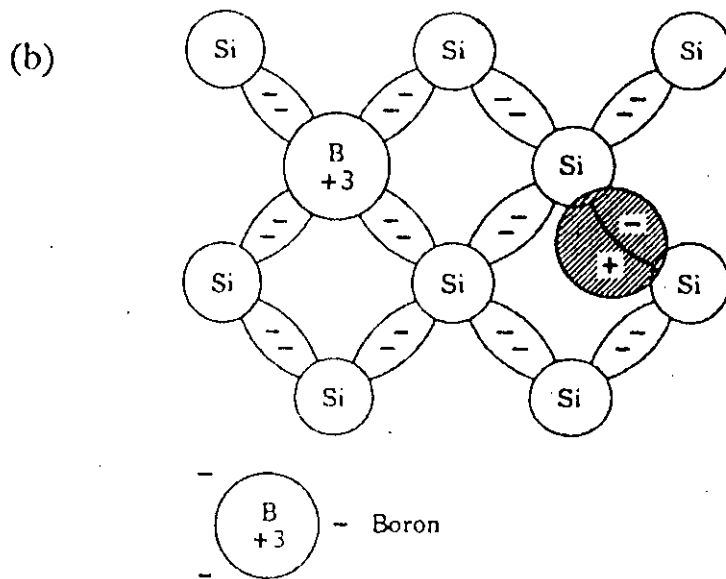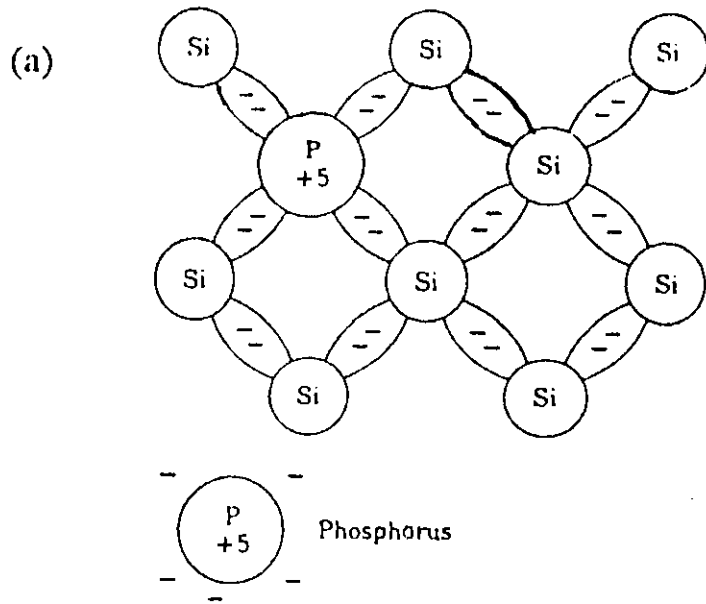
Fig. 1.2.2:   Types of impurity semiconductors (a) n-type (b) p- type.

18

The absorption and reflection properties of rutile have been studied extensively. At 4K, the short wavelength absorption edge for rutile is 410 nm (bandgap energy = 3.05 eV) [6, 7]. The lowest energy electronic absorption at 3.05 eV is an indirect transition. On the other hand, the bandgap of anatase is reported as 3.2 eV [8]. The absorption coefficients for both crystal phases are reported as $\sim 10^5$ cm^{-1} at 340 nm [9].

Ultraviolet radiation below $\sim$390 nm stimulates valence-band electrons in TiO_2 particles that are suspended in contaminated water. These electrons are promoted to the conduction band (e^-_{cb}), creating holes in the valence band (h^+_{vb}). These electron / hole pairs can either recombines, producing thermal energy, or interact

$$TiO_2 \xrightarrow{\text{h}\nu} TiO_2\, (e^-_{cb}, h^+_{vb})$$
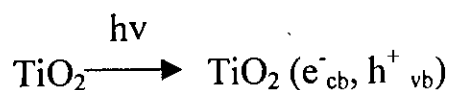
with the external environment to perform oxidation and reduction reactions.

C.   Composites

Since 1965 has a distinct discipline and technology of composite materials begun to emerge. That is 80% of all research and development on composites has been done since 1965 when the Air Force launched its-all out development program to make high performance fiber composites a practical reality. There are two major reasons for the revived interest in composite materials. One is that the increasing demands for higher performance in many product areas specially in the aerospace, nuclear energy and aircraft fields is taxing to the limit our conventional monolithic materials. The second reason, the most important for the long run is that the

composites concept provides scientists and engineers with a premising approach to designing, rather than selecting, materials to meet the specific requirements of an application.

The term 'composite' refers to something made up of various parts or elements. In definition of composite depends on the structural level of the composite we are thinking about. At the submicroscopic level that of simple molecules and crystal cells all materials composed of two or more different atoms or elements would be regarded as composites. This would include compounds, alloys plastics and ceramics. Only the pure elements would be excluded. At the microscopic level (or microstructural level) that of crystals, polymers, and phases a composite would be a material composed of two or more different crystals, molecular structures or phases. By this definition most of our traditional materials which have always been considered monolithic would be classified as composites. At the macrostructural level which is most useful for composites, the definitions of composites is that they are a mixture of macroconstituent phase composed of materials which are in a divided state and which generally differ in form and/or chemical composition. Note that, contrary to a widely held assumption, this definition does not require that a composite be composed of chemically different materials, although this usually the case. The more important distinguishing characteristics of a composite are its geometrical features and the fact that its performance is the collective behavior of the constituents of which it is composed. A composite material can vary in composition, structure, and properties from one point to the next inside the material.

The major constituents used in structuring composites are fibers, particles, laminas, flakes, filters, and matrix. The matrix which can be

thought of as the body constituent gives the composite its bulk form. The other four, which can be referred to as structural constituents determine the character of the composites internal structure. An special type of composite, fiber glass embedded in a polymer matrix is a relatively recent invention but has in a few decades, become a common place material. Characteristic of good composites, fiber glass, provides the 'best of both worlds', it carries along the superior properties of each component, producing a product that is superior to either of the components separately. The high strength of the small diameter glass fibers is combined with the ductility of the polymer matrix to produce a strong material capable of with standing the normal loading required of a structural material.

D.   Conductive polymers

The discovery in 1973 that poly sulfur nitride $(SN)_x$ was intrinsically conducting provided a proof that polymers could be conducting and thus greatly stimulated the search for other conducting polymer [10]. During the last two decades, a new class of organic polymers has been devised with the remarkable ability to conduct electrical current. These class of materials are called conducting polymers [11].

One of the earliest approaches to make the polymers conductive is to prepare a composite of polymers and conductive filler, such as, metal powder, graphite powder, flake or wire etc. Conductive fillers remain embedded more or less evenly dispersed in the polymer matrix and conduct electric current. But these composites can not be regarded as conducting polymers because the polymers presents in such composites are non-conducting [12-15].

In 1964, W. A. Little [16] synthesized a superconductor at room temperature with polymeric backbone and large polarizable side groups which led the discovery of new organic compounds with high electrical conductivity.

In the early 1980s, excitement ran high when several prototype devices based on conductive polymers, such as rechargeable batteries and current rectifying p-n junction diodes [17] were announced. Among the many polymers known to be conductive, polyacetylene (PAT), polyaniline (PANI), polypyrrole (PP) and polythiophene (PT) have been studied most intensively [18-24]. However, the conductive polymer that actually launched this new field of research was PAT.

Research has been expanded into the studies of heteroatomic conductive polymers because of their better chemical stability and the interest in the polaron and bipolaron conduction mechanism [25, 26]. Among the heteroatomic polymers PP, PT and PANI have been studied extensively.

During the 1980s, PANI was subjected to intense structural, physical, and electrical characterization, using modern experimental techniques. A brief survey, out of numerous features and studies made on PANI is presented below:

Structural features: Organic conducting polymer, PANI, is being studied more and more, and up to the recent years has been the centre of considerable scientific interest. However, PANI is not really a new material

and its existence has been known for the past 150 years or over, since it had already been made by Runge in 1834.

PANI has been described in many papers [27] usually as ill-defined forms such as 'aniline black' emeraldine, nigraniline, *etc.* synthesized by the chemical or electrochemical oxidation of aniline. Figure 1.3.1 shows the idealized oxidation state of PANI: leucoemeraldine, emeraldine, pernigraniline and emeraldine salt. Different structures result in different electrical behaviours of the material. Emeraldine salt is a partially oxidized
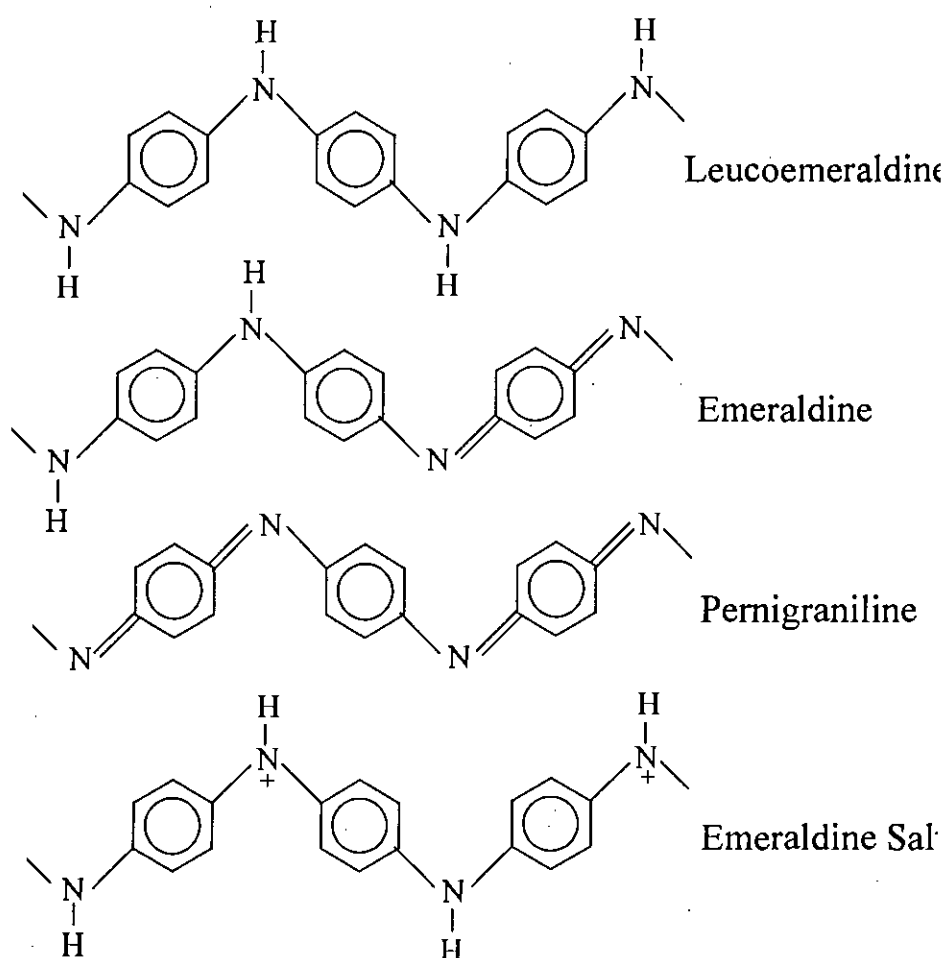
Fig. 1.3.1 Representation of idealized oxidation states of PANI.

23

compound, protonated, with electrical conducting characteristics. Leucoemeraldine is a fully reduced compound with electrical insulating characteristics. There are no double bonds between the aromatic rings and the N-H groups. Emeraldine base is an insulating compound, partially oxidized with few N-H groups in the main chain. Emeraldine changes from insulator to conductor when it is protonated with proton donor acids, such as, hydrochloric acid. This change is one of the most interesting properties of PANI. The structure of emeraldine PANI can be changed to emeraldine salt by removing an electron from the N-H group. Pernigraniline is a fully oxidized compound without conducting characteristics. There are no N-H groups in the structure. The level of protonation in the structure causes dramatic changes in the conductivity. The base form of the polymer in the emeraldine oxidation state (y = 0.5)
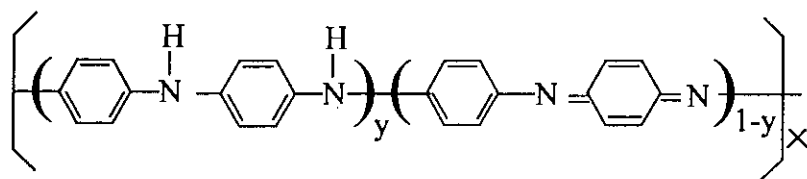
which contains equal number of alternating reduced,

   and oxidized
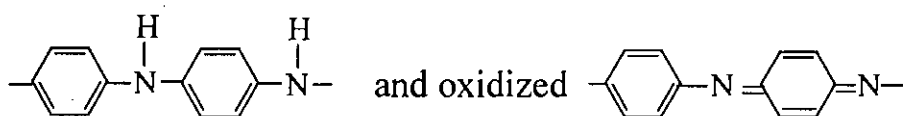
repeat units can be protonated by dilute aqueous acid to produce the corresponding salt (A=anion)
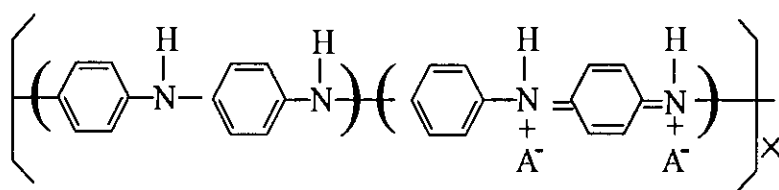
which is believed to exist as polysemiquinone radical cation [28-30].
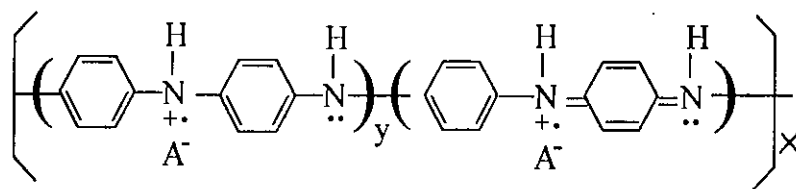
The polymer exhibits conductivities of ~ 1-5 S cm^{-1} when approximately half of its nitrogen atoms are protonated as shown above.

Methods of preparation : PANI is generally prepared by direct oxidation of aniline using an appropriate chemical oxidant or by electrochemical oxidation on different electrode materials.

Various chemical oxidizing agents have been used by different authors: potassium bichromate [31, 32], ammonium persulfate or peroxydisulfate [33, 34], hydrogen peroxide, ceric nitrate and ceric sulfate [35, 36]. The reaction is mainly carried out in acid medium, in particular sulfuric acid, at a pH between 0 and 2 [31, 32]. However, MacDiarmid *et al.* [33, 34] used hydrochloric acid at pH 1. Genies *et al.* [37] used a eutectic mixture of hydrofluoric acid and ammonia, the general formula of which is NH$_4$F: 2.3 HF, for which the pH is probably less than 0.

When aniline is mixed with the chemical oxidant in a reaction vessel and left for a certain period of time (the duration of which depends on the temperature and the concentration of active species), the solution gradually becomes colored and a black precipitate appears [38]. The coloration of the solvent is possibly due to the formation of soluble oligomers.

Anodic oxidation of aniline on an inert metallic electrode is the most current method for the electrochemical synthesis of PANI. This method offers the possibility of coupling with physical spectroscopic technique such as visible, IR, Raman, ellipsometry and conductimetry, for *in situ* characterization.

The anodic oxidation of aniline is generally effected on an inert electrode material which is usually Pt [39, 40]. However, several studies have been carried out with other electrode materials: iron [41], copper [42], zinc and lead [43], chrome-gold [44], palladium [45] and different types of carbon vitreous, pyrolic or graphite [46] or on semiconductor [47, 48]. When the polymerization is carried out at constant current, a maximum current density of 10 mA cm^{-2} is rarely exceeded.

Morphology and structure : The adherence and the homogeneity of a PANI film on an electrode varies according to the method of synthesis employed. Diaz [49] has observed weak adherence for a polymer prepared by electrochemical oxidation at constant potential, whereas good adherence results when potential cycling is employed. Kitani *et al.* [50] have reported that, using the same method, a thin homogenous film is initially deposited on the electrode, followed by the formation of an amorphous powder which eventually becomes detached from the electrode surface. Electrochemical investigations on the polymer growth by Thyssen *et al.* [51] yielded evidence for cross-linking reactions leading to the formation of hemispheres.

There is, therefore, a myriad of possible chemical structures for the polymeric backbone of PANI. Elucidation of the precise molecular

arrangement is complicated by the fact that these structures are affected by both electronic excitation and reduction and by concomitant protonation and deprotonation of the nitrogen atoms in the polymer.

Optical properties : A wide range of colors from pale yellow to blue for the PANI is observed. From the optical data obtained for PANI, it is possible to assign three absorption zones which are dependent on the oxidation state of the polymer. In the reduced state, PANI is an insulating material, the energy band structure of which is comparable to that of an intrinsic semiconductor, with the resulting absorption being associated with the transition between the valence band and the conduction band. However, when the potential is increased, the polymer oxidizes and intermediate mid-gap states appear in the forbidden band (radical cations and then dications) and thus results absorption in the longer wave length. Elucidation of band model of a polymer can be made based on optical data.

Conductivity : From conductivity measurements, Travers et al. [32] have observed that the PANI exhibits a metal-to-insulator transition which is a function of the pH. The conductivity of the polymer is 5 ohm^{-1} cm^{-1} when the polymer is previously equilibrated at pH 6. MacDiarmid et al. [33, 34] has also described a variation in the conductivity of both chemically and electrochemically prepared polymers with the pH of the aqueous solution to which the polymer was exposed before drying. The polymer exhibits a conductivity of 1 ohm^{-1} cm^{-1} when it is equilibrated at a pH between -1 and $+1$, and 10 ohm^{-1} cm^{-1} when it is equilibrated at a pH between 5 and 6. Elsewhere, they indicates that the conductivity of the polymer is a function of the level of doping, with a value of 1 ohm^{-1} cm^{-1} for 15% doping, and

varying from 10^{-10} to 10^{-1} ohm^{-1} cm^{-1} for 0% to 10% doping. Measurements carried out by Brahma [52] revealed that PANI doped with iodine exhibits a conductivity four orders of magnitude greater than the undoped polymer.

Solubility :It is generally accepted that PANI is insoluble in most common organic and aqueous solvents, irrespective of the method of synthesis. Nevertheless, Mohilner *et al.* [39] have shown that the polymer is easily dissolved in pyridine and DMF, strongly tinting the solutions blue.

The synthesis of soluble PANI is of great interest since the formation of a soluble material is essential in order to post-synthesis processing. There are two possible methods for preparing soluble polymers: (i) formation of the polymer salt using an anionic dopant which favors dissolution, or (ii) prefunctionalization of the starting monomer with a suitable group prior to polymerization. Chemical synthesis of soluble PANI by the former method has been successfully accomplished by Li *et al.* [53] and involves proton acid dopants of large molecular size such as toluene-*p*-sulfonic acid, sulfanilic acid or polymeric electrolyte-polystyrene sulfonic acid.

Applications: PANI can be used as material for modified electrodes [46, 49], as a corrosion inhibitors for semiconductors in photoelectro-chemical assemblies [54], in microelectronics [55] and as electrochromic material [56]. The application which has inspired most interest is in the area of electrochemical batteries. The possible use of PANI as active anodic material is in rechargeable batteries [57].

More recent systematic studies have been undertaken by numerous groups [33, 34, 54] on the possible use of PANI as an active electrode material. These investigations deal with the behaviour of PANI in aqueous and organic media as a function of the mode of synthesis.

1.3 Electroplating of Nickel

A. Principles

Fundamental to an understanding of modern nickel plating is a thorough knowledge of the chemistry of the Watts bath [58] and the effects of all controllable variables on the properties of the deposits made from this type of electrolyte. In actual tonnage of nickel deposited the bright and semibright nickel baths are of predominant importance, but they all include the basic Watts ingredients. Other ingredients of commercial baths are used for very specific purposes. The fundamentals of nickel plating are observed in the effects of such variables as temperature, nickel concentration, current density, pH, and agitation on deposits from the Watts bath. This bath opened the way for rapid plating at elevated temperatures. This improvement was, in large part, due to bath compositions and operating conditions favoring a rich and constantly replenished cathode film and high anode efficiency.

B. Nickel Bath: The Watts Bath

Nickel Sulphate: Most of the nickel ion content is contributed by nickel sulfate. This salt is used because it is the least expensive salt of nickel with a stable anion that is not reduced at the cathode, oxidized at the anode, or volatilized. It is also highly soluble and readily available commercially. The limiting cathode current density for sound nickel deposits is a function of the

29

nickel ion concentration in the cathode film, which in turn depends on the metal ion concentration of the bath itself.

Chloride ion: Chloride ions are introduced by adding nickel chloride instead of sodium chloride to simplify the composition and control of the bath and to avoid secondary effects such as an increase in stress of deposits ascribed to the presence of sodium ions. A principal function of the chloride ion is to improve anode dissolution by reducing polarization. It also increases the conductivity of the bath and has marked effects at the cathode. It increases throwing power as a result of increasing cathode efficiency, electrolyte conductivity, and slope of the cathode potential curve [59]. These effects are at a maximum in the all-chloride bath [60], and at a lesser degree in the high-speed bath developed [61], which contains chloride and sulfate in about equal normalities.

Boric acid : Boric acid serves as a buffer in a nickel plating solution. Its principal effect is that of controlling the pH in the cathode film. In the absence of a buffer, nickel deposits at ordinary temperatures tend to be hard, cracked, and pitted [62]. Nevertheless, made excellent heavy deposits from unbuffered boiling electrolytes [63]. A secondary effect of the buffer is that of maintaining the pH in the operating range of the specific bath. The maximum buffering action is obtained at a pH of 5-6.

Addition agents : Addition agents to prevent pitting are employed in all types of nickel plating baths. Wetting agents are used exclusively for this purpose in bright nickel plating baths. One disadvantage of using wetting agents is that oil or grease dropped on the bath becomes emulsified, reduces

ductility of the deposit, and may be the cause of serious pitting. Decomposition products of wetting agents may also accumulate in time and have a similar effect until the bath is repurified. Where the highest ductility is required and where other mechanical properties must be rigidly controlled, hydrogen peroxide is used as needed to prevent hydrogen pitting. It operates by depolarization of the cathode, as well as by oxidation of iron (II) and decomposition of undesirable organic contaminants of the bath. The amount of peroxide required to prevent pitting is a function of bath purity. The usual recommendation for a Watts bath is an addition, once a day, of 1 part 30% hydrogen peroxide per 2000 parts solution. A grade free of organic and metallic stabilizers should be used. Localized additions of peroxide next to the cathode should be avoided; instead, it should be added in a manner favoring its intimate and complete mixture with the whole electrolyte. By frequent analysis and additions, a constant concentration of hydrogen peroxide has been successfully maintained in a large-scale nickel plating plant with uniformly good results. The rate of decomposition of peroxide increases rapidly with increase in pH [64], hence this addition agent is more efficient in low-pH baths. An excess of hydrogen peroxide increases the contractile stress and causes burning and embrittlement of the deposit. Other agents used occasionally to control pitting are sodium perborate, which decomposes to form hydrogen peroxide; and nitrates. Nickel plating baths commonly contain a small amount of cobalt derived from the anodes and salts. This fractional percentage of cobalt is considered to have no significant effect on the properties of the deposit.

Composition range: The function of the ingredients of a Watts bath shows that their concentrations can be varied over rather wide ranges. The typical

formula is excellent for an average cathode current density of 5 amp/dm^2 at a temperature of 50 ^{o}C. Under such conditions local current densities of one-half or twice this value will still result in excellent deposits. For plating at a lower average current density, for example 2 amp/dm^2, the nickel sulfate and nickel chloride contents may be halved. For higher current densities than normal, their concentrations can be increased, but the practical difficulty of excessive drag-out losses and crystallization sets a limit to such changes. Current densities higher than 10 amp/dm^2 are better achieved by increase in agitation, temperature, and ratio of chloride to sulfate.

C.   Effects of other controllable variables

Other factors also influence the nature of the cathode film and thereby the quality of the deposit. They are current density, temperature, pH, and degree of agitation or relative motion of cathode and solution. These are all interrelated; if a variable such as current density is altered considerably without the other factors being altered at the same time, adverse effects on the deposit. The typical modern Watts bath can be operated at 54 C and pH 2.0 to give sound, ductile, gray deposits at 6 amp/dm^2 with a moderate degree of agitation. If the current density is lowered to 0.2 amp/dm^2 without reduction of the temperature or increase of the pH, bright, brittle deposits will be obtained. The relation between limiting current density, temperature, and pH in a bath of the original Watts composition (240 g/l nickel sulfate, 20 g/l nickel chloride, and 20 g/l boric acid) was determined [65] and is summarized graphically. The curves would also be displaced to the right for increasing rates of agitation of the electrolytes over the cathode surface. The range of permissible current densities is greatly extended at low pH, where

smoother deposits are obtained because of the greater solubility of metallic impurities.

Metal distribution (throwing power): The electrochemical properties which determine metal distribution over a cathode of a given shape are cathode polarization, solution conductivity, and cathode efficiency. A steep slope of the cathode potential-current density curve, a small or negative slope of the cathode current efficiency- current density curve, and a low specific resistivity of the electrolyte favor more uniform metal distribution or higher throwing power. These characteristics of a Watts bath are affected by changes in the plating variables indicates their probable effect on throwing power. The specific resistivity of the Watts bath is about 11 ohm-cm at 60 C, and it decreases in the usual way with increase in temperature [67]. It also decreases with increasing total concentration [67] and increasing chloride ion concentration [60]. It is but little affected by pH within the range 2.0-5.5 [69]. Like the cathode efficiency of all nickel plating baths, that of the Watts bath rises with increase in current density until the limiting current density is reached. It also rises with increase in temperature and with total concentration [67, 68]. Increase in chloride ion concentration has a more markedly beneficial effect, but the effect of pH is the most pronounced: the current efficiency decreases rapidly with a fall in pH [59, 67].

Hydrogen peroxide reduced the throwing power of the low-pH bath, but the effect did not last long after the addition had been made. Iron (III) sulfate is very detrimental to throwing power, but iron (II) sulfate is not. Throwing power of nickel plating solutions using a Hull cell [69]. A

moderate improvement over a Watts solution was obtained by changing the anion.

Structure and mechanical properties of deposits : The effects of pH, temperature, current density, and solution composition on the metallographic structure and mechanical properties of nickel deposits from the modern Watts bath [66, 70, 71].

When plated at 55 °C and pH 2.0, deposits from the modern Watts bath show a columnar or conical structure which grows coarser with increasing thickness. Grain refinement occurs as the pH or the chloride content is increased or the temperature is decreased. The effect of current density varies with conditions. The hardness, tensile strength, and ductility of nickel deposits are almost always consistently related; that is, an increase in hardness is accompanied by an increase in tensile strength and a decrease in ductility. Soft, ductile deposits are obtained at pH 4.5 or lower.

The increase in hardness and strength of nickel deposits produced at high pH to be related to the amount of occluded basic compounds of nickel. These are believed to be codeposited in a finely divided or colloidal form dispersed through the nickel lattice in such a way as to interfere with slip. The relationship was as simple as that, since other factors, such as the structure and the cobalt content, play a role [72]. Nickel can be deposited with a wide variety of metallographic structures and with controlled physical and mechanical properties over a wide range of values. When other than a soft, ductile nickel is required, bath compositions quite different from the Watts solution are employed.

Ostress in nickel deposits: Characteristic of nickel deposits is that all are deposited in a condition of internal contractile (tensile) stress, except when one of certain specific organic addition agents is present. The study of this phenomenon received a great impetus in 1946 from the outbreak of spontaneous cracking of bright nickel deposits in the automotive industry at a time when a high production rate was imperative [73-75], which described how to measure such internal stresses quantitatively. All measurements were based on the amount of bending of a strip nickel plated on only one side. The theory of Wyllie [76] that stress is due to hydride formation and subsequent escape of hydrogen, does not explain some of the experimental results, such as the marked increase in tensile stress produced by small amounts of certain impurities in nickel baths (iron, manganese, zinc, carbon dioxide, organic colloids) or the effect of certain organic addition agents in decreasing or reversing tensile stress [77]. It is now in disrepute for metallurgical reasons [78]. Still a different cause of tensile stress, namely that it is simply a manifestation of the greater internal energy of the newly deposited nietal equivalent to the overvoltage involved in deposition [73]. An expanded lattice would have a higher energy content and would then tend to contract.

The performance of a stressreducing agent in a Watts bath and interpreted the results by means of a vacant-site and dislocation theory [79]. It was postulated that tensile stress results from the formation of an oriented array of edge dislocations initiated by surface vacant-sites.

Effect of Bath Variables: There is disagreement on stress [80-84] regarding the effects of some variables, but the preponderance of evidence supports the following conclusions.

1. Positive (tensile) stress increases with increase in chloride content of the bath.

2. The effect of temperature on stress is not consistent: it varies with the composition of the bath (principally the chloride content) and the current density.

3. The effect of pH varies with composition of the electrolyte.

4. The effect of current density is not marked over the range 1-5 amp/dm^2 but is usually in the direction of an increasing tensile stress with increasing current density.

5. Superimposing alternating current on the direct plating current tends to reduce stress, other conditions remaining the same.

6. Agitation has little effect.

7. Evidence regarding effects of impurities and addition agents is conflicting, apparently because these effects change with variation in solution composition and pH. Hydrogen peroxide, carbon dioxide, certain organic brighteners of the second class, wetting agents, and iron, zinc, lead, and sodium salts can all act as stress raisers under some conditions. Ammonium sulfate reduces stress in high-pH baths, but the reverse or no effect may occur at lower pH values [66].

8. Several types of addition agents, such as fluorides and fluoborates, tend to reduce tensile stress, and some, such as the brighteners of the first class, can cause the stress to pass through zero and even reverse in direction so as to make the nickel expand or be under compression if restrained from expanding.

1.4 Theoreticals of experimental techniques

A. Cyclic voltammetry

Electrochemical process is widely used in the polymerization of organic polymer. Most of the system for electrochemical polymerization consists of compartment where three electrons are dipped into the solution containing monomer and electrolyte solution. Appropriate potential is applied to the working electrode for polymerization of the monomers. The potential of the working electrode, where deposition of the polymer film takes place, is controlled versus the reference electrode using a feed-back circuit or a potentiostat. Feed-back circuit drives the circuit between the working and counter electrode while ensuring that none passed through the reference electrode circuit.

The nature of the working electrode is a critical consideration for the preparation of these films. Since the films are produced by an oxidative process, it is important that the electrode is not oxidized concurrently with the aromatic monomer. For this reason, most of the available films have been prepared using a platinum or a gold electrode.

Potentiostatic, galvanostatic and potential sweep techniques such as cyclic voltammetry are widely used for electrochemical polymerization of aromatic compounds. In potentiostatic technique, a constant potential is applied to the working electrode which is sufficient to oxidize the monomers to be polymerized on the electrode. In galvanostatic process, a constant current density is maintained to polymerize the monomers while film thickness can be monitored in the similar way as described for potentiostatic

technique. On the other hand, cyclic voltammetry involves sweeping the potential between potential limits at a known sweep rate. On reaching the final potential limit, the sweep is reversed at the same scan rate to the initial potential and the sweep may be halted, again reversed, or alternatively continued further. In such experiments, cell current is recorded as a function of the applied potential.

B. Optical microstructure

In comparison with a biological microscope, the optical one differs in the manner by wich the specimen is illuminated [57]. In optical microscope, a horizontal beam of light source is reflected, by means of a plane-glass reflector, downward through the microscope objective onto the surface of the specimen. Some of the incident light reflected from the secimen surface will be magnified in passing through the lower lens system, the objective, and will continue upward through the plane-glass reflector and be magnified again by the upper lens system, the eyepiece. The initial magnifying power of the objective and the eyepiece is usually engraved on the lens mount. When a particular combination of objective and eyepiece is used at the proper tube length, the total magnification is equal to the product of the magnification of the objective and the eyepiece.

The maximum magnification obtained with the optical microscope is about 2000x. The principal limitation is the wavelength of visible light, which limits the resolution of fine detail in the optical specimen. The magnification may be extended some what by the use of shorter-wave length radiation, such as ultraviolet radiation, but the sample preparation technique is more involed. The specimen is polished and etched following normal

38

metallographic practice before taking photograph. In the optical microscope the image is brought into focus by changing the spacing Fig. 1.4.1. illustrates the principle of the optical compound microscope and the trace of rays through the optical system from the object field to the final visual image.

C. SEM technique

The scanning electron microscope (SEM) uses a finely focused beam of electrons to scan over the area of interest. The beam-specimen interaction is a complex phenomenon. The electrons actually penetrate into the sample surface, ionizing the sample and cause the release of electrons from the sample. These electrons are detected and amplified into a SEM image that consists of Back Scattered Electrons and Secondary Electrons. Since the electron beam has a specific energy and the sample has a specific atomic structure, different image will be collected from different samples, even if they have the same geometric appearance.

The specimen stage of SEM allows movement of the specimen along 5 axis. The basic stage is controlled manually by micrometers and screw-type adjusters on the stage door. The motorized stage has motors driving the X, Y, Z and rotation controls, all with manual over ride.

The stage can be tilted over 90°. The tilt axis always intersects the electron optical axis of the column at the same height (10 mm). When the specimen positioned at this height, the specimen can be tilted in the eucentric plane. This means that during tilt, almost no image displacement occurs. The tilting
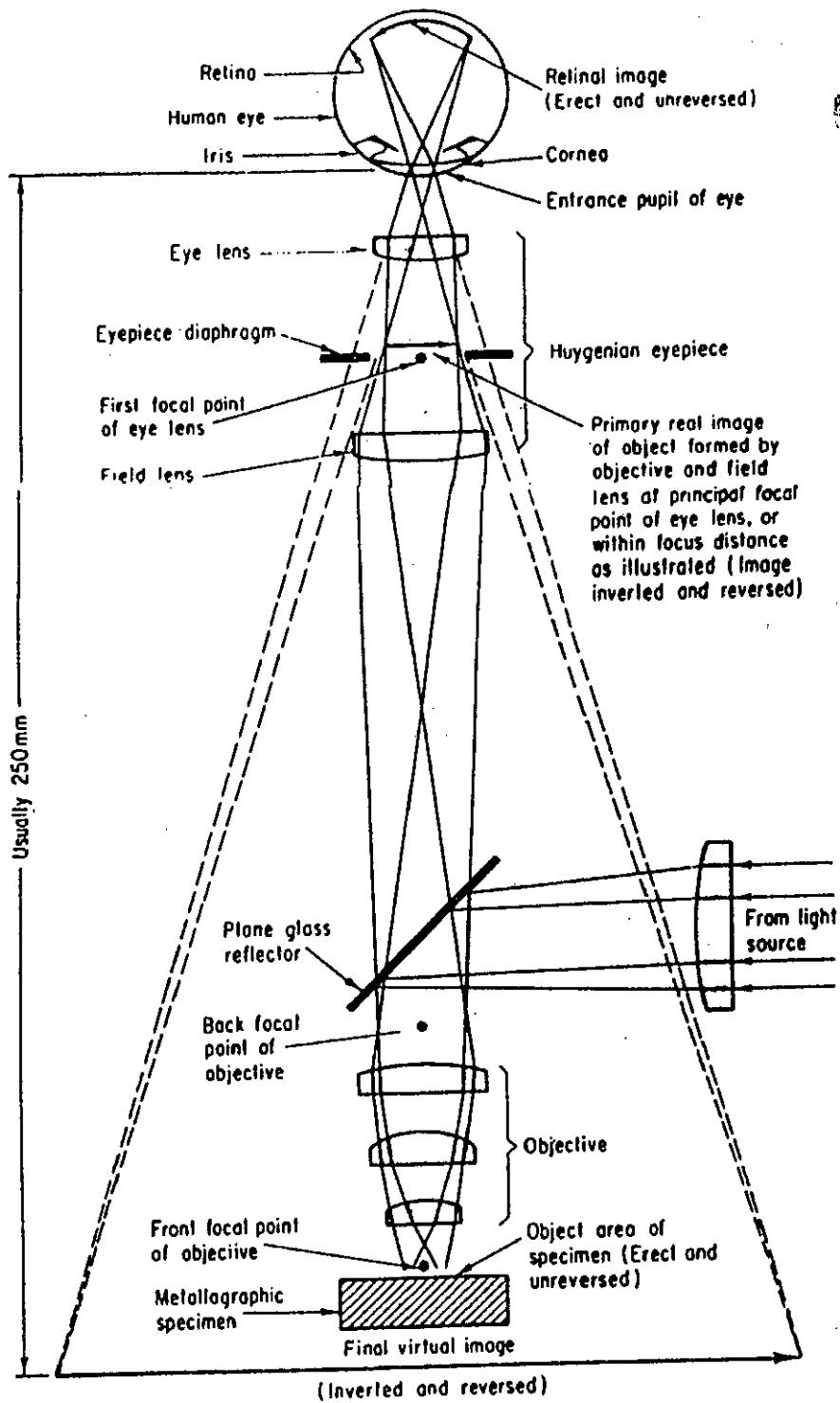
Fig. 1.4.1: The Illustrating the principle of the optical compound microscope and the trace of rays through the optical system from the object field to the final virtual image.

mechanism can be locked for more stability at high magnification. A schematic diagram of scanning electron microscope is shown in Fig. 1.4.2.

D. IR spectroscopy

Emission or absorption spectra arise when molecules undergo transition between quantum states corresponding to two different internal energies. The energy difference ΔE between the states is related to the frequency of the radiation emitted or absorption by the quantum relation

$$\Delta E = h\nu \hspace{4cm} 1.4.1$$

where $h \rightarrow$ planck's constant $\nu \rightarrow$ frequency. Infrared frequencies have the wave length range from 1 μm to 50 μm are associated with molecular vibration and vibration-rotation spectra. Detection of chemical groups and bonding are done by the typical spectra.

In polymer, the IR absorption spectrum is often surprisingly simple, if one considers the number of atoms involved. This simplicity results first from the fact that many of the normal vibrations have almost the same frequency and therefore appear in the spectrum as one absorption band and second, from the strict selection rules that prevent many of the vibrations from causing absorptions. In our experiment, we tried to observe the change in frequency of different samples and detection of SiO_2 by following the Si-O or O-Si-O frequencies. IR spectrum of all the compounds were recorded on IR spectrophotometer in the region of 4000-400 cm^{-1}. Samples were introduced as KBr pellets. A block diagram of an IR spectrophotometer is shown in Fig. 1.4.3.

41

Rotation in the
tilted plane

Y ± 75 mm in the plane
of tilt, perpendicular to
the tilt axis

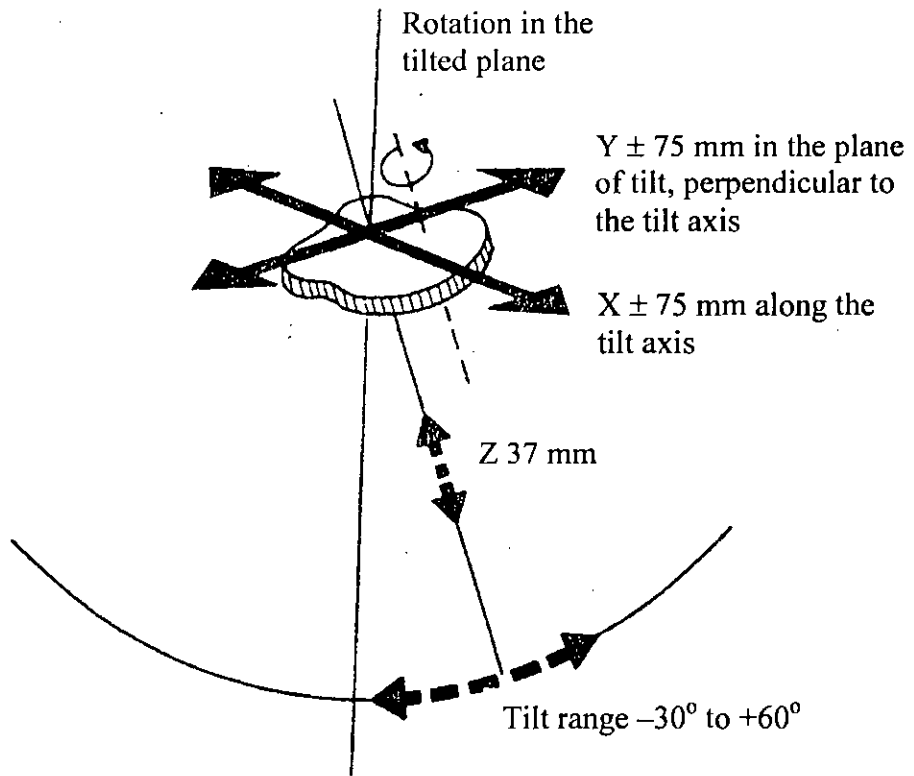X ± 75 mm along the
tilt axis

Z 37 mm

Tilt range −30° to +60°

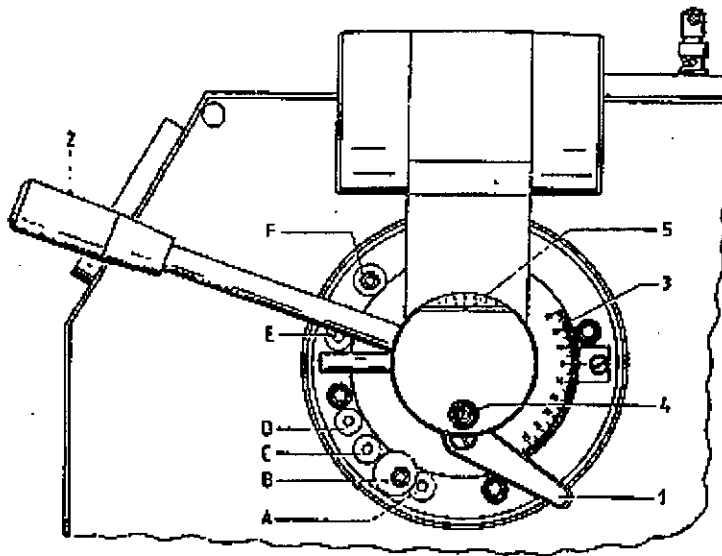Fig. 1.4.2a: Illustration of specimen stage movement
in SEM arrangements.

Fig. 1.4.2b: Mechanical controls and tilt stops on the stage
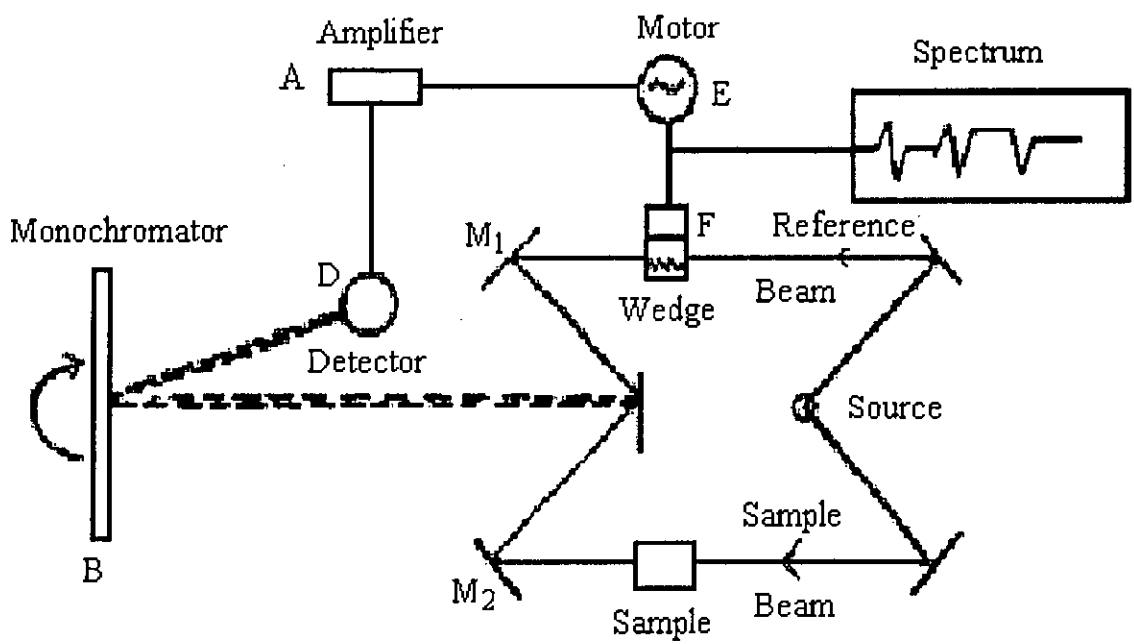door of SEM.

42

Fig. 1.4.3: A bloc diagram of an IR spectrophotometers.

E.   X-ray diffraction

The X-ray diffraction (XRD) provides substantial information on the crystal structure. This method is applied for the investigation of orderly arrangements of atoms or molecules through the interaction of electromagnetic radiation to give interface effects with structures comparable in size to the wave length of the radiation. Studies on the crystal structures developed, based on methods using single crystals after the discovery of X-ray diffraction by crystals made by the Von Laue [85]. Now a days XRD is used not only for the determination of crystal structure but also chemical analysis, such as chain conformations and packing for polymers, for stress measurements and for the measurement of phase equilibria and the measurement of particle size, for the determination of the orientation of the crystal and the ensemble of orientations in a polycrystalline material.

X-rays are the electromagnetic radiation whose wavelength are in the neighborhood of 1° A. The wave length of an X-ray is thus of the same order of magnitude as the lattice constant of crystals, and it is this which makes X-rays so useful in structures analysis of crystals whenever X-ray are incident on a crystal surface they are reflected. The reflection abides by the celebrated Bragg's law as given below:

$$2d\, Sin\theta = n\lambda \qquad\qquad\qquad 1.4.4$$

where d is distance between crystal planes, θ is the incident angle, λ is the wave length of X-ray and n is a positive integer. The diffracted X-ray may be detected by their action on photographic films or plates or by means of a radiation counter or electronic equipment feeding data to a computer [86].

The main purpose of using this technique for the analysis of the studied polymeric samples is to observe, from the X-ray diffraction pattern, the change in crystallinity in the series upon same condition.

F.   Solid state conductivity

The conductivity of polymer or polymeric composites depends on dopant level, protonation level of oxidation morphology and moisture content of the sample. Electrical resistivity of the polymer samples may be measured by two probe and four probe technique. The electrical conductivity may be measured by using ohm's law

$$E/I = R \qquad\qquad 1.4.5$$

where I is the current in amperes, E is the potential difference in volts, R is the resistance in ohms. The reciprocal is termed the conductance, this is measured in siemens (S) which is reciprocal of ohms (ohm^{-1}). The resistance of a samples of length L, and cross-sectional area A, is given by

$$R = \rho L/A \qquad\qquad 1.4.6$$

where ρ is a characteristic property of the material termed the resistivity. If L and A will be measured respectively in cm and then ρ refers to cm cube of the material and

$$\rho = RA/L \qquad\qquad 1.4.7$$

The reciprocal of resistivity is the conductivity, (formerly specific conductance)

$$K = 1/\rho \qquad or \qquad K = L/RA \qquad\qquad 1.4.8$$

which is SI units is the conductance of a one cm cube of substance and has the units ohm^{-1} cm^{-1} or S cm^{-1} [87].

In this experiment, Electrochemistry prepared sample was dried by sunlight and annealing the samples at 80°C temperature for 24 hours. Thus the powdered samples are converted into pellet by pressing appropriate pressure 10^4 pounds per squire inch. For electrical connection silver paste and copper wire is used on the palette.

Two electrodes of electrometer are connected with silver pasted copper wire and resistance (R) is measured directly at room temperature 23°C after some time interval.

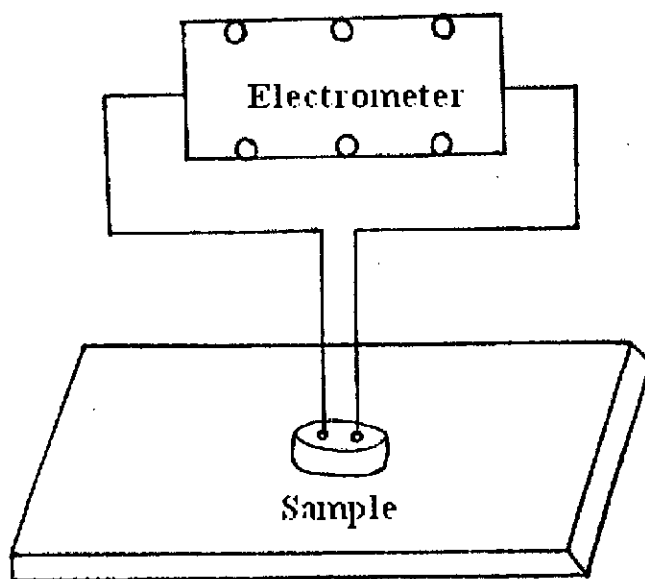A schematic diagram of the construction for d.c. conductivity measurements is shown in Fig. 1.4.4.

Fig. 1.4.4 : The construction for the measurement of d.c. conductivity.

G. Magnetic susceptibility

Magnetic susceptibility is given by $\chi = \dfrac{I}{H}$ and thus expresses the extent to which the material is susceptible (sensitive) to the external magnetic field or susceptible to magnetization. Here χ = simply volume susceptibility, I = magnetic moment and H = magnetic field strength, If I and H are measured in the same unit, χ becomes dimension quantity. By placing $\dfrac{B}{H}$ =P and χ = I/H in Gaess's law equation, we get $P = I + 4\pi\chi$

In practice, susceptibility is usually expressed, gram susceptibility (χ_g) and molar susceptibility (χ_m).

Gram susceptibility(χ_g): Gram susceptibility is usually expressed per unit mass. χ_g is given by

$$\chi_g = \frac{\text{volume susceptibility}}{\text{Density}} = \frac{\chi}{d}.$$

The molar susceptibility: Molar susceptibility (χ_M) expressed by

$$\chi_M = \text{gram susceptibility} \times \text{mol.wt}$$

$$= \chi_g \times M$$

$$= \frac{\chi}{d} \times M$$

For normal paramagnetic and diamagnetic substraces χ, χ_g and χ_M are constants independent of field strength.

In this work, electrochemically prepared samples were dried and measured their gram susceptibility with the help of magnetic susceptibility balance. Susceptibility, χ_g, is calculated using:

47

$$\chi_g = \frac{C_{Bal} * l * (R - R_0)}{10^9 * m}$$

1.4.9

Where: l = the sample length (cm)

m = the sample mass (gm)

R = the reading for tube plus sample

R_0 = the empty tube reading

C_{bal} = the balance calibration constant

When the various substances are placed between the poles of a magnet (magnetic field) they do not become in a similar way, i.e. they show different behaviours which are known as magnetic behaviors. These are classified as diamagnetism, paramagnetism. antiferromagnetism and ferrimagnetism. Of these, the last three at rare occurrence. On the other hand, diamagnetism, paramagnetism are of great importance. A schematic diagram of magnetic susceptibility balance is shown in Fig. 1.4.5.

Diamagnetism: The substances which, when placed in a magnetic field, decrease the intensity of the magnetic field than in vacuum are called diamagnetic substances and the property due to which they show this behaviour is called diamagnetism.

Paramagnetism: The substance which, when placed in a magnetic field, allow the magnetic lines of force to pass through them rather than due to which they show this behaviour is called paramagnetism.
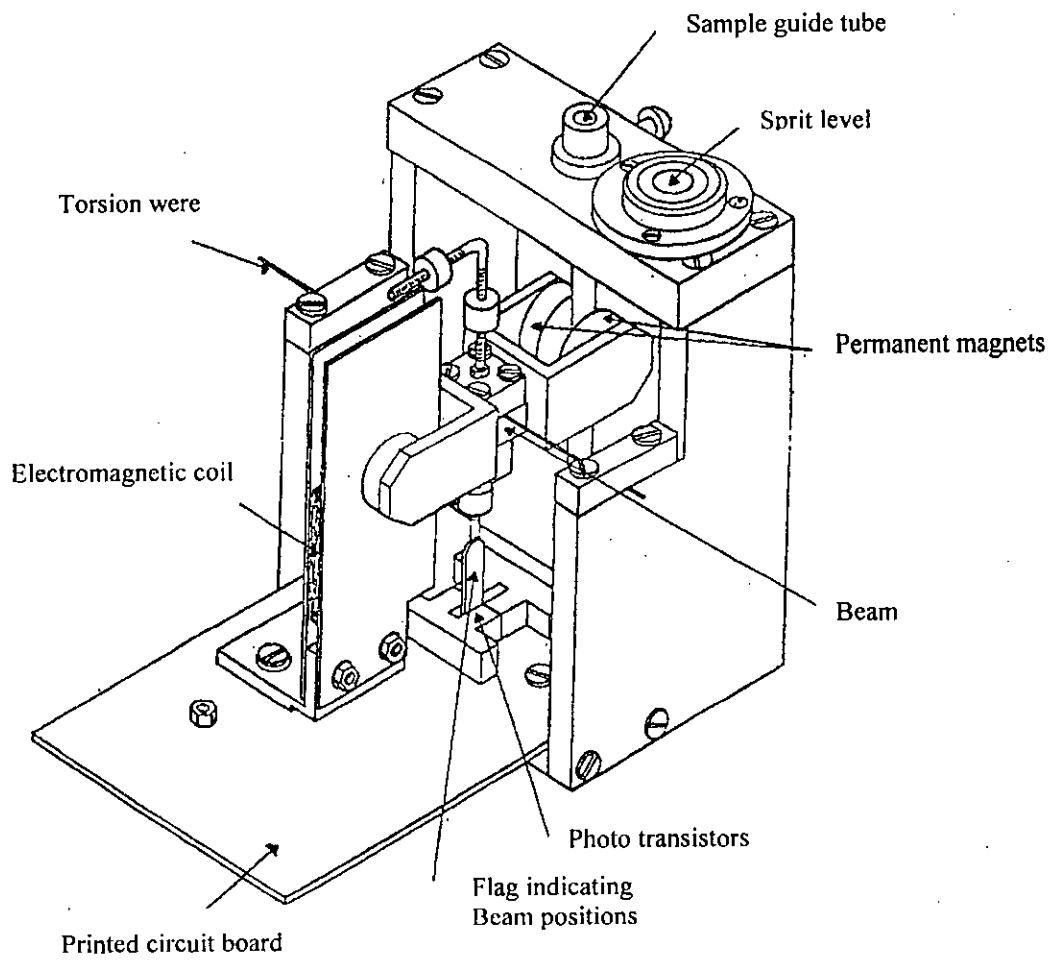
Fig. 1.4.5: Schematic diagram of magnetic susceptibility balance.

1.5 Aim of the present work

Taking into account the early works, it is evident that a good progress has been made in preparing conducting polymers with well-defined structure. Interest in the electrical properties of highly conjugated polymers has increased rapidly during the past decades. In the early 1980's excitement ran high when several prototype devices based on conducting polymer were announced.

PANI is unique among the other conducting polymer that its electrical properties can be reversibly controlled both by charge-transfer doping and by protonation. The wide range of associated electrical, electrochemical and optical properties coupled with good stability made PANI potentially attractive for application as an electronic material. Metal and semiconductor particles comprise a fundamentally and technologically interesting class of materials. The possibility of dispersing metallic and semiconductor particles inside the conducting polymer to form hybrid conducting matrices has received a special attention in recent times. Inorganic oxides, such as, TiO_2, ZnO and organic dyes are also very interesting materials in this regard.

Although electrochemically conducting polymers are known to be very important materials due to the large field of their potential applications, polymeric system do not have any intrinsic catalytic or magnetic activity of their own. They have been used as host matrices where different chemical species have been incorporated. In the present work, metallic Ni particle is planned to disperse into the PANI host with an aim to acquire catalytic and magnetic functionalities of the resulting matrix.

References

1. H. Lund, in organic electrochemistry, Eds., M. M. Baizer and H. Lund, Marcel Dekker, 1983.

2. S. Barnartt, *J. Electrochem. Soc.*, **99** (1952) 549.

3. Reports on the IUPAC Convention on Electrochemistry, *Electrochim. Acta,* **27** (1982) 629 and *Pure and Appl. Chem.*, **37** (1974) 503, **51** (1979) 1159.

4. L. Smart and E. Moore, *Solid State Chemistry*, Chapman and Hall, 1992, 126.

5. *The Oxide Handbook,* Samsonov, G. V. Ed.; IFI / Plenum, New York, p23, 1982.

6. Grant, F. A. *Riv. Modern Phys.*, **31** (1959) 646.

7. Cronemeyer, D.C. Phys. Rev. **87** (1952) 876.

8. Bickley, R. I. *Chem. Phys. of Solids and Their Surface* 7 (1978) 118.

9. Salvador, P. *Solar Energy Matter.*, **6** (1982) 241.

10. V. V. Walatka, M. M. Labes and J. H. Perlstein, *J. Phys.Rev. Lett.*, **31** (1973) 1139.

11. A. J. Heeger, G. B. Street and G. Tourillon, *Hand Book of Conducting Polymers* (T. A. Skotheim, ed.), Marcel Dekker, Inc., New York, vol. **1** (1986) 265, 293.

12. R. B. Seymour, *Conducting Polymers*, Plenum Press, New York, (1981) 23.

13. E. K. Sickel, *Carbon Black Polymer Composites,* Marcel Dekker, New York, (1982).

14. A. Malliaris and D. T. Turner, *J. Appl. Phys.*, **42** (1971) 614.

15. H. Inokushi and H. Akamatu, *Solid State Physics*, (F. Seitz and D. Turnbull, ed.)., **12** (1955) 93.

16. W. A. Little, *Phys. Rev.* **134A** (1964) 1416.

17. C. K. Chiang, A. J. Hegger and MacDarmid, *Ber. Bunsenges. Phys. Chem.*, **83** (1979) 407.

18. R. de Surville, M. Jozefowicz, L. T. Yu, J. Perichon and R. Buvet, *Electrochim. Acta.*, **13** (1968) 1451.

19. A. G. MacDiarmid, J.-C. Chiang, M. Halpen, W.-S. Huang, S.-L. Mu, N. L. D. Somasiri, W. Wu and S. 1. Yaniger, *Mol. Cryst. Liq. Cryst.*, **121** (1985) 173.

20. E. M. Genies, A. A. Syed and C. Tsintavis, *Mol. Cryst. Liq. Cryst.*, **121** (1985) 181.

21. E. W. Paul, A. J. Ricco and M. S. Wrington, *J. Phys. Chem.*, **89** (1985) 1441.

22. P. M. McManus, S. C. Yang and R. J. Cushman, *J. Chem. Soc., Chem Commun.*, (1985) 1556.

23. D. McInnes, M. A. Druy, P. J. Nigrey, D. P. Nairns, A. G. McDiarmid and A. J. Hegger, *J. Chem. Soc., Chem. Commun.*, **317** (1981).

24. A. G. Hegger, G. B. Street and G. Tourillon, in *Hand Book of Conducting Polymers* (T. A. Skotheim, ed.), Marcel Dekker, Inc., New York, vol **1** (1986) 46, 51.

25. J. L. Bredas, G. B. Street, *Acc. Chem. Res.*, **18** (1985) 309.

26. M. G. Kanatzldls, *Chemical Engineering News,* Dec. 03 (1990) 38- 42.

27. A. G. Green and A. E. Woodhead, *J. Chem. Soc.*, (1910) 2388; R. de Surville, M. Josefowicz, L. T. Yu, J. Perichon and R. Buvet, *Electrochem. Acta,* **13**, (1968) 1451; F. Cristofini, R. de Surville, M. Josefowicz, L. T. Yu and R. Buvet, *C. R. Acad. Sci. Paris, Ser. C*, **268** (**15**), (1969) 1346; A. F. Diaz and J. A. Logan, *J. Electroanal. Chem. Interfacial Electrochem.*, **111** (1980) 111; R. Noufi and A. J. Nozic, *J. Electrochem. Soc.*, **129**, (1982) 2261.

28. A. J. Epstein, J. M. Ginder, F. Zuo, H.-S. Woo, D. B. Tanner, A. F. Richter, M. Angelopoulos, W. S. Hung and A. G. MacDiarmid, *Synth. Met.*, **21**, (1987) 63.

29. A. G. MacDiarmid, J.-C. Chiang, A. F. Richter, N. L. D. Somasiri and A. J. Epstein, (L. Alcacer, ed.), *Couducting Polymers*, D. Redel Publishing Co., Dordrecht, The Netherlands (1987).

30. A. G. MacDiarmid, J.-C. Chiang, A. F. Richter and A. J. Epstein, *Synth. Met.*, **18** (1987) 285.

31. E. M. Genies and C. Tsintavis and A. A. Syed, *Mol. Cryst. Liq.Cryst.*, **121** (1985) 181.

32. J. P. Travers, J. Chroboczek, F. Devreux, F. Genoud, M. Nechtschein, A. A. Syed, E. M. Genies and Tsintavis, *Mol. Cryst. Liq. Cryst.*, **121** (1985) 195.

33. A. G. MacDiarmid, J. C. Chiang, M. Halpern, W. S. Huang, S. L. Mu, N. L. D. Somasiri, W. Wu and S. I. Yaniger., *Mol.Cryst. Liq. Cryst.*, **121** (1985) 173.

34. A. G. MacDiarmid, N. L. D. Somasiri, W. R. Salaneck, I. Lundstrom, B. Liedberg, M. A. Hasan, R. Erlandsson and P. Konrasson, *Springer Series in Solid State Sciences,* Vol. 63, Springer, Berlin, 1985, p-218.

35. R. L. Hand and R. F. Nelson, *J. Electrochem. Soc.*, **125** (1978) 1059.

36. R. L. Hand and R. F. Nelson, *J. Am. Chem. Soc.*, **96** (1974) 850.

37. *Fr. Patent No. EN* 8307958 (1983); *U.S. Patent No.* 698 183 (1985).

38. L. T. Yu, M. S. Borredon, M. Jozefowicz, G. Belorgey and R. Buvet., *J. Polym. Sci.*, **10** (1987) 2931.

39. D. M. Mohilner, R. N. Adams and W. J. Argersinger, *J. Am. Chem. Soc.*, **84** (1962) 3618.

40. J. Bacon and R. N. Adams, *J. Am. Chem. Soc.*, **90** (1968) 6596.

41. G. Mengoli, M. T. Munari, P. Bianco and M. M. Musiani, *J. Appl. Polym. Sci.*, **26** (1981) 4247.

42. G. Mengoli, M. T. Munari and C. Folonari, *J. Electroanal. Chem.*, **124** (1981) 237.

43. E. M. Genies and C. Tsintavis, unpublished work.

44. E. W. Paul, A. J. Ricco and M. S. Wrighton, *J. Phys. Chem.*, **89** (1981) 1441.

45. B. Pfeiffer, A. Thyssen, M. Wolff and J. W. Schultze, *Int. Workshop – Electrochemistry of Polymer Layers, Dutsburg, F. R. G., Sept.* 15-17, 1986.

46. C. M. Carlin, L. J. Kepley and A. J. Bard, *J. Electrochem. Soc.*, **132** (1985) 353.

47. R. Noufi, A. J. Nozik, J. White and L. F. Warren, *J. Electrochem. Soc.*, **129** (1982) 226.

48. B. Aurian-Blajeni, I. Taniguchi and J. O'M. Bockris, *J. Electroanal. Chem.*, **149** (1983) 291.

49. A. F. Diaz and J. A. Logan, *J. Electroanal. Chem.*, **111** (1980) 111.

50. A. Kitani, J. Yano and K. Sasaki, *Chem. Lett.*, (1984) 1565.

51. A. Thyssen, A. Hochfeld, R. Kessel, A. Meyer and J. W. Schulzte. *Synth., Met.*, **29** (1989) E357; T. A. Borgerding and J. W. Schulzte, *Makromol. Chem., Macromol. Symp.*, **8** (1987) 143.

52. A. Brahma. *Solid State Commun.*, **57** (1986) 673.

53. S. Li. Y. Cao and Z. Xue., *Synth. Met.*, **20** (1987) 141.

54. E. M. Genies, M. Lapkowski, C. Santier and E. Vieil, *Synth. Met.*, **18** (1987) 631.

55. (a) E. P. Lofton, J. W. Thackeray and M. S. Wrighton, *J. Phys. Chem.*, **90** (1986) 6080; (b) S. Chao and M. S. Wrighton, *J. Am. Chem. Soc.*, **109** (1987) 6627.

56. T. Kobayashi, H. Yoneyama and H. Tamura, *J. Electroanal. Chem.*, **161** (1984) 419; **177** (1984) 281, 293.

57. F. Cristofini, R. De Surville, M. Josefowicz, L. T. Yu and R. Buvet, *C. R. Acad. Sci., Ser. C.* **268** (1969) 1346.

58. E. B. Saubestre, Plating, **45** (1958) 927.

59. W. A. Wesley and E. J. Roehl, *Trans. Electrochem. Soc.*, **86** (1944) 419.

60. W. A. Wesley and J. W. Carey, *Trans. Electrochem. Soc.*, **75** (1939) 209.

61. W. L. Pinner and R. B. Kinnaman, *Monthly Rev. Am. Electroplates' Soc.*, **32** (1945) 227.

62. D. J. Macnaughtan, *Rev. Am. Electroplates' Soc.*, **22**(7) (1935) 49.

63. W. Blum and C. Kasper, *Trans. Faraday Soc.*, **31** (1935) 1203 .

64. G. U. Greene, *Trans. Electrochem. Soc.*, **76** (1939) 391.

65. W. M. Philips, Trans. Am. Electrochem. Soc., **58** (1930) 387.

66. A. Brenner, V. Zentner and C. W. Jennings, *Plating.*, **39** (1952) 865.

67. R. E. Harr, *Trans. Electrochem. Soc.*, **64** (1933) 249.

68. L. C. Flower and J. C. Warner, *Trans. Electrochem. Soc.*, **62** (1932) 77.

69. S. A. Watson, *Trans. Inst. Metal Finishing.*, **37** (1960) 28.

70. E. J. Roehl, *Monthly Rev. Am. Electroplates' Soc.*, **34**, (1947) 1129; *Plating* 35, (1948) 452.

71. C. E. Heussner, A. R. Balden and L. M. Morse, *Plating.*, 35 (1984) 554, 719.

72. A. Brenner and C. W. Jennings, Plating, **35** (1948) 1228; *Proc. Am. Electroplaters' Soc.*, **35** (1948) 31.

73. K. G. Soderberg and A. K. Graham, *Proc. Am. Electroplater' Soc.*, **34** (1947) 74.

74. W. M. Phillips and F. L. Clifton, *Proc. Am. Electroplater' Soc.*, **35** (1948) 87.

75. A. Brenner and S. Senderoff, *Proc. Am. Electroplates, Soc.*, **35** (1948) 53.

76. M. R. J. Wyllie, J. Chem. Phys., **16** (1948) 52.

77. A. W. Hothersall, Symposium on Internal Stresses in Metals and Alloys, The Institute of Metals, London, 1948, p.107.

78. D. P. Smith,, Hydrogen in Metals, University of Chicago Press, Chicago, 1948, p-4.

79. T. P. Hoar and D. J. Arrowsmith, *Trans. Inst. Metal Finishing.*, **36** (1958).

80. C. L. Faust and P. D. Miller, US. patent **2** (1948) 440, 715.

81. S. Wernick, *J. Electrodepositos' Tech. Soc.*, **18**, (1943) 103; Sheet Metal Ind., **19** (1944) 613, 979; 20, 1178, 1541, 2095 (1944); **21** (1945) 844; **22** (1945) 1951.

82. H. R. Clauser, *Mater. Methods.*, 24 (1946) 112.

83. R. F. Ledford, *Plating.*, **36** (1949) 560.

84. Electrodeposition Memorandum No. 9, Armament Research Dept., Ministry of Supply, England (1946).

85. M. J. Buerger and L. V. Azraf, the powder method in X-ray crystallography, McGraw. Hill, New York, (1958).

86. B. D. Cullity, Elements of X-ray diffraction, Weseley publishing Inc., Phillipines, (1978).

87. G. H. Jeffery, J. Baggett, J. Mendham and R. C. Denney, Vogel's Text book of Quantitative Chemical Analysis, 5th edition ed. ELBS, England, (1991), P-519.

Chapter 2

EXPERIMENTAL

2.1 Materials and Devices

A. Chemicals

Reagent grade chemicals were used through out this work. The organic monomer aniline was distilled twice prior to its use in polymerization reactions. Ammonium nickel (II) sulphate (Ni-II salt) was recrystallized twice from distilled water. Double distilled water (H_2O) was used as solvent to prepare most of the solutions utilized in this work. The important chemicals and solvents utilized throughout the experiments are listed below:

i)   Aniline [E. Merck, Germany]

ii)   Sulphuric acid (97%) [E. Merck, Germany]

iii) Ammonium nickel (II) sulfate [General Chemical, USA]

iv)   Boric acid [E. Merck, Germany]

v)   Potassium ferrocyanide [Loba Chemical, India]

vi)   Lithium perchlorate [E. Merck, Germany]

vii) Potassium chloride [E. Merck, Germany]

viii) Acetonitrile [E. Merck, Germany]

B. Instruments

Analysis of the samples performed in this work employed the following devices:

i)   Potentiostat / Galvanostat / Coulombmeter [HABF 501, Hokuto Denko, Japan]

ii)   X-Y recorder [F–5C, Riken Denshi Co. Ltd, Japan]

iii) Optical microscope [SWIFTMASTER II, Swift Instruments. Inc. Japan].

iv)   Canon camera [AE-1, Japan]

v)   Infra-red spectrophotometer [IR–470, Shimadzu, Japan]

vi)   Automatic X- ray diffractometer [JDX-8P, JEOL Ltd., Japan]

vii)   Electrometer [6514 System, Keithley, USA]

viii) Magnetic susceptibility balance [MSB MK1, Sherwood Scientific Ltd. England]

ix)   Scanning electron microscope [Philips XL 30, Holland]

x)   Digital balance [FR-200, Japan]

xi)   Controlled heating oven [Gallencame, England]

2. 2 Electrochemical Synthesis

The electrochemical preparation of PANI, PANI/Ni films were carried out at room temperature in a standard three-electrode one-compartment electrolysis cell. A schematic representation of the electrochemical cell employed in this work is illustrated in Fig. 2.2.1. The cell consisted of a 0.5 cm^2 working electrode (WE) made of platinum (Pt), a 1.0 cm^2 Pt foil as counter electrode (CE) and a saturated calomel electrode (SCE) as the reference electrode (RE). Prior to each experiment, the working Pt electrode was carefully polished with fine grained abrasive paper, followed by rinses in distilled water and 5 minutes immersion in concentrated sulphuric acid (H_2SO_4), before it was finally dried on clean laboratory tissues. The reproducibility of experimental results was greatly improved with this pretreatment of the working electrode. The films were grafted onto the working Pt electrode either by sweeping the potential or constant potential mode. Voltammetric sweeps were always started in the anodic direction from 0.0V at 100 mV/s, unless stated otherwise. A Hokuto Denko (HABF 501] electrochemical measurement system provided necessary potential and current control.
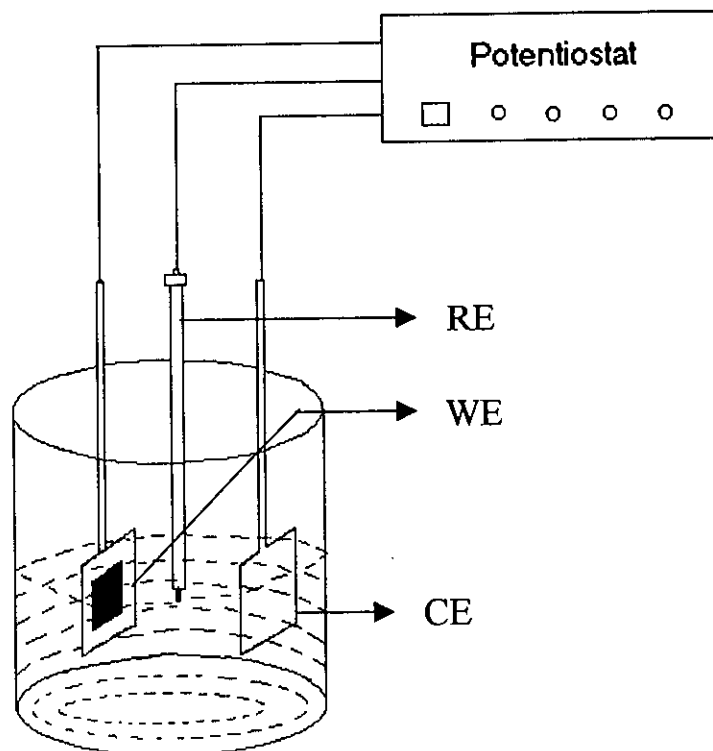
Fig. 2.2.1: Three electrodes system for electrochemical measurements.

A. PANI on Pt : Pt/PANI

The electrochemical preparation of PANI film on the Pt working electrode was carried out by the ordinary anodic polarization method [1-7]. The working Pt electrode was the anode and counter Pt foil was used as the cathode. A 0.8M sulphuric acid (H_2SO_4) in distilled water containing 0.5 M aniline was used as the electrolytic solution. Electrolysis was carried out either by sweeping the potential between $-0.2V$ to $+1.0V$ *vs* SCE or the constant potential mode at $+1.0V$ and passing a fixed amount of charge. After polymerization, the potential of the PANI film coated Pt electrode was held at 0.0V until the cathodic current disappeared to dedoped the PANI film. The film as grown and dedoped was washed three times in distilled water to remove any traces of monomer or any other reactants or by-products that might produced during electrolysis.

B. Ni on Pt : Pt/Ni

Electrochemical deposition of Ni on the Pt electrode was attempted from the following bath composition:

i)   0.1M ammonium nickel (II) salt solution.

ii) 0.1M ammonium nickel (II) sulfate (Ni-II salt), 0.1M boric acid and $10^{-4}M$ sulphuric acid solution.

iii) 0.1M ammonium nickel (II) sulfate (Ni-II salt) and 0.1M boric acid solution.

pH of the three solution were i) 5.45, ii) 5.42 and iii) 5.12 respectively. The deposition of Ni particle on the Pt substrate employed either of potential sweeping or controlled potential method.

In the potential sweeping method, the potential was swept from -1.6V to 0.5V at different scan rate of 50 mV/sec, 100 mV/sec or 200 mV/sec while in constant potential mode, a of potential of $-1.6V$ was used for passing a fixed amount of charge. In the preparation of Pt/Ni electrode, a potentiogalvanostate (Hokuto HABF 501) with function generating ability was used for generation of potential and supply of current. The current-potential response was recorded in a X-Y recorder (F-5C, Riken Denshi). The Ni partical grown onto the Pt electrode was washed several times in distilled water to remove any residual solution or salts.

C. Ni on PANI : PANI/Ni

For this purpose, PANI film was grown first on the Pt substrate. It was prepared on the working Pt electrode at constant potential of 1.0V allowing the passage of 50 mC charge. A 0.8M H_2SO_4 in distilled water containing 0.5M aniline was used as the electrolytic solution for the preparation of PANI films. After polymerization, the potential of the PANI film coated Pt electrode was held at 0.0V until the cathodic current disappeared to dedoped the PANI film. The film as grown and dedoped was washed several times in distilled water to remove any traces of monomer or any other reactants or by-products that might produced during electrolysis. This Pt/PANI matrix was then used for the preparation of Ni-PANI matrix. For Ni disposition, the Pt/PANI matrix was placed in the electrochemical cell containing the electrolytic solutions having bath composition as described in 2.2B. A constant potential of $-1.6V$ was applied and allowed to pass the charge of 50 mC. After the run, PANI/Ni film was carefully washed repeatedly in distilled water to remove any traces of by-products, salts or electrolytic solution.

2.3 Surface Morphology

A. PANI

PANI matrices thus prepared electrochemically following the methods described in section 2.2 were examined for their surface morphology. For this purpose, both optical microscopy and scanning electron microscopy techniques were adopted. In the optical microscopy technique, electrochemically synthesized PANI film was washed in distilled water several times and dried under vacuum. The sample was placed in an optical microscope (SWIFTMASTER II) coupled with a very high precision canon camera. Polarized light was transmitted or reflected and a magnified image of the sample was formed in the plane of image formation of the objective lens. This magnified image was recorded by cannon camera.

Scanning electron microscopic technique was also adapted to analyzed the surface morphology of the dried powder PANI. The samples was dispersed on a conduction carbon glued strip. The sample loaded strip was then mounted to a chamber that evacuated to $\sim 10^{-3}$ to 10^{-4} torr and then a very thin gold layer was supttered on the sample to ensure the conductivity of the sample surface. The system was computer interfaced and thus provides recording of the surface imaging in the computer file for its use as hard copy.

B. Ni on Pt : Pt/Ni

To analyze the surface morphology of Pt/Ni matrix, optical microscopic technique was adapted. For this purpose, Ni deposited Pt electrode was properly washed in distilled water and then dried under

vacuum. The clean Pt/Ni electrode was then placed on optical microscope the magnified image of the sample was recorded as before with a cannon camera. Analysis was carried out at room temperature.

C.   Ni on PANI : PANI/Ni

The surface morphology of PANI/Ni sample was analyzed by both scanning electron microscope and optical microscope. For scanning electron microscopy, the dried PANI/Ni matrix was dispersed on a conducting carbon glued strip, the loaded strip was then mounted to a chamber. The sample was then placed in the main SEM chamber to view its surface. The system was computer interfaced and thus provides recording of the surface images in the computer.

Optical microscopic technique was applied for the analysis of optical microstructure of the PANI/Ni sample. Electrochemically nickel dispersed PANI film was washed repeatedly in distilled water and dried carefully in the vacuum. The film was then placed on optical microscope for its surface analysis. The magnified image of the sample was recoded by canon camera. Optical image of PANI/Ni sample was taken at the different location of the sample surfaces. All of the analysis were carried out at room temperature.

2.4   Spectral Analysis

A.   IR spectra

IR spectra of the dried PANI, PANI/Ni and Ni-II salt samples were recorded on an IR spectrometer in the region of 4000-400 cm^{-1}. IR spectra of the solid samples was obtained by mixing and grinding a small portion of

the materials with dry and pure KBr crystals. Thorough mixing and grinding were done in a motar by a pestler. The powder mixture was then compressed in a metal holder under a pressure of 8–10 tons to make a thin transparent pellet. The pellet was then placed in the path of IR beem for measurements.

B.   XRD pattern

PANI, PANI/Ni and Ni-II salt samples were analyzed for their XRD diffraction pattern in the powder state. The dried samples were thoroughly crushed to powder that employed for XRD diffraction measurements. The powdered samples were pressed in a square aluminium sample holder (40 mm × 40 mm) with a 1 mm deep rectangular hole (20 mm × 15 mm) and pressed against an optically smooth glass plate. The upper surface of the sample was labeled in the plane with the sample holder. The sample holder was then placed in the diffractometer. The XRD pattern was recorded in an automatic X-ray diffractometer using Mo(Zr) radiation having wave length of 1.5 A°. The diffractometer was operated at 30 KV, 20 mA with a scan speed of 2° min^{-1}. The samples that examined for XRD characteristics were processed and operated under ambient atmospheric conditions.

2.5   Electrical Conductivity

Electrochemically synthesized PANI and PANI/Ni samples conductivity were measured in the solid states employing conventional two probe method [8, 9]. For this purpose PANI and PANI/Ni samples were synthesized following the procedure describe in section 2.2. Synthesized samples were pressed with high pressure to form uniform pellets having diameter and thickness of 1.2 and 0.3 cm, respectively. With this state of the

rigid compressed pellet, conductivity measurement was performed. An auto ranging electrometer (Keithley 6514 system, USA) was employed to get the voltage drop between the arbitrary two points on the pellet samples. The distance between two points for the samples were constant for the measurement. Electrical contacts to the points were made by conducting silver paste. The observed resistance for each sample was read directly from the electrometer and allowed to calculate the specific conductance of the PANI and PANI/Ni samples by using the relation (1.4.8) presented in chapter 1. The measurement was conducted under laboratory temperature (~ 25°C) condition. A schematic diagram for the construction for d.c conductivity measurement is shown in Fig. 2.5.1.

2.6 Magnetic Susceptibility

PANI and PANI/Ni matrices thus prepared following the methods described in section 2.2 were examined for their magnetic susceptibility. For this purpose, magnetic susceptibility balance was adopted. The dried PANI and PANI/Ni samples were taken into tube (R) and measured the samples mass in gram and samples length (l) in cm. The balance calibration constant (C_{Bal}) was measured by the formula: $C = \dfrac{C_{Bal}}{10^9}$. The balance was warm-uped about 10 minutes and adjust the zero knob then packed sample tube were placed into tube guide and taken the sample reading (R).

Putting the value of R, l, and C_{Bal} in equation (1.4.9) magnetic susceptibility (χ_g) was calculated. Magnetic susceptibility measurement was performed under ambient atmospheric condition.
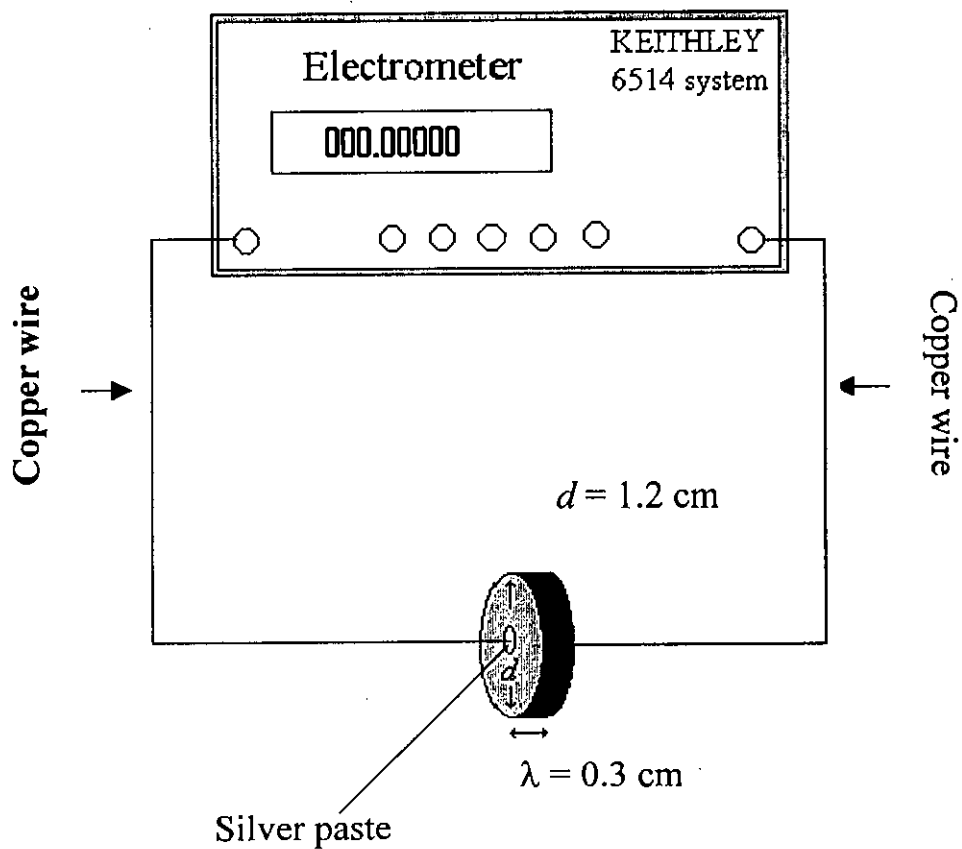
Fig. 2.5.1: Schematic diagram for the measurement of two-point probe d.c conductance of PANI and PANI/Ni.

2.7 Redox Activity

The synthesized matrices were examined for their electroactivity in the electrochemical system. For this purpose, some redox reaction was carried out on the surface of PANI and PANI/Ni film electrodes. The films were grown onto Pt substrate as thin or thick structured as described in section 2.2. In brief, the film were synthesized on the Pt working electrode having an area of 1 cm^2 and passing charge of 0.2 coulomb and 0.5 coulomb for thin and thick films, respectively. The Pt electrodes thus modified with the film were tested both in the aqueous and non-aqueous media for the redox reaction studied. Aqueous solution of 0.1M lithium perchlorate, 0.1M potassium ferrocyanate were employed. Non-aqueous solvent *viz.* acetonitril containing lithium perchlorate was utilized on the other hand.

In order to study their electrochemical redox behaviour, the voltammetric behaviour of the film coated electrodes was followed both in the aqueous and non-aqueous medium. This was done in the electrochemical one compartment cell (Fig. 2.2.1) connected with a potentiostate, galvanostate and a X-Y recorder, the potential was swept between either 0.2V and +0.8V or −2.2V and +0.7V *vs* SCE. Any changes in the peak position and current response was monitored and recorded in the respective voltammograms.

2.8 Electrochemical Stability

The electrochemical stability of the Pt/PANI film and PANI/Ni film electrodes were examined in aqueous 0.1M lithium perchlorate solution. For this purpose, electrochemical synthesis of Pt/PANI and PANI/Ni films were

carried out following the procedure : the working electrode area was 1 cm^2 and counter electrode area 2 cm^2. In order to study their electrochemical stability, the voltammetric behaviour of the film coated electrodes was followed. The rinsed electrodes was placed into 0.1M lithium perchlorate solution in electrochemical cell (Fig. 2.2.1) connected with potentiostat / galvanostate and a X-Y recorder. The potential was swept between –0.2V to +0.8V *vs* SCE and taken cyclic voltammogram at different no. of scan cycles *viz.* 1st, 2nd, 5th, 10th , 10th and 30th. The voltammograms were than compared with that of first scan to address its electrochemical stability.

The other test of stability was attempted by examining the application of high anodic (positive) potentials, such as, +1.0V and +2.0V *vs* SCE and then comparing the voltammograms to detect any changes either in peak position or current response with that obtained with unbiased (i.e, without application of high positive potentials).

References

1. Y. Ohnuki, T. Ohsaka, H. Matsuda and N. Oyama, *J. Electroanal. Chem .*, **158** (1983) 55.

2. N. Oyama, Y. Ohnuki, K. Chiba and T. Ohsaka, *Chem. Lett.*, (1983) 1759.

3. R. Noufi, A. J. Nozik, J. White and L. F. Warren, *J. Electrochem. Soc.*, **129** (1982) 2261.

4. A. Volkov, G. Tourillon, P. C. Lacaze and J. E. Dubois, *J. Electroanal. Chem.*, **115** (1980) 279.

5. A. F. Diaz and J. A. Logan, *J. Electroanal. Chem.*, **111** (1980) 111.

6. A. Kitani, J. Izumi, J. Yano, Y. Hiromoto and K. Sasaki, *Bull. Chem. Soc. Jpn.*, **57** (1984) 2254.

7. A. G. MacDiarmid, J.-C. Chiang, M. Halpern, W-S. Huang, S-L. Mu, N. L. D. Somasiri, W. Wu and S. I. Yaniger, *Mol. Cryst. Liq. Cryst.*, **121** (1985) 173.

8. I. J. van der Pauw, *Philips Res. Repts.*, **13** (1958) 1.

9. J. Lange, *J. Appl. Phys.*, **35** (1964) 2659.

Chapter 3

RESULTS AND DISSCUSSION

3.1 Electrochemical Synthesis

A. Preparation of PANI

Cyclic voltammetry is a useful method to investigate the process of electrochemical polymerization. The anodic oxidation of aniline is generally affected on an inert material which is generally Pt [1-7]. Typical cyclic voltammogram (CV) for electrochemical polymerization of aniline is presented in Fig. 3.1.1. On sweeping the potential, as in the first scan, from − 0.2 to +1.0V vs SCE, a sharp rise in current is seen at a potential ca. +0.8 V indicating the oxidation of aniline to yield PANI [8, 9]. A thin deep blue film is seen to be adhere on the Pt surface. As the sweeping repeated, i.e, in the second and subsequent cycles, the peak current increases further indicating the formation of more deposits of PANI on the substrate. Potential cycling was repeated upto 6 cycles for the deposition of a thin film of PANI. The anodic peak at ca. +0.18 V is seen to be observed from the second scan. This peak can be assigned to the oxidation of PANI film deposited on the electrode corresponding to the conversion of amine units to radical cations in the polymer chain [10, 11]. The deep blue color of the film turned to greenish-yellow when potential sweeping approached to the cathodic direction at ca. +0.0 V or lower.

Figure 3.1.2 shows the CV of PANI film thus synthesized on the Pt substrate in an aqueous solution containing 0.8M H_2SO_4. The CV involved sweeping the potential between −0.2 to +0.5V vs SCE at a scan rate of 100 mVs^{-1}. The result clearly shows that PANI can be switched between their oxidized (conductive) and reduced (insulator) state. It can be seen from the figure that the CV of the present system is composed of two redox couples.
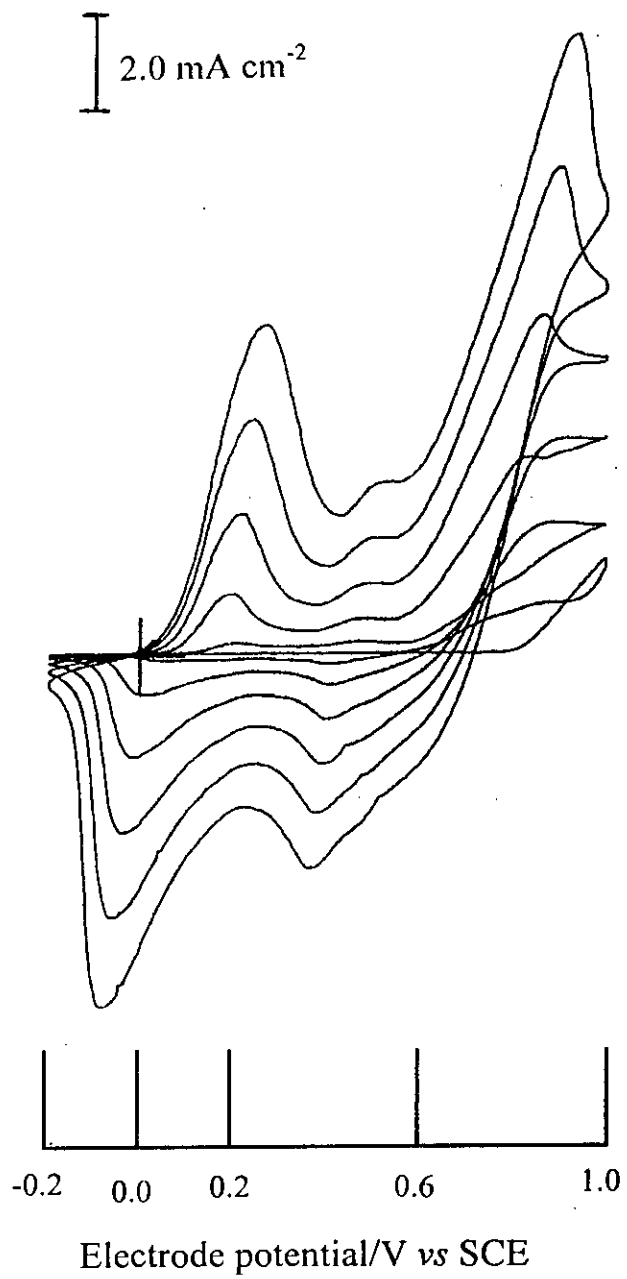
2.0 mA cm^{-2}

-0.2   0.0   0.2   0.6   1.0

Electrode potential/V *vs* SCE

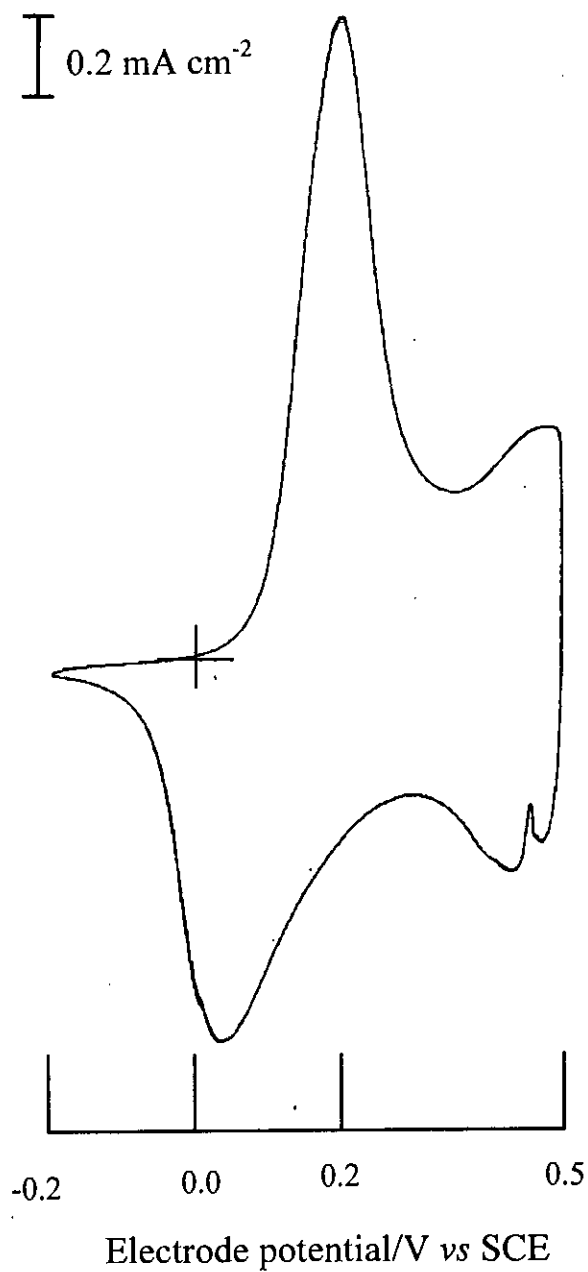Fig. 3.1.1: CV during electrochemical synthesis of PANI.

71

Fig 3.1.2: CV for the doping-dedoping of PANI in 0.8 M H_2SO_4.

This behaviour indicates the presence of variable electroactive region in the polymer film. From the result of CV, it may be assume that the oxidation of the PANI film takes place at the potentials 0.15V while the corresponding reduction of the film take place at 0.03V *vs* SCE. Similar results has also been reported by several authors [12-19].

During electrochemical oxidation (doping), the anions in the solution become incorporate into the polymer to compensate the positive charge in the chain while in the reduction (dedoping) processes the incorporated anions get removed out of the polymer film [20-22]. In case of PANI, most of the authors proposed that the redox processes appeared in its CV are associated to the protonation as well as to the insertion of anion in the film [16, 18, 19, 23-26]. However, Shacklette *et. al.* [27] proposed that the first set of volumetric peaks correspond to the formation of the radical cation (polaron) and the second set of peaks corresponds to the dication (bipolaron).

Switching from doped to dedoped states was accompanied by concomitant colour change of the polymer. In the present system, doping and dedoping of the SO_4^{-2} anion caused a colour change of the PANI film. A deep green colour was seen in the doped state of PANI while a greenish yellow colour was observed in its dedoped state. Diaz [15] was the first to show that PANI changes colour, giving from yellow to green depending on the potential applied. Kobayashi [28] has reported that the colour change from yellow through green, blue and finally black generally results following the redox reaction which occur between −0.2 and 1.0V *vs* SCE. However, in the present case, the dedoped PANI film was not purely yellow

rather it was greenish yellow. It may be that under the experimental conditions employed in this work PANI was not dedoped fully.

B. Ni deposition on Pt

Ni was deposited electrochemically on the Pt substrate from the following aqueous electrolytic solutions having bath compositions of (i) 0.1M Ni-II salt, (ii) 0.1M Ni-II salt + 0.1M boric acid and (iii) 0.1M Ni-II salt + 0.1M boric acid + 10^{-4}M H_2SO_4. The corresponding CV during the deposition of Ni are shown in Figs. 3.1.3, 3.1.4 and 3.1.5, respectively. In all the cases, potential was sweepted between +0.5 and −1.6V vs SCE. The result shows an abrupt rise in the cathodic current when potential reach at − 1.0 or more. In the reverse scan, a small but prominent peak is observed at ~ −0.3V. At potential −1.2 and more, a shiny gray particles were found to be deposit on the Pt electrode. This gray deposit seems to be metallic Ni which may produced by the electrochemical reduction of Ni^{+2} from its electrolytic solution. Similar result was observed with all the electrolytic media employed for Ni deposition in the work. Thus, the present result clearly indicates that all the three electrolytic media used in the present work can potentially be used for the deposition of Ni by the electrochemical means adopted.

Attempt was made to check the dissolution of the Ni thus deposited on the Pt electrode. This was done by sweeping the potential between −0.5 and 0.0V in the same electrolytic solution from which Ni was originally deposited. Figure 3.1.6 shows the typical CV for the dissolution process of Ni. Sweeping started from −0.5V. As soon as the sweeping proceeds towards
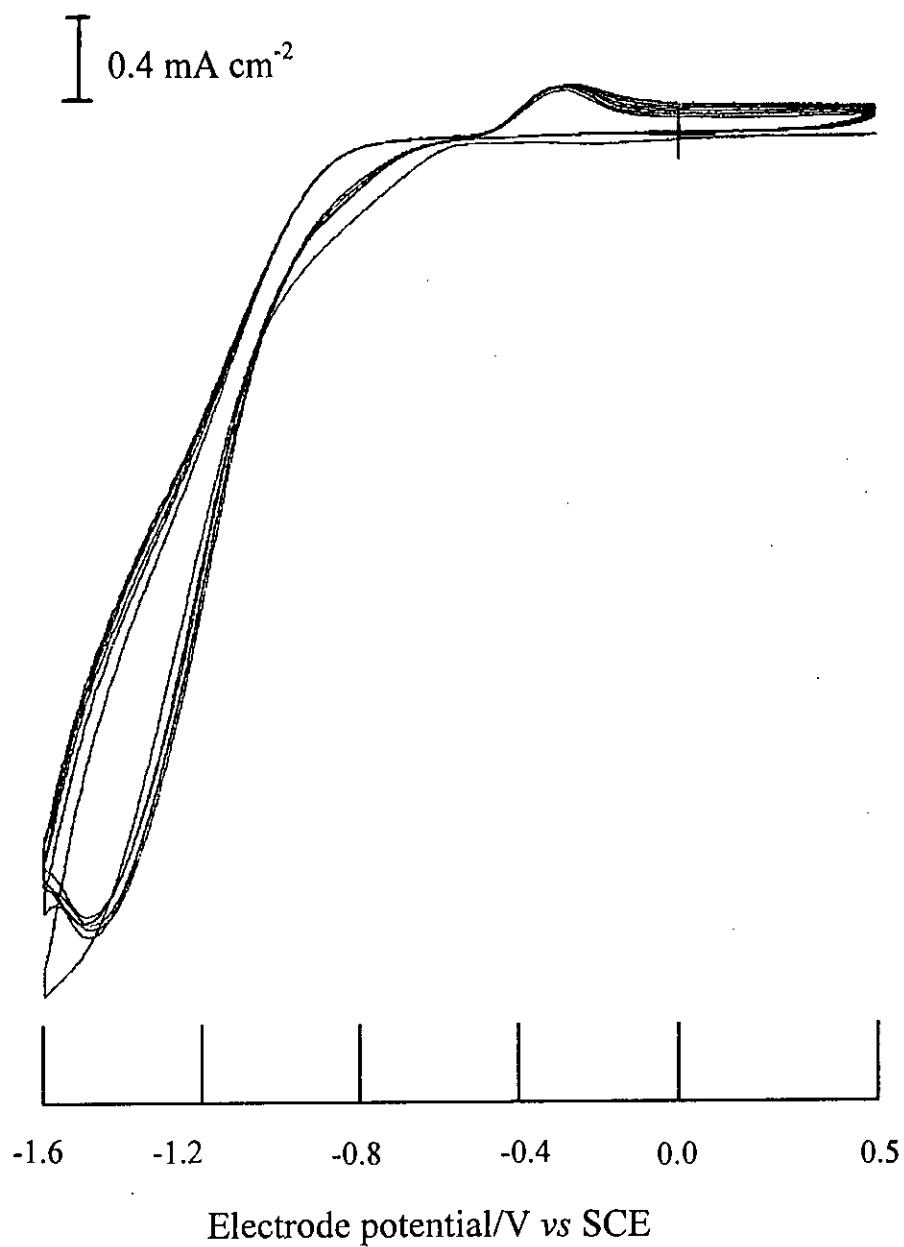
74

0.4 mA cm^{-2}

Electrode potential/V *vs* SCE

-1.6 -1.2 -0.8 -0.4 0.0 0.5

Fig. 3.1.3: CV during electrochemical Ni-deposition on Pt from
0.1M Ni-II Salt solution.

0.4 mA cm^{-2}
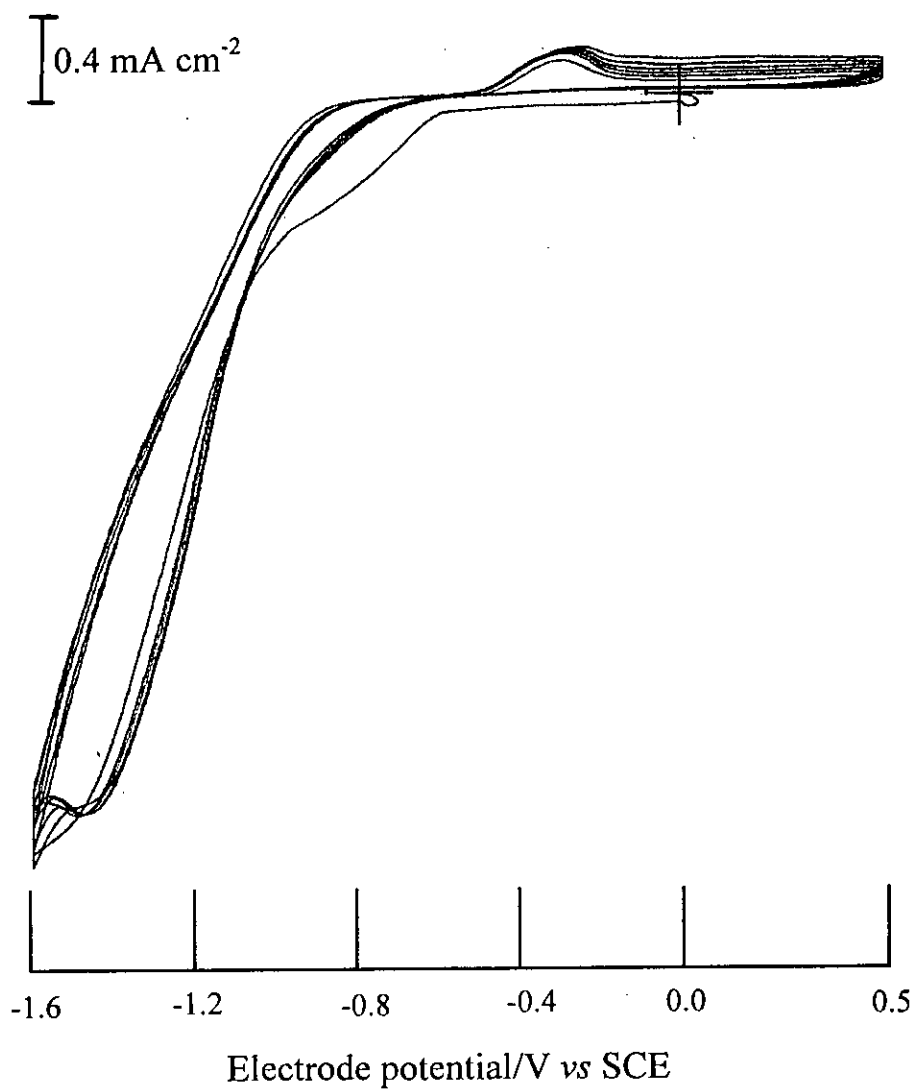
Electrode potential/V *vs* SCE

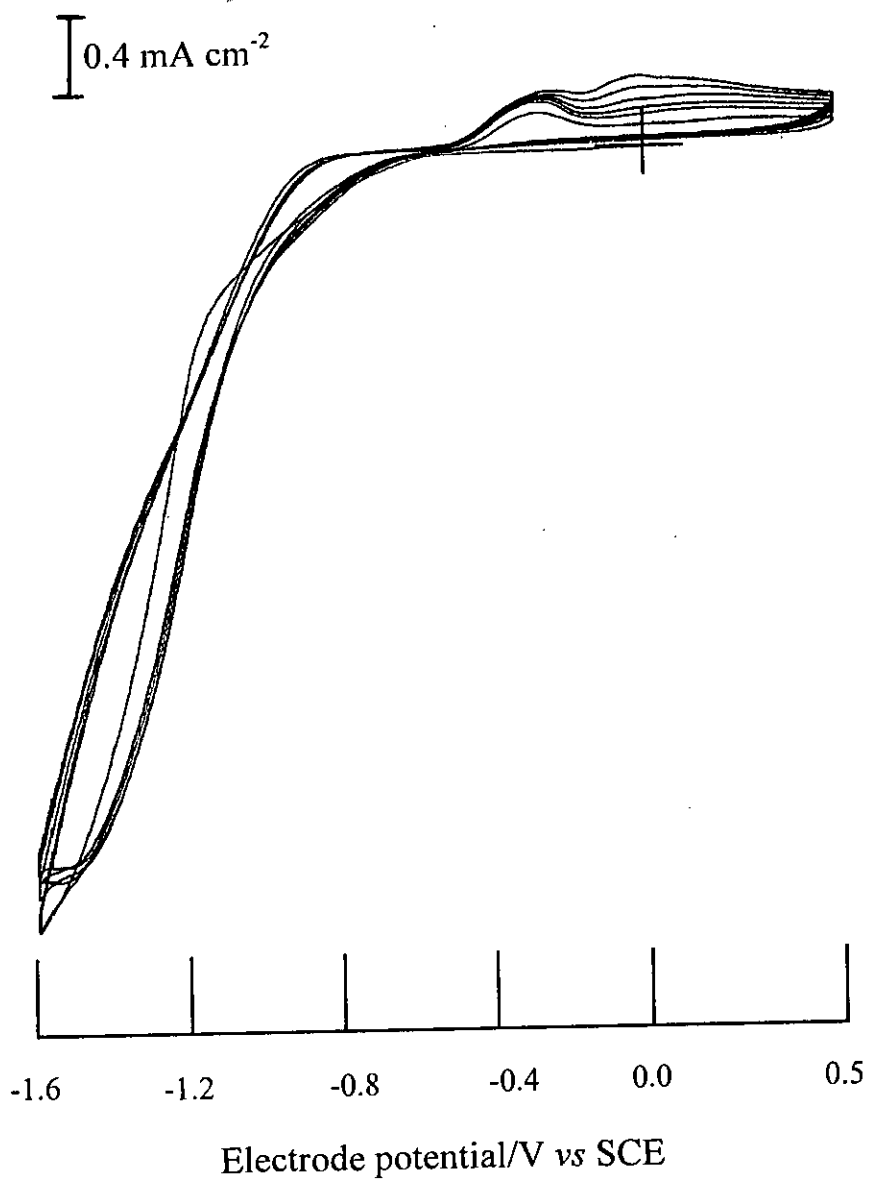Fig. 3.1.4: CV during electrochemical Ni-deposition on Pt from 0.1M
Ni-II Salt + 0.1 M boric acid solution.

Fig. 3.1.5: CV during Ni-deposition on Pt from 0.1M Ni-II salt + 0.1M boric acid + 1×10^{-4} M H_2SO_4 solution.
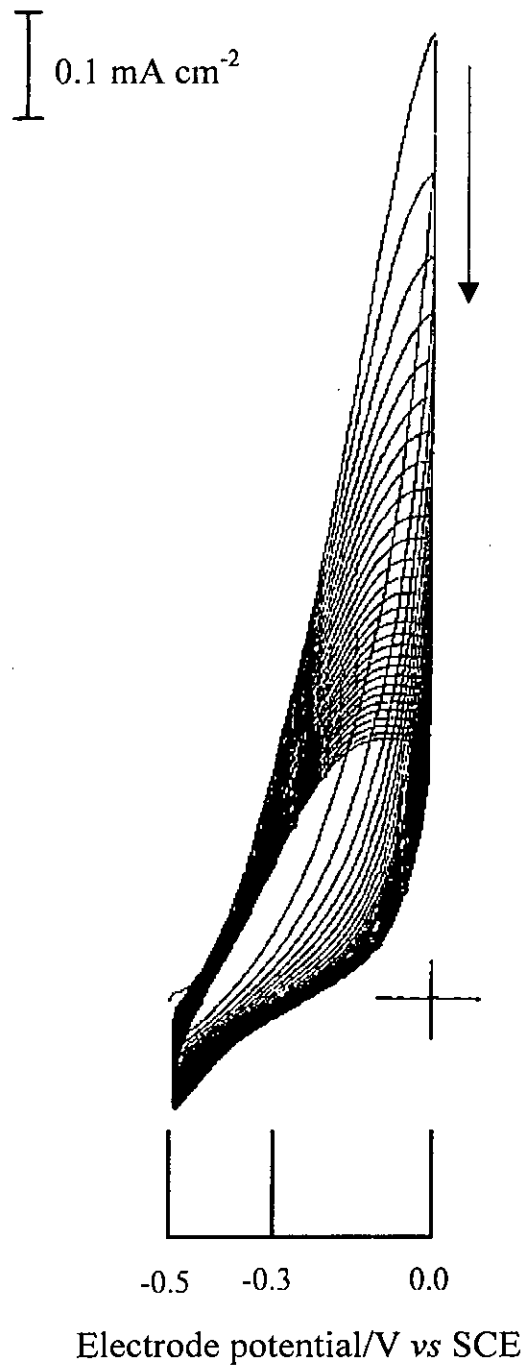
0.1 mA cm^{-2}

-0.5   -0.3   0.0

Electrode potential/V *vs* SCE

Fig. 3.1.6: CV for the dissolution of Ni from Pt.

0.0V, the peak current at −0.3V is observed. In the repeated scan, the peak current around −0.3V decreases. This indicates that the dissolution of Ni depositions was taking place with the repeated scan. This is because, sweeping is restricted between −0.5 and 0.0V, i.e., only dissolution potential of Ni is allowed; in this potential window, deposition of Ni can not take place. Deposition is seem to be occurred at more negative potential than − 1.2V as observed in the CV's presented in Figs. 3.1.3- 3.1.5.

C.   Ni dispersed on PANI

Attempt was made to disperse Ni onto the PANI matrix. For this purpose a thin PANI film was electrochemically coated onto a Pt substrate. The PANI film was grown by scanning the potential three times between −0.2 and +1.0V from an aqueous electrolytic solution containing 0.5M aniline + 0.8M H_2SO_4 at a seen rate of 100 mV^{-1}. The washed PANI film was then placed in an another electrolytic bath containing 0.1M Ni-II solution and performed scanning the potential between +0.5V and −1.6V. Typical CV for the dispersion of Ni in the PANI film is shown in Fig. 3.1.7. The CV consists of several peaks, *viz.* at about 0.18 and 0.0V. These peaks may correspond to the oxidation and reduction of PANI as discussed in section 3.1A. In addition, two more peaks, at about −1.6 and −0.3V can also be seen in the CV. The sharp rise in current at −1.6V may associated with the reduction of Ni^{+2} to Ni metal that might incorporated into the PANI matrix while the peak at −0.3V may corresponds its dissolution. Indeed, energy dispersed X-ray analysis of the synthesized PANI/Ni matrix shows a Ni content of 4.26%.

0.4 mA cm^{-2}

Electrode potential/V *vs* SCE
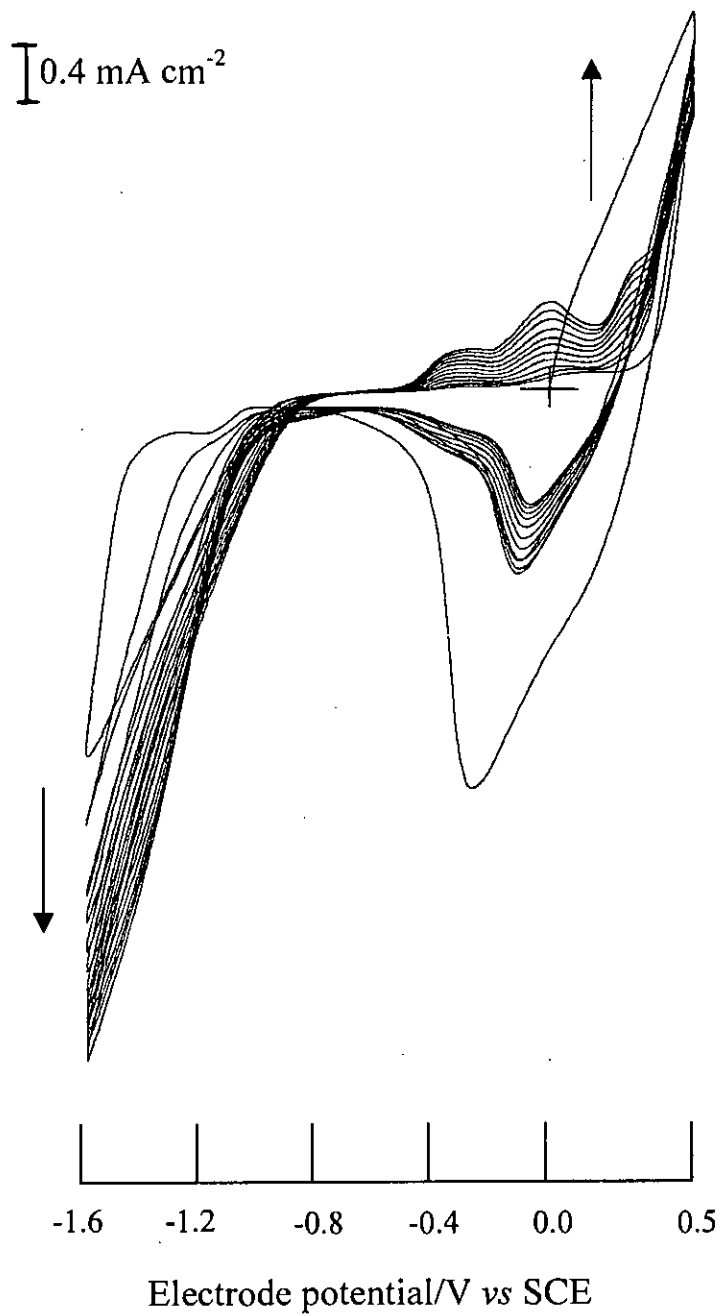
-1.6   -1.2   -0.8   -0.4   0.0   0.5

Fig. 3.1.7: CV during Ni-deposition on PANI film.

Incorporation of the metallic Ni particles into the PANI film was further investigated by following its electrochemical dissolution. Typical CV for the dissolution of Ni from the PANI matrix is depicted in Fig. 3.1.8. The potential scan was restricted between −0.5V and 0.3V and thus during this scanning, no deposition of Ni was possible. The peak current having shoulder started from −0.3V gradually decreases as the scanning repeated. In other words, dissolution progresses as the scanning repeated. This observation may indicate that Ni particles were previously deposited in the PANI matrix and that are gradually oxidized back to Ni^{+2} in the electrolytic media.

D.   Charge-discharge characteristics

Incorporation of Ni into the polymer film was controlled by passing a fixed amount of charge (Q) at a constant potential. Again, in the dissolution process of Ni that was incorporated into the polymer film, the charge was discharged at a fixed potential. The injection and removal of the charge (thus termed was charge-discharge) to and from the polymer were studied in the present work. Charge *vs* time (Q-t) plot for the incorporation of Ni into the PANI film is shown in Fig. 3.1.9. The PANI film that utilized in this experiment was prepared on a Pt electrode (3.0×2.0 cm^2) by passing 50 mC of charge at a constant potential of +1.0V. The polymer film thus prepared was then placed in a cell containing 0.1M Ni-II solution. Ni was deposited on it by passing charge at −1.6V. This was recorded with time as shown in Fig. 3.1.9. The result shows that injection of charge for the initial periods seems to be very rapid. Then it slows down compared to the initial periods. The dissimilar nature of the charge passed with time may arises due to other
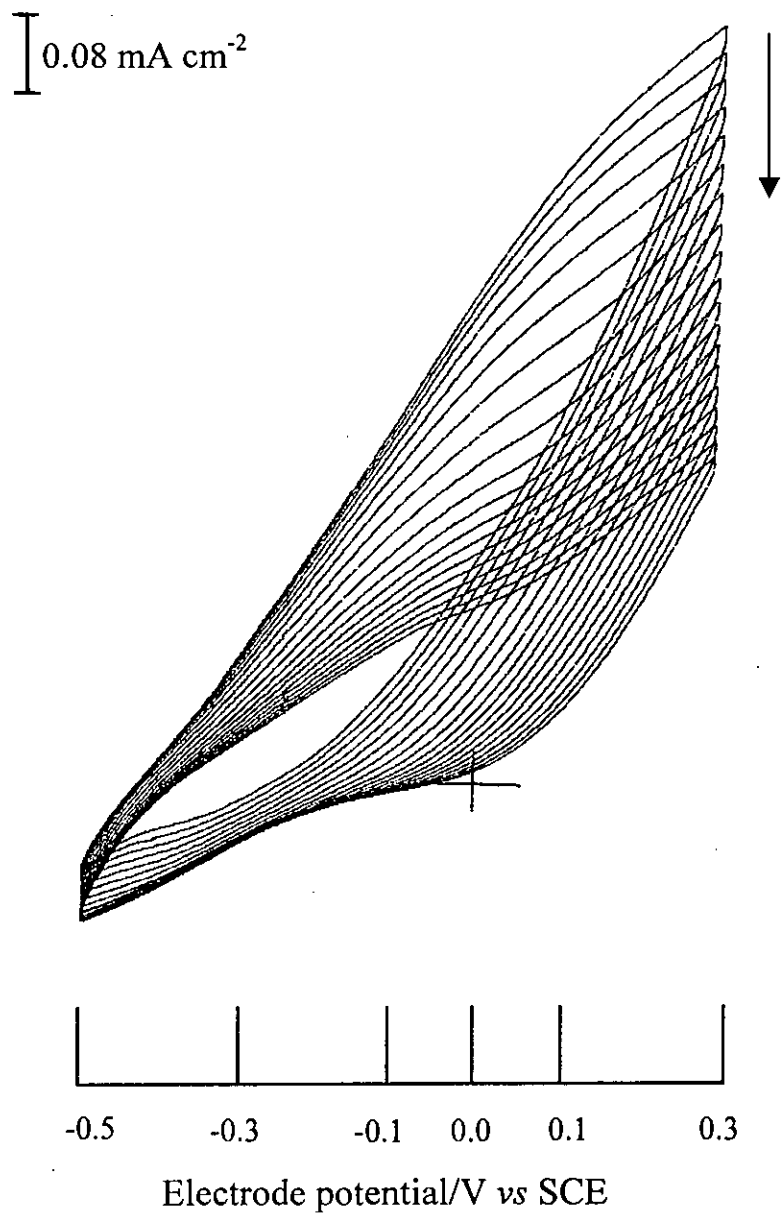
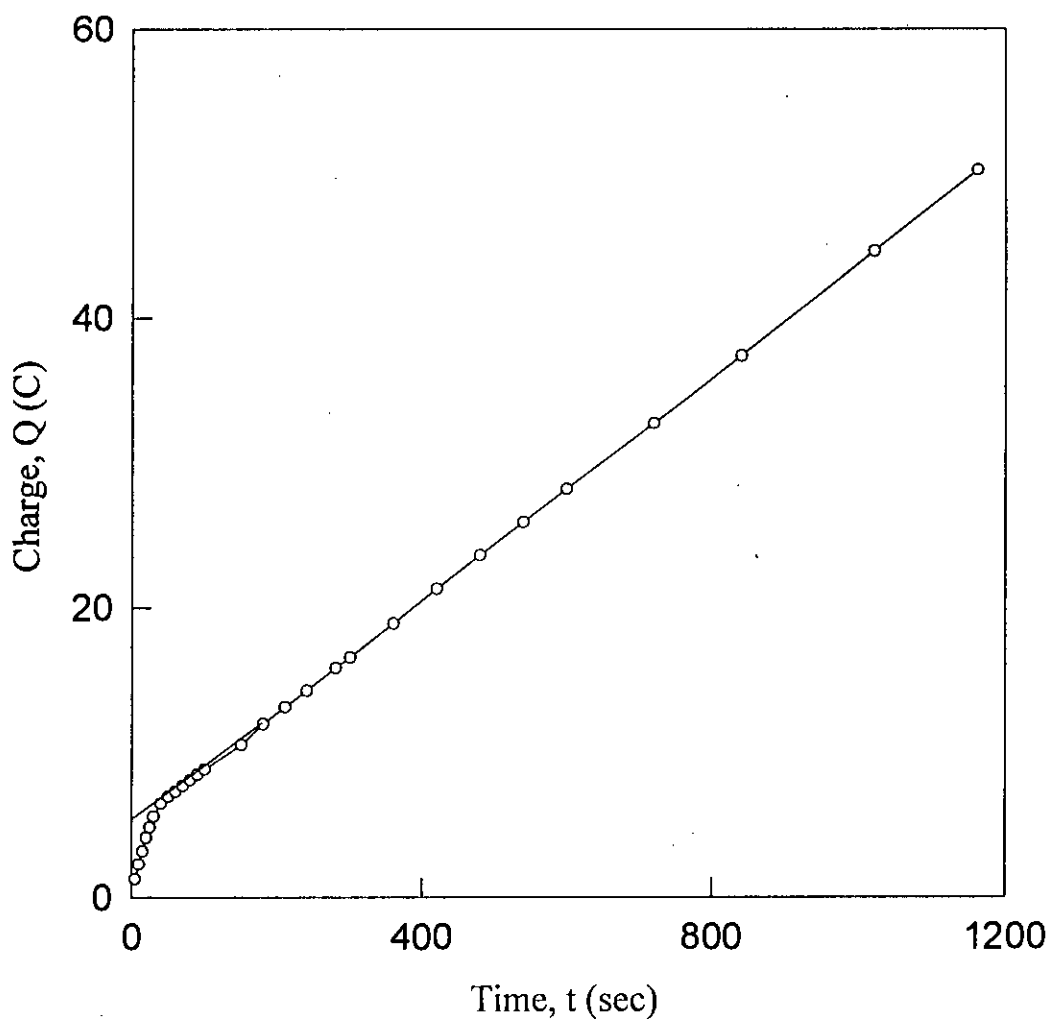Fig. 3.1.8: CV for the disolution of Ni from PANI film.

Fig. 3.1.9: Charge, Q *vs* time, t plot of Ni-deposition onto PANI matrix.
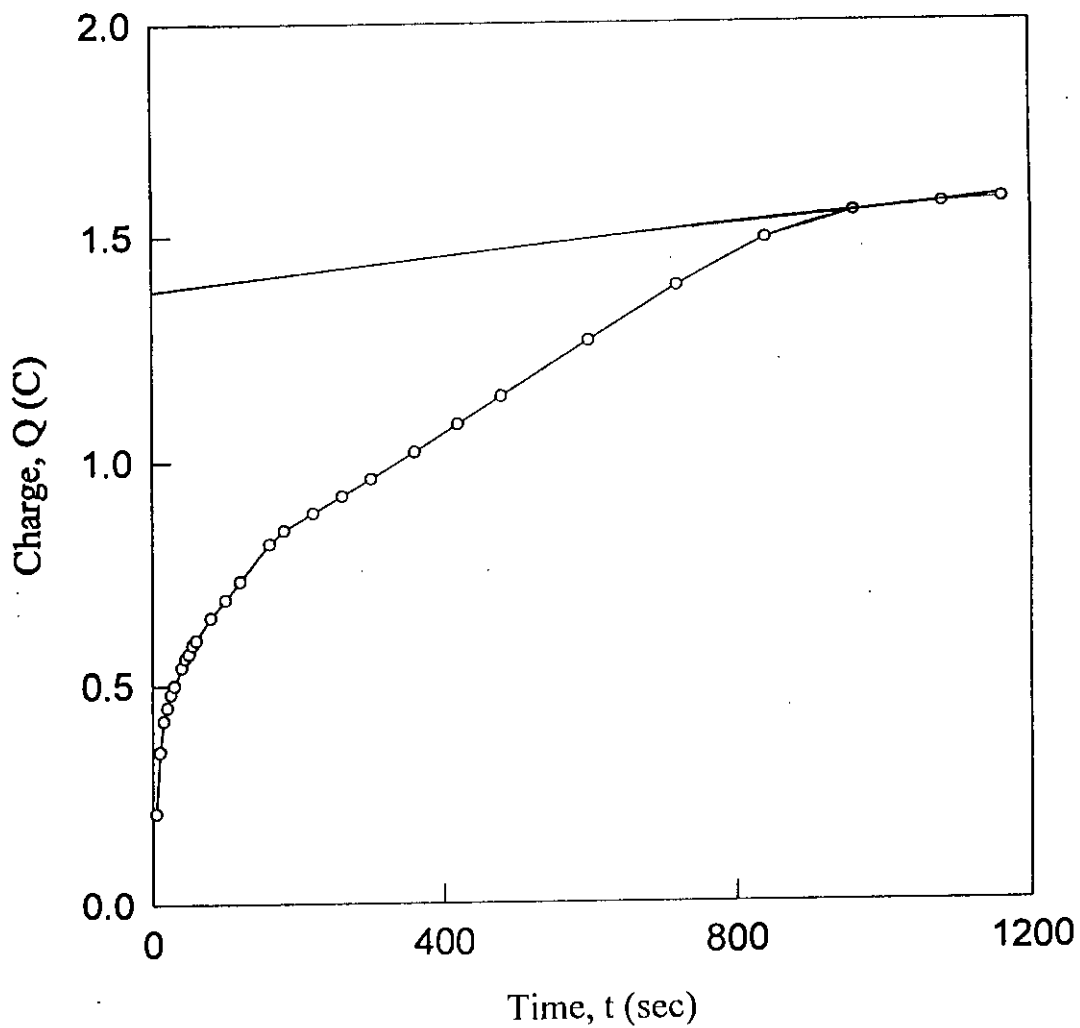
Fig. 3.1.10 Charge, Q *vs* time,t plot of Ni-dissolution from PANI/Ni matrix.

processes that might took place along with Ni deposition in course of the time of the experiment. However, to get the actual charge consumed for Ni deposition it is wise to find the intersection of the two process by drawing two straight lines and extrapolate one to the Y-axis to drive the actual charge for Ni deposition. For the present case, although 50 mC charge was passed, only about 4 mC charge (obtained by extrapolation in the Fig. 3.1.9) seems to be used for Ni deposition. The dissolution of this Ni that deposited in the PANI was then again examined by Q-t plot as given in Fig. 3.1.10. It is expected that the charge consumed for Ni dissolution i.e. 4 mC (as obtained by the extrapolation of the curve in Fig. 3.1.9) should be discharged in the dissolution process. This was checked by extrapolating the Fig. 3.1.10 and obtained a charge of about 1.35 mC that removed during dissolution process. The discharge charge is lower than it was predicted as of 4 mC. This discrepancy may happen due to the insufficient time allowed for the dissolution process. However, Q-t process employed in this work may give a more or less precise value of injected charge that consume for the deposition of Ni in a electrode matrix. Similar Q-t plot was utilized by Chowdhury *et. al* [29] for the determination of doping level of conducting polymers.

3.2   Characterization of Electrode Matrices

A.   Optical microstructure

Ni deposit on Pt and PANI surfaces was characterized by optical microscopy. Figure 3.2.1 shows the optical microstructures of Ni deposits on Pt under various electrochemical bath and sweeping conditions. The microstructures as displayed in the row 1, 2 and 3 are the Ni particles
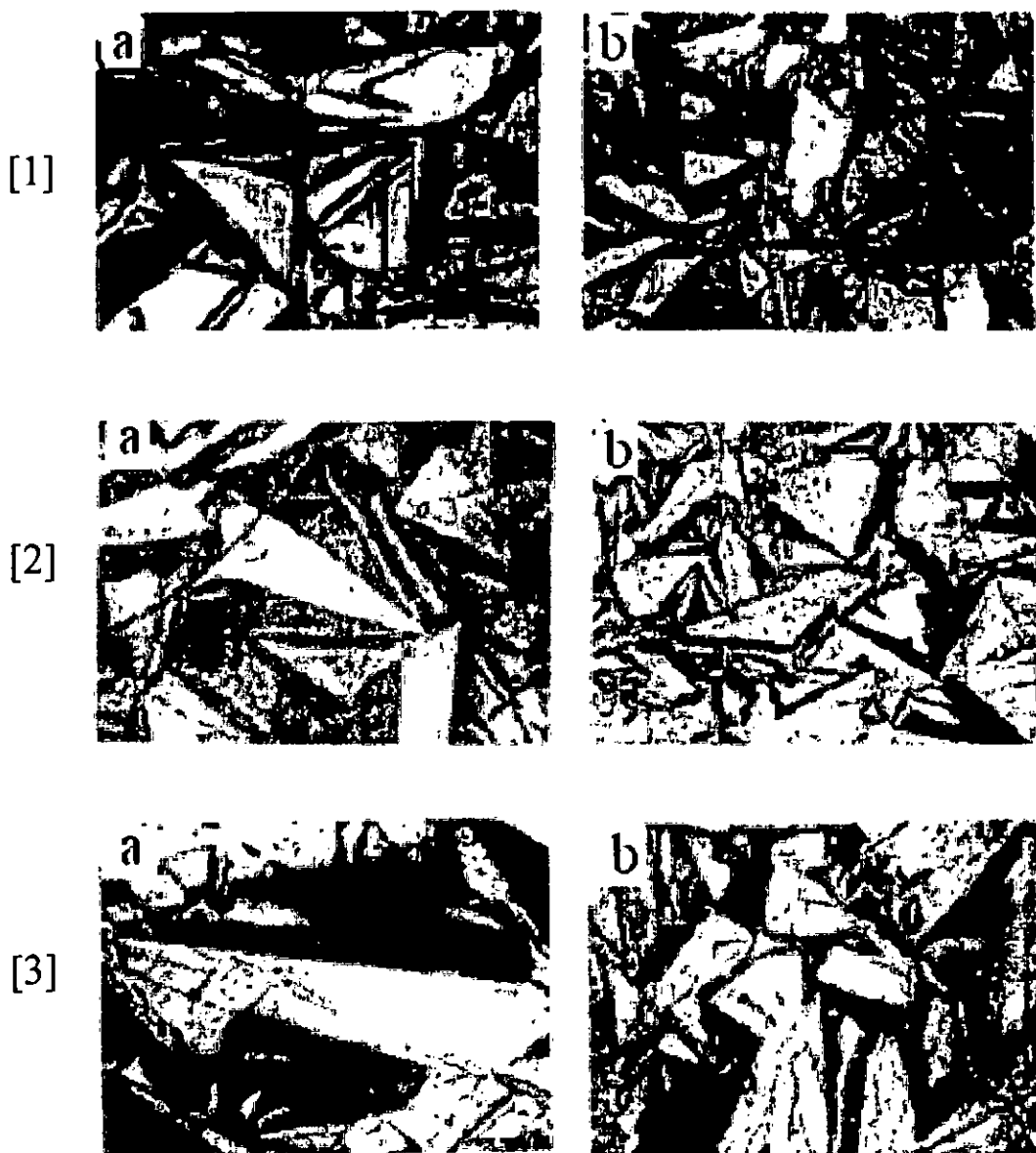
Fig. 3.2.1: Optical microstructures of Ni-deposits from [1] Ni-II salt,
[2] Ni-II salt + boric acid and [3] Ni-II salt + boric acid +
H_2SO_4 solution.
Scan speed (a) 50 mV /sec and (b) 200 mV/sec.

deposited from the electrolytic bath composition of (i) 0.1M Ni-II salt, (ii) 0.1M Ni-II salt + 0.1M boric acid and (iii) 0.1M Ni-II salt + 0.1M boric acid + 10^{-4}M H_2SO_4 solutions, respectively. On the other hand, columns "a" and "b" show the microstructures of Ni deposits from the above mentioned electrolytic baths at a sweeping rate of 50 and 200 mV/sec, respectively. In depositing the Ni particles, potential was sweept ten times between −1.6 and 0.5V *vs* SCE. From the microstructures, it appears that a good amount of Ni can be deposited on the Pt substrate under the conditions employed here. The Ni particles are distributed randomly on the surface in all the cases studied. However, the micrographs clearly shows that the bath condition and scan speed both effects the particle size of Ni deposit. The size of the particle follows the order 1a < 2a < 3a ; i.e. the bath consists of 0.1M Ni-II salt gives the smaller particles of Ni. Again the microstructures labeled "b" <"a", i.e., a scan speed of 200 mV/sec^{-1} gives smaller particles than that of 50 mV/sec^{-1}. This means that higher scan speed favors smaller deposition of Ni. This result seems highly interesting in the sense that a control of particle size of the Ni can be achieved by controlling bath condition and scan speed. Previous works [30] have also reported influence of varying deposition conditions and electrolyte composition on the growth of electroplated metals and allows.

Microstructure of Ni dispersed on PANI matrix was also analyzed by the optical microscopy. Figure 3.2.2 shows the optical microstructure of (a) PANI film and (b) PANI/Ni film. The PANI films was prepared by sweeping the potential ten times −between 0.2 and +1.0V from the electrolytic solution described earlier. The similar PANI film was also adopted for Ni deposition that done at constant potential of −1.6V by passing
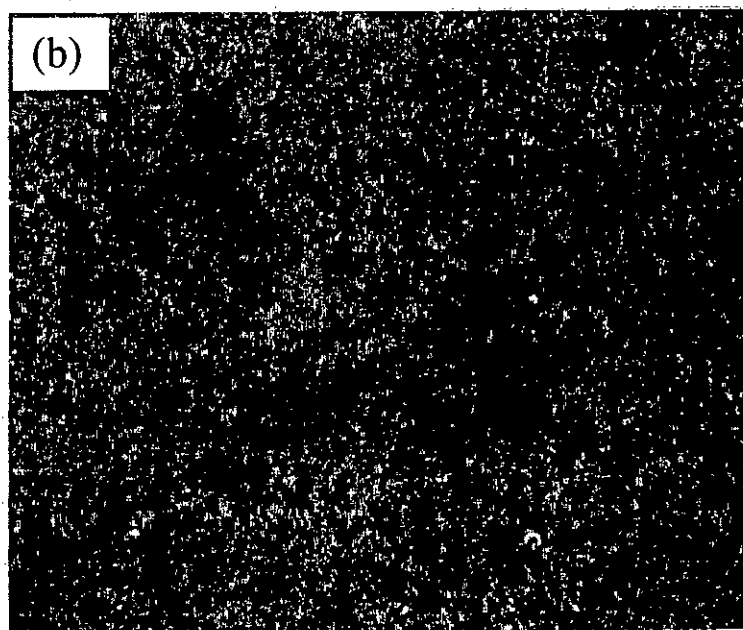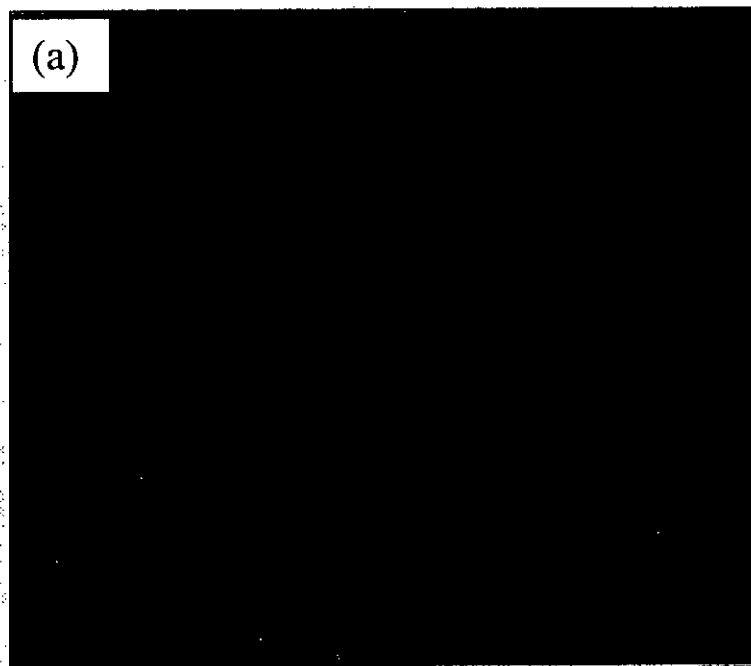
87

Fig. 3.2.2: Optical microstructures of (a) PANI and (b) PANI/Ni.

50 mC of charges. The microstructure of PANI seems to be uniform and continuous and formed a pack structure on the surface. On the other hand, a wide variety of white images is found to be dispersed on the surface of the PANI/Ni matrix. The white image may reflect the Ni particles that could have deposited by the electrochemical treatment of the PANI film made at −1.6V in the Ni-II electrolytic solution.

B.   Scanning electron microscopy

To get more clear insight about the surface morphology, scanning electron microscopic (SEM) analysis was attempted. SEM is known to the best choice because of its potential in precise analysis of a solid surface. Chemical composition and morphological structure of a material strongly depends on the mode of synthesis condition such as pH, concentration of reactants and products, electrochemical parameters. Thus, there is a variety of morphology of a material could be possible. In the present work, PANI was synthesis electrochemically by sweeping ten times the potential between −0.2 and +1.0V at a scan rate of 100 mV/sec^{-1}. The film thus formed on the Pt electrode was washed thoroughly with distilled water and then dried under vacuum. The PANI becomes powdered in its dry state. The powdered mass was taken for its SEM analysis. Similarly, identical PANI film was first synthesized and then dispersion of Ni in it was performed. Ni was incorporated by passing 50 mC of charge at −1.6V. The film thus cathodically treated was washed and dried as earlier. The SEM images of (a) PANI (b) PANI/Ni are presented in Fig. 3.2.3. It can be seen that grain-like morphology is appeared for PANI. Its surface is uniform and covered with the PANI grain. The present observation is in good agreement with a previous work reported earlier [31]. On the other hand, the surface
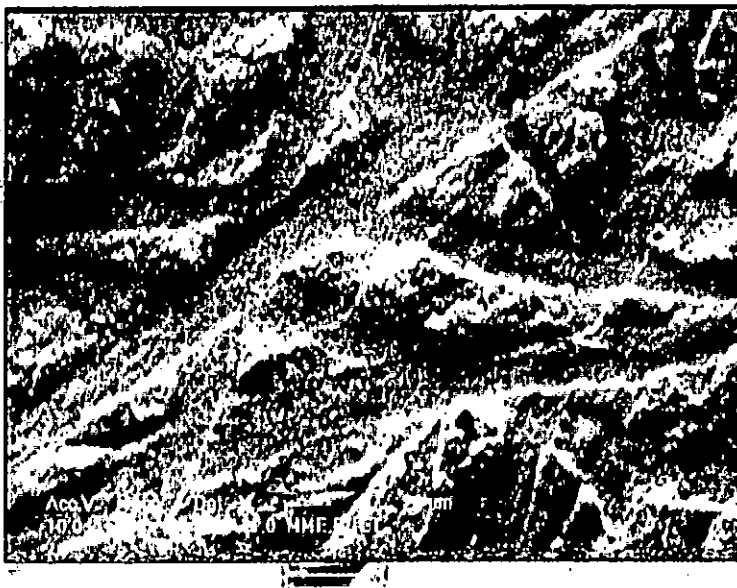
[a]
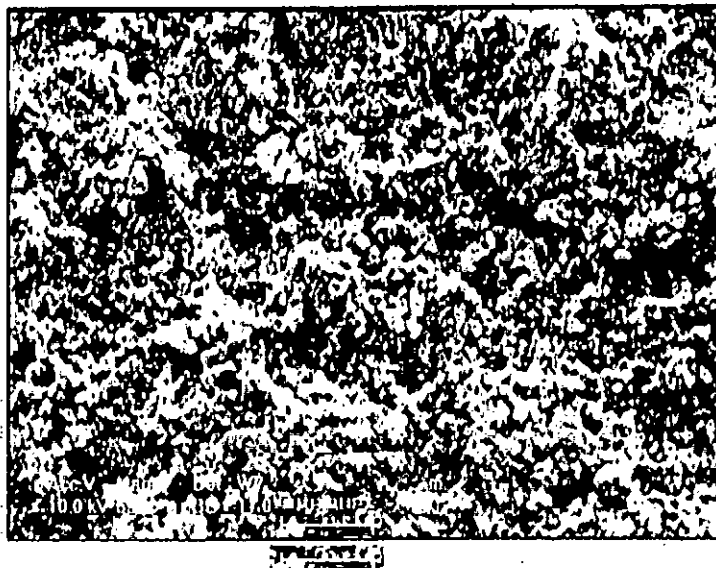
[b]

Fig. 3.2.3: SEM micrographs of (a) PANI and (b) PANI/Ni.

morphology of PANI is drastically changed when Ni was dispersed in its surface. Small islands seems to developed in the morphology. The islands are distributed randomly in the surface. The island as well as the whole surface seems to be covered with soft grainy particles. The islands appear to have definite shape and sharp edges. Similar geometric shape was also observed in the optical microstructures of Ni when deposited on Pt (Fig.3.2.1).

C. IR spectral analysis

IR spectral studies provide some useful, albeit qulitative information on the identification of compounds. Particularly organic substances absorb IR ligh and thus IR active. Since we are not solely depends on IR spectra for identification, a detail analysis of the spectrum will not be required. In order to get some insight about the structure of the synthesized matrices, IR spectra analysis were performed. IR spectra of PANI and PANI/Ni are presented in Fig. 3.2.4. and 3.2.5 while for the control sample Ni-II salt is shown in Fig. 3.2.6. The tentative assignment of the IR spectrum of PANI is listed in Table -1.
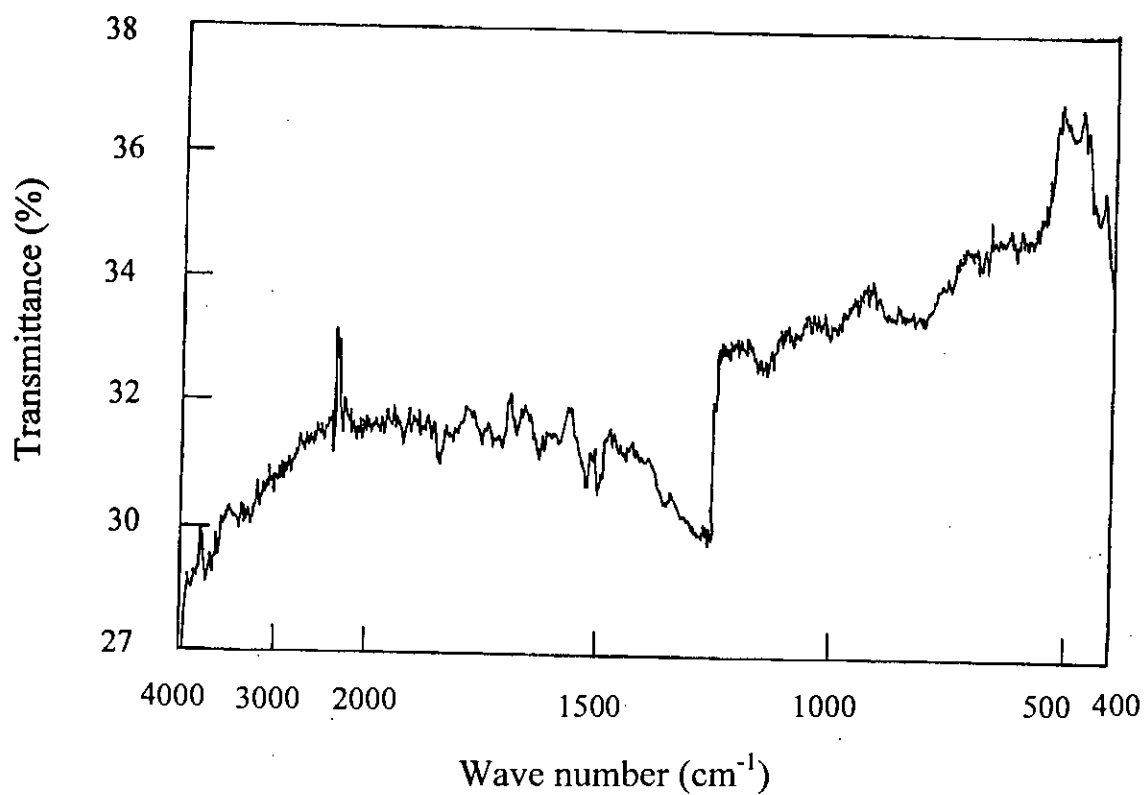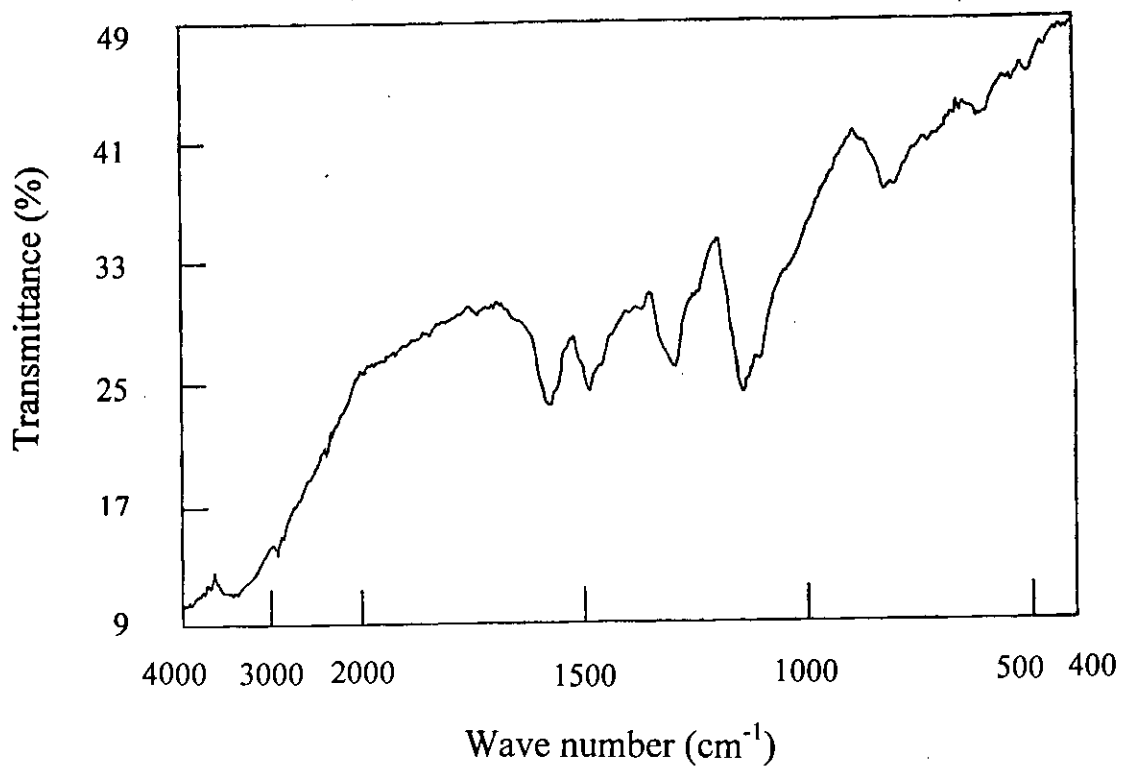
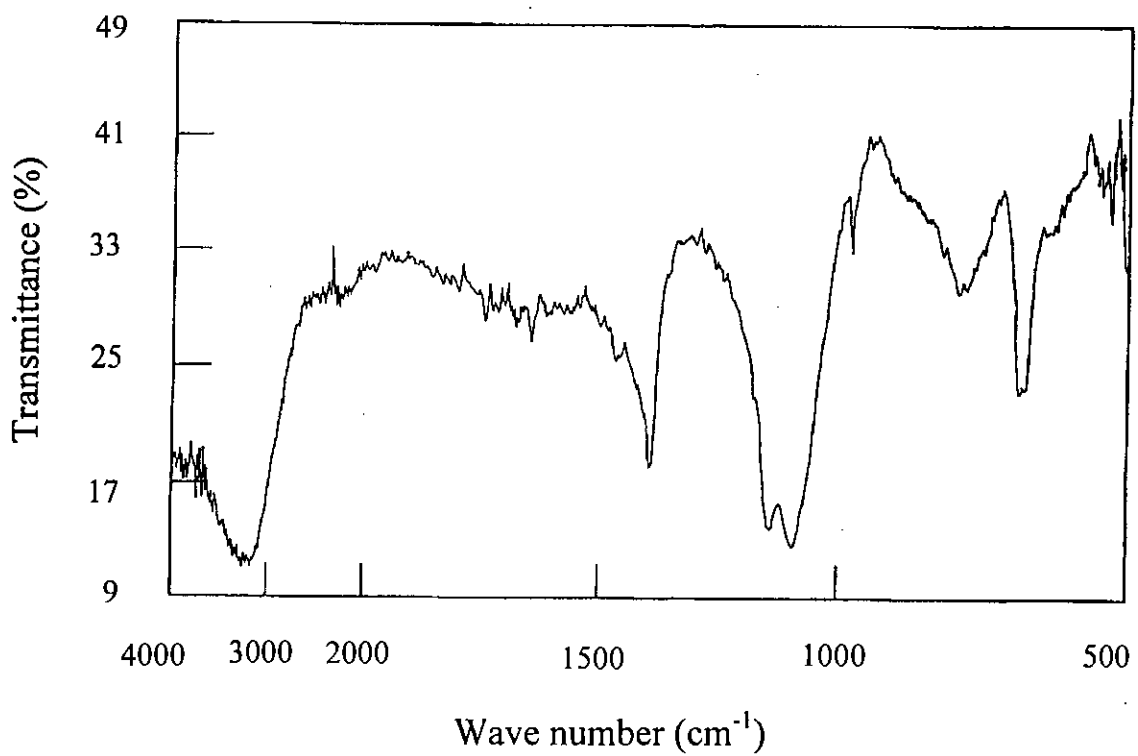Fig. 3.2.4: IR spectrum of PANI.

Fig. 3.2.5: IR spectrum of PANI/Ni.

Fig. 3.2.6: IR spectrum of Ni-II salt.

Table-1: Tentative assignment of the IR spectra of PANI sample

Frequency (cm^{-1})	Assignment*
3710	presence of H_2O
3470	NH_2 asym. str.
3360	NH_2 sym. str., NH str
3175	=NH str.
1563	str. of N=Q=N
1538	str. of N−B−N
1450	str. of benzene ring
1368	C−N str. in QB_tQ
1315	C−N str. in QB_cQ, QBB, BBQ
1245	C−N str. in BBB
1160	a mode of N=Q=N
1140	a mode of $Q=\overset{+}{N}H$-B or B-$\overset{+}{N}H$-B
1225	
1104	C−H *ip* on 1,4-ring
1128	
1046	C−H *ip* on 1,2,4-ring
952	
917	
875	C−H *op* on 1,2,4-ring
847	
807	C−H *ip* on 1,4-ring
759	
690	C−H *ip* on 1,2-ring
659	
534	aromatic ring deformation
494	

* Abbreviations: asym = asymmetric, sym = symmetric, str = stretching, *ip* = in-plane bending, *op* = out-of-plane bending, Q = quinoid unit, B = benzoid unit, B_t= *trans* benzoid unit, B_c= *cis* benzoid unit.

It is the worthwhile to mention here that the observed spectrum is consistent with the previous studies [32-38] and discussed below according to the frequency region:

3500-3100 cm^{-1}: This is the N-H stretching region. The absorption of PANI in this region is rather weak. The main absorption peaks are located at 3380 and 3310 cm^{-1}, with shoulders at 3460 and 3170 cm^{-1}. With increasing acid concentration in the polymerization system, the peak at 3380 cm^{-1} increases and the shoulder at 3170 cm^{-1} decreases.

3100- 2800 cm^{-1} : This is the C-H stretching region. The absorption of PANI in this region is even weaker, but it is observable at 3050 – 3030 and 2960 – 2850 cm^{-1}. With increase of acid concentration in the polymerization system, the relative intensity of the 3040 cm^{-1} decreases indicating that the number of H atoms bonded to benzene ring is reduced.

1600-1450 cm^{-1}: Aromatic ring breathing, N-H deformation and C=N stretching all give absorption in this region. In general, The N-H deformation band is very weak. A 1, 4- substituted benzene ring may give absorption band at 1600-1580 and 1510-1500 cm^{-1}. However, the former is very weak and even observable if the two substituents are the same and the latter is strong in the IR in this range. Therefore, it is reasonable to assign the band at 1510 cm^{-1} mainly to benzoid ring (B) stretching in PANI. Based on the following arguments, we consider the 1587 cm^{-1} band as a characteristic band of nitrogen quinone (Q).

1400-1240 cm^{-1}: This is the C-N stretching region for aromatic amines. The intrinsic PANI shows three peaks: medium absorption at 1240 cm^{-1} and weak ones at 1380 and 1240 cm^{-1}. The 1315 cm^{-1} peak is rapidly strengthened by acid treatment. Here it would be worthy to point out that the reaction mechanism of PANI with acid may involve the structure $\overset{+}{=}$NH and $-\overset{\bullet\bullet+}{N}$H. The introduction of the positive charge leads to a great increases in molecular dipolar moment and thus IR activity. This is why all peaks in this region grow obviously during acid doping or treatment. The band at 1160 and 1140 was referred as "electronic like band" and was considered as a measure of the degree of delocalization of electrons on PANI and thus are the characteristic peaks of PANI conductivity [26, 27]. The band at 1160 and 1140 cm^{-1} be assigned separately: 1160 cm^{-1} to intrinsic structure and 1140 cm^{-1} to the doped (acid treated) structure. The 1140 cm^{-1} band is a vibrational mode of B-NH = Q or B$-\overset{\bullet\bullet+}{N}H-$B which is formed in doping reactions. This may be attributed to the existence of the positive charge and the distribution of the dihedral angle between the B and Q rings [28].

1220-500 cm^{-1} : This is the region of in-plane and out-of-plane bending of C-H bonds on aromatic rings. The main absorption bands for intrinsic PANI are located at 1160 and 830 cm^{-1} and some weak bands can be observed. It is easy to judge the substitution pattern on the benzene ring from the frequencies of these peaks. For example, 1220, 1105, 1010 and 830 cm^{-1} stands for 1,4- substitution, 1115, 1060, 960, 895 and 850 cm^{-1} for 1, 2, 4-substitution and 740 and 690 cm^{-1} for 1,2- or mono-substitution.

Peaks at 1120 and 625 cm^{-1} are also observed in the spectra of the PANI film and correspond to the presence of SO_4^{-2} ions, which were used as an electrolytic anion in the film [39].

The spectrum for PANI/Ni as shown in Fig. 3.2.5 shows prominent absorption peaks at 501, 603, 811, 1133, 1283, 1483, 1570 and 3455 cm^{-1}. Indeed the observed IR spectrum is identical with that of undoped PANI reported earlier [40]. The PANI matrix was reduced at $-1.6V$ during Ni deposition. In this respect, the resumblance of the present IR data with that of undope PANI is quile reasonable. However, the absorption for identifying the Ni in the matrix is not probably possible. One reason of the fact is that free Ni particle should not be IR active.

D.   XRD pattern

Both PANI and PANI/Ni matrices were examined for their structural analysis in the powdered state by using wide angle X-ray diffraction. The scattering patterns as a function of Bragg angle, 2θ at $\lambda = 1.54$ Å for the samples are presented in Figs. 3.2.7 and 3.2.8. The XRD pattern for the control Ni-II salt sample is depicted in Fig. 3.2.9.

The results show that the patterns consist of only diffuse x-ray scattering i.e., the peaks appear in the pattern are responsible for the amorphous nature of the sample. Most of the conducting polymers are reported to be extremely poor crystalline. During polymerization, although most of the aniline units are linked through the 1,4-position, a significant units are couple through other positions. This introduces defects in the hypothetical ideal linear chain arrangement of the polymer and also causes
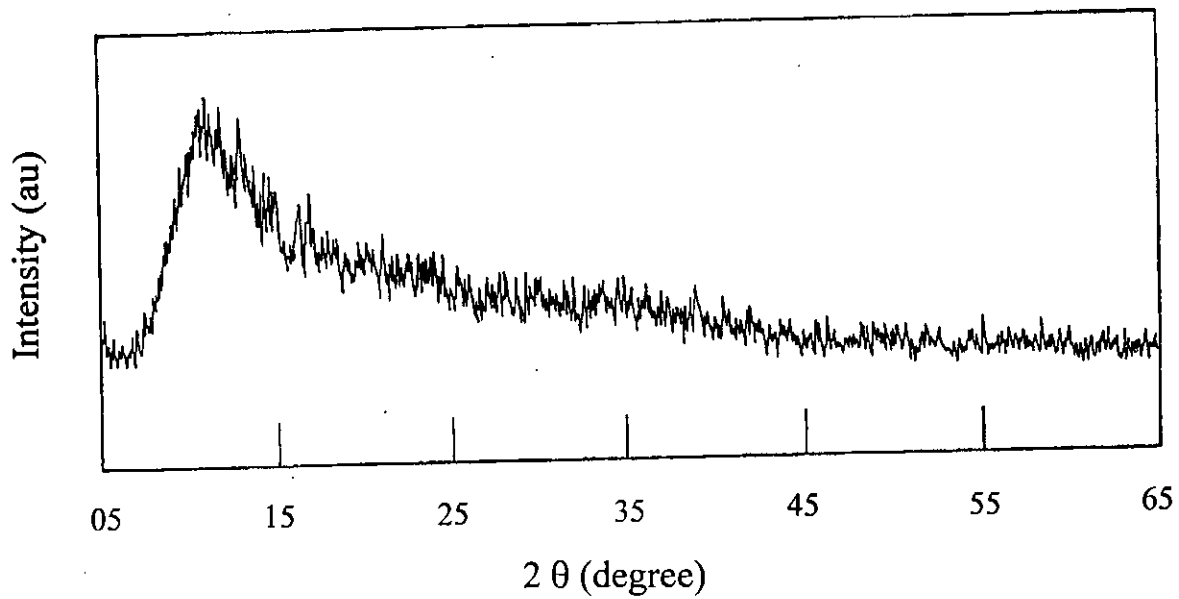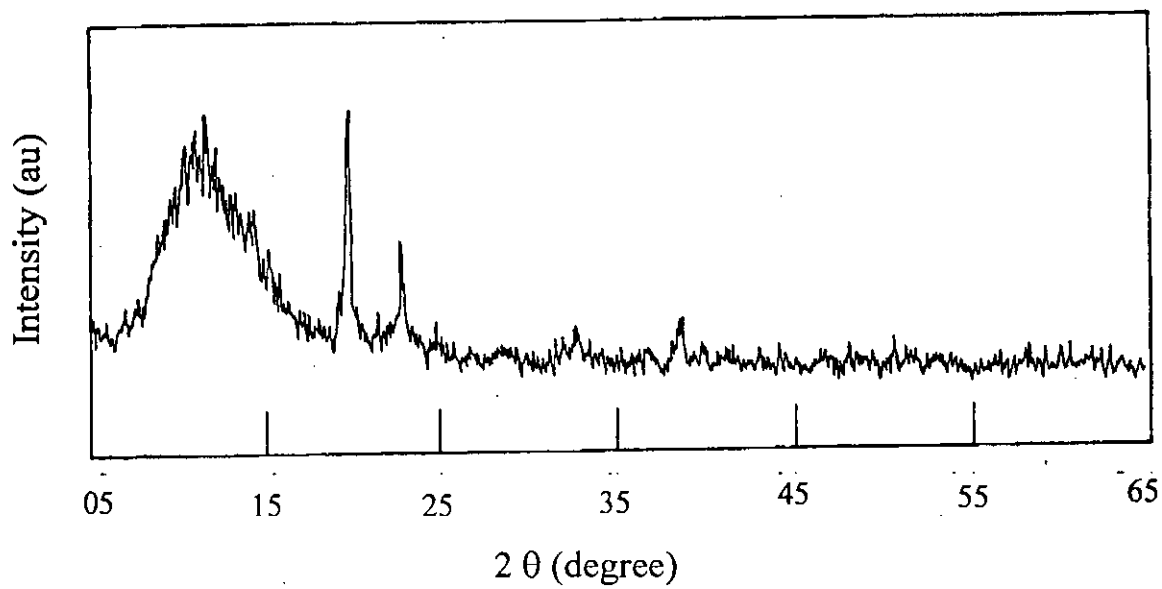
Fig. 3.2.7: XRD pattern of PANI.

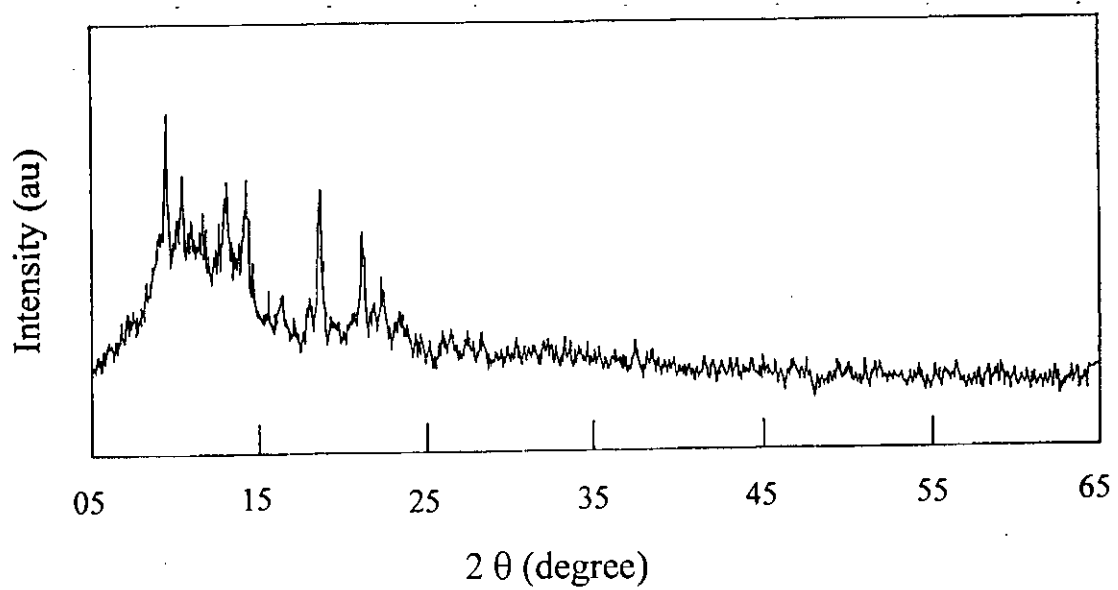Fig. 3.2.8: XRD pattern of PANI/Ni.

Fig. 3.2.9: XRD pattern of Ni-II salt.

some cross-linking of the polymer and consequently, results in a significant decrease in the crystallographic order of the chain [41, 42]. As a result, the polymer loses its crystallinity and leads diffuse diffraction pattern as exhibited in Fig. 3.2.7. Other well studied conducting polymer PP, has also been reported to be amorphous in nature [43]. The importance of a better intermolecular arrangement, i.e., a level of crystallinity in the PANI samples for obtaining a higher conductivity has become a well-accepted factor all around the world, and this idea is not restricted to PANI but involves most of the more prominent electronically conductive polymers.

On the other hand, the XRD pattern of PANI/Ni shows few sharp peaks in addition to the diffuse peaks. This result indicates the presence of some crystalline entities in the matrix. The observation seems to be reasonable if one consider the presence of Ni particles in the PANI matrix. The electrochemical reduction of Ni^{+2} yielded Ni metal that has incorporated into the polymer matrix following the electrochemical procedure described earlier. The Ni particles thus embedded into the PANI may responsible for the observed crystallinity as reflected in the XRD pattern shown in Fig. 3.2.8.

E.   Electrical and magnetic properties

Conductance measurement reflects the electrical property of a material. In general conductivity is the function of number of charge carrier and its mobility. In the present work, conductivity measurements of the samples, PANI and PANI/Ni were carried out involving their compressed-pellet states and adopting conventional d.c two point-probe conductance technique [44, 45]. For measuring electrical and magnetic properties, PANI

was prepared on a Pt electrode (2.0×3.0 cm^{-2}) at constant potential of +1.0V by passing 50 mC of charge. The PANI mass was then washed several time with distilled water (pH=6.86). Thus, it is expected that, after washing, the PANI matrix switch to its undoped state. Similarly, PANI/Ni was prepared by depositing Ni particles on the PANI film (prepared by following the method just described above) at a constant potential of −1.6 and allowed the charge 50 mC to be passed. The PANI/Ni film thus synthesized was also washed repeatedly in distilled water (pH = 6.86) to adjust its doping level as that of PANI. The measured conductivity of PANI and PANI/Ni were found to be 4.83×10^{-3} and 3.16×10^{-7} Scm^{-1}, respectively. The measured conductance of PANI seems to be consistent with the previous work [46] reported for an undoped PANI. The conductance of PANI/Ni seems to be four order of magnitude smaller than that of PANI. This might happen due to the insertion of Ni particles in the polymer matrix. The decrease in conductivity may be due to the partial blockage of conductive path by Ni particles embedded in the PANI matrix. Similar, decrease in conductivity of PANI was also reported by the Zhang *et. al.* [47] when Fe_3O_4 nanoparticles were embedded in the polymer.

Magnetic susceptibility provides a proof on the magnetic nature of a material. It gives the extent to which the material susceptible, (i.e., sensitive) to the external magnetic field. In practice, susceptibility is usually exposed per unit mass (i.e. gram) rather than per unit volume. In the present work, gram susceptibility of PANI and PANI/Ni powder were measured. The gram susceptibility of PANI and PANI/Ni were measured to be -3.68×10^{-7} and 9.025×10^{-5} (in c.g.s unit), respectively. The result shows a negative and

small susceptibility for PANI and it appears to be large for PANI/Ni samples. The positive and negative dimension of gram susceptibility are the indicator of the nature of the magnetism [48]. Thus the present finding clearly indicates that PANI is diamagnetic whereas PANI/Ni is paramagnetic one. The observed paramagnetic nature of the polymer may arises due to the incorporation of Ni particles in its matrix.

3.3 Redox Behaviour

A. PANI in aqueous and non-aqueous media

Electrodes are the sites where electrochemical oxidation and reduction are take place. For the redox process electrodes, play the critical and effective role. Usually noble metals, *viz.* Pt, Au are utilized mostly as active electrodes. However, because noble metals are costly and their abundance is limited and thus effort is given to search for new electrode materials. The conductive polymers are the class of material which are conductive, easy to prepare and less costly and thus appeared as potential candidates for electrode materials. In the present work, Pt electrode are coated with PANI and PANI/Ni films. Thus, from the potential application print of view, these matrices are examined as electrode materials by carrying out some redox process electrochemically. Figures 3.3.1 and 3.3.2 show the CV's of a PANI coated Pt electrodes in the electrolytic solutions containing 0.1M $LiClO_4$ in water and acetonitril (CH_3CN), respectively. The PANI films coated on the Pt were obtained by sweeping the potential ten times between −0.2 and +1.0V at a scan rate of 100 $mVsec^{-1}$. In the CV's, potential sweeping were carried out between −2.0 and +0.5V for aqueous (H_2O) media and −0.2 and +0.8V for non-aqueous (CH_3CN) media. In both the cases, any sharp peak
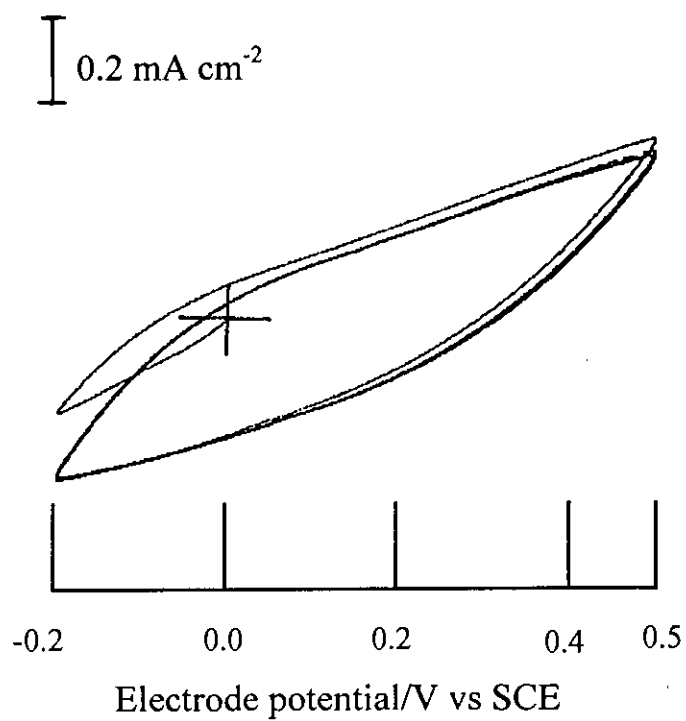
0.2 mA cm^{-2}

-0.2   0.0   0.2   0.4   0.5

Electrode potential/V vs SCE

Fig. 3.3.1: CV for PANI in aqueous 0.1M LiClO$_4$ solution.

0.2 mA cm^{-2}

-0.2   0.2   0.6   0.8

Electrode potential/V *vs* SCE.
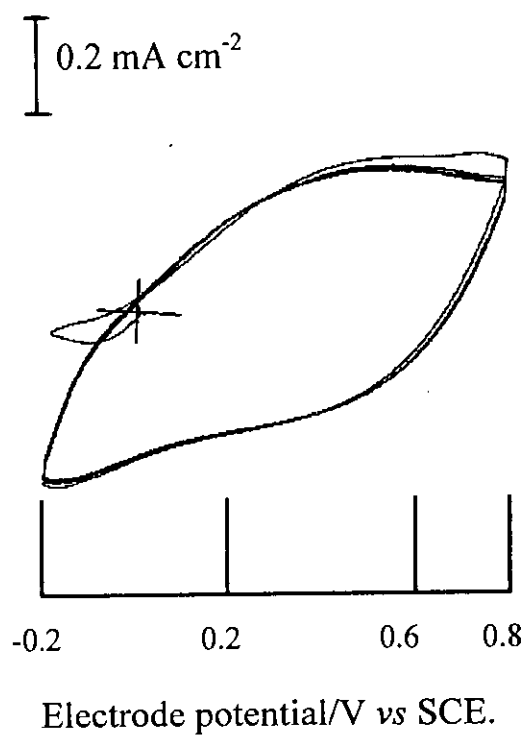
Fig. 3.3.2: CV for PANI in CH_3CN solution containing 0.1M $LiClO_4$.

can be seen hardly. However, current shoulder is appeared, indicating that the coated films are electroconducting. In the redox process employed here, the oxidation and reduction of the polymer film is expected. That is, during oxidation, doping of the ClO_4^- ion and its reduction, dedoping of ClO_4^- ion should occur by exhibiting peaks in the CV's. The doping- dedoping process in this case seems to be difficult. It may be due to the nature of the film thus coated, that is, films hardness, procity etc. makes the ion difficult to insert or remove from the polymer. However, the CV still shows that current can conduct through it and thus electrically conductive.

B.   PANI/Ni in aqueous and non-aqueous media

To examine the electrochemical redox i.e. doping-dedoping behaviours of PANI/Ni film electrode both in aqueous (H_2O) and non-aqueous (CH_3CN) media voltammetry technique was adopted. The typical CV's are presented in Figs. 3.3.3 and 3.3.4. The PANI/Ni film was prepared as described earlier, i.e.. PANI film, as grown onto the Pt electrode following the procedure described above, was treated at constant potential of $-1.6V$ and allowed 50 mC of charge for Ni deposition. The PANI/Ni film thus synthesized was then emerged in 0.1M $LiClO_4$ salt dissolved in H_2O and CH_3CN. In both cases, voltammogram shows good current spectrum between the potential window as shown in the CV. This matrix also shows no peak indicating difficult insertion and removal of the ClO_4^- ion to and formed the film. Under the experimental condition, the doping-dedoping seems to be ineffective, but the film shows sufficient electroactivity. Thus, the result indicates the possibility of its use as a new electrode material in the electrochemical process. The possibility of the PANI and PANI/Ni film electrodes in the electrode processes will be further discussed in the following sections.
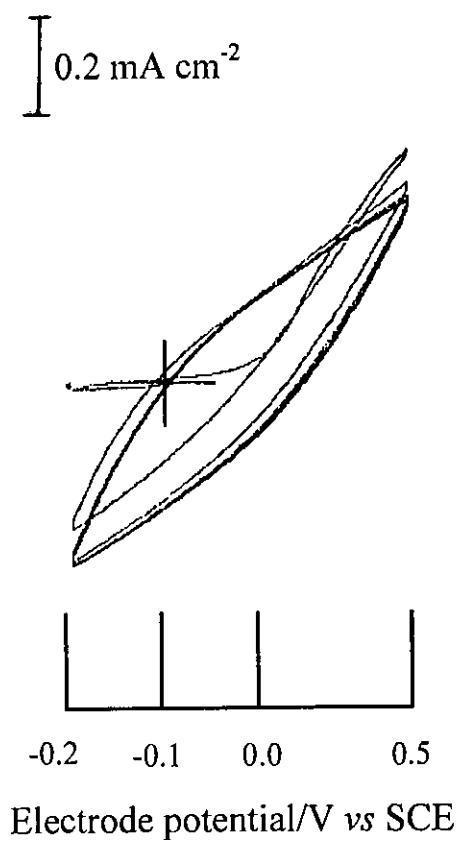
107

$0.2\ mA\ cm^{-2}$

-0.2	-0.1	0.0	0.5

Electrode potential/V *vs* SCE

Fig. 3.3.3: CV for PANI/Ni in aqueous 0.1M LiClO$_4$ solution.

0.2 mA cm^{-2}

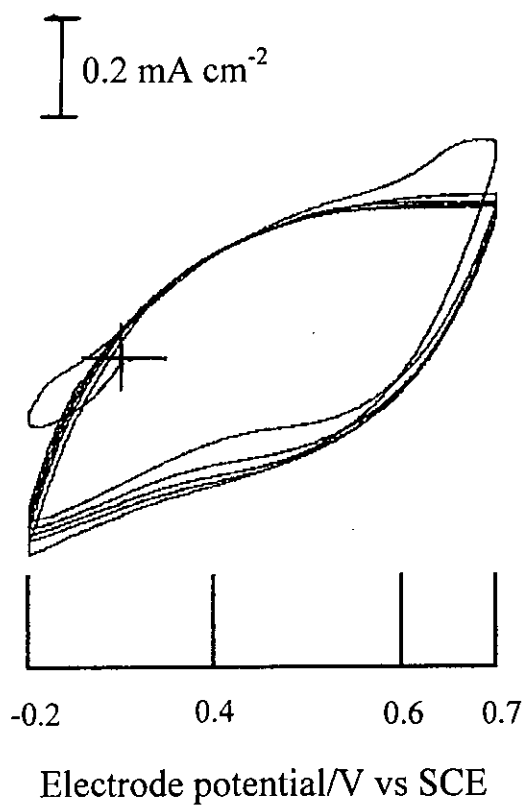-0.2   0.4   0.6   0.7

Electrode potential/V vs SCE

Fig. 3.3.4: CV for PANI/Ni in CH_3CN solution containing 0.1M $LiClO_4$.

3.4　Electrode Activity

A.　PANI electrode

Electrode activity meant here the capacity of reactivity of an electrode matrix toward a specific electrochemical reaction. As described above that the PANI and PANI/Ni films are electroactive, this made us interested to examine a standard redox process using the new PANI and PANI/Ni materials as electrode. Fe^{+2}/Fe^{+3} is a common redox process that can be investigated electrochemically by a simple arrangement. Fig. 3.4.1 shows the CV during the redox process: $Fe^{+2} \rightarrow Fe^{+3} + e^-$. This was carried out onto a Pt working electrode. For this purpose, a Pt electrode having dimension of 0.25 cm^2 was employed. The process was performed in an electrolytic medium containing aqueous solution of 0.1M $K_4Fe(CN)_6$. Potential sweeping was restricted between −0.2 and +0.7V. The CV shows excellent redox process performed on the Pt surface. The anodic and cathodic peaks in the CV correspond to the oxidation and reduction of the Fe species, respectively. Similar experiment was performed with the PANI coated Pt electrode. The result is depicted in Fig. 3.4.2. PANI was coated on Pt by sweeping the potential ten times between −0.2 and +1.0V from an electrolytic solution containing 0.5M aniline + 0.8M H_2SO_4 at a scan rate of 100 mVsec^{-1}. The CV seems to be identical with that observed for bare Pt electrode (Fig. 3.4.1), expect the redox peaks shifted to some extent. Thus, it indicates that the similar oxidation and reduction processes have taken place on the PANI modified Pt electrodes. The shifting of the peaks indicates that the potential required to perform the redox process is different. It is quite reasonable in the sense that the electrode materials, Pt and PANI are different and consequently their activity could also be different to perform specific reaction on their surface and thus showing the redox peak potential different (shifted) from one another.

110

0.2 mA cm^{-2}

-0.2   0.0   0.2   0.4   0.7

Electrode potential/V *vs* SCE
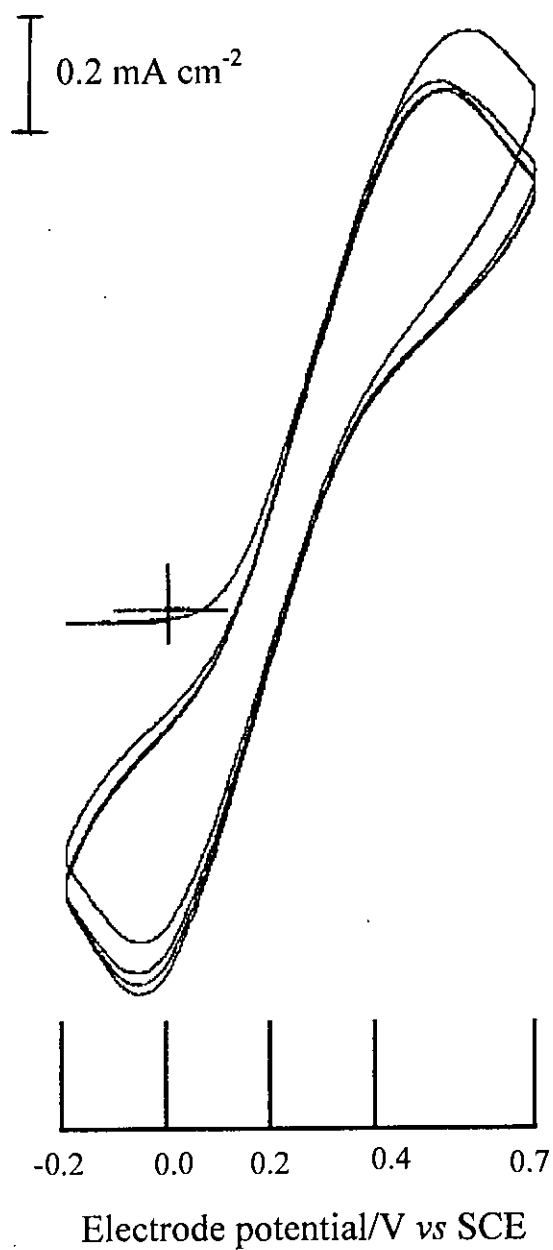
Fig. 3.4.1: CV of a Pt electrode (1.0 cm^2) in aqueous 0.1M K$_4$Fe(CN)$_6$ solution.

111

0.2 mA cm^{-2}

-0.2   0.2   0.7
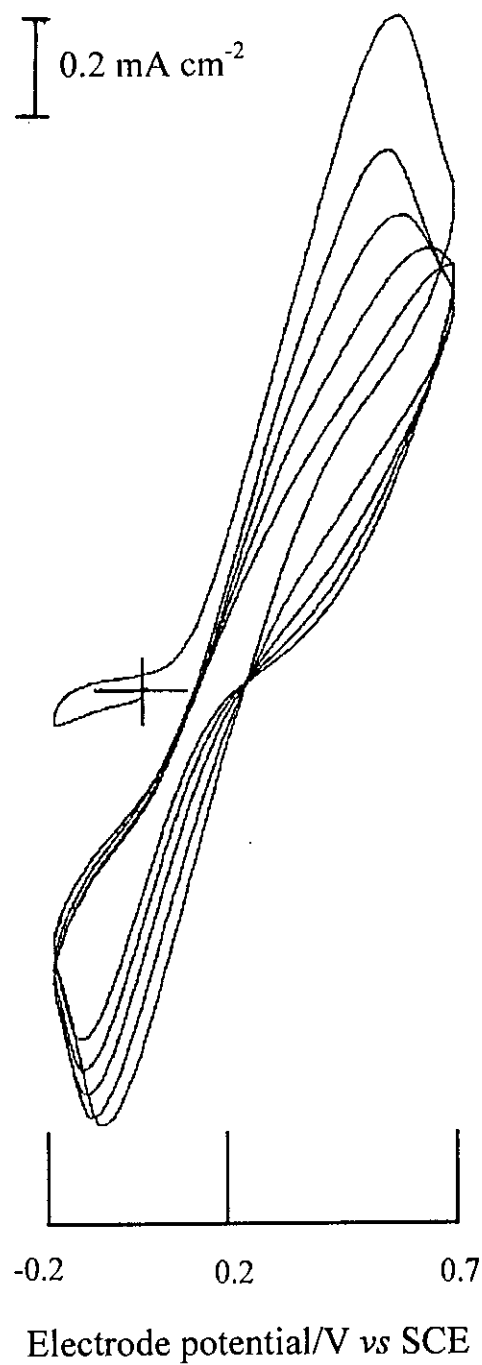
Electrode potential/V *vs* SCE

Fig. 3.4.2: CV for PANI in aqueous $K_4Fe(CN)_6$ solution.

B.   PANI/Ni electrode

In the present work, PANI was further modified by incorporating Ni particles in the film. The PANI/Ni film thus prepared shows good electroactivity both in aqueous and non-aqueous electrolytic media (section 3.3). Thus, we were interested to examine its redox activity by studying the $Fe^{+2} \rightarrow Fe^{+3} + e^-$ reaction on it. Figure 3.4.3 shows the CV of 0.1M $K_4Fe(CN)_6$ aqueous solution with the modified PANI/Ni electrode. It can be seen from the CV that, the oxidation and reduction processes are occured efficiently on the surface of the electrode. The anodic peak at about ~0.1V and cathodic peak at about –0.1V corresponds to the oxidation and reduction processes, respectively. The result is consistent with those that observed with bare Pt (Fig. 3.4.1) and Pt/PANI (Fig. 3.4.2) electrodes suggesting that the Fe^{+2}/Fe^{+3} redox process can be performed with the PANI/Ni electrode under the experimental conditions employed. It is worthwhile to note here that the redox peak potentials observed for the PANI/Ni electrodes is nearly coincident with that observed with bare Pt electrode. In case of PANI electrodes peaks are shifted to some extent than that occurred on the Pt electrode. However, both PANI and PANI/Ni films matrices seem to be excellent electrode modifier to applicable in the electrode processes as an alternative new electrode materials. Chowdhury *et. al.* [49] also reported PANI coated Pt electrode as modifier to control electrochemical reaction.

3.5   Electrode Stability

A.   PANI electrode

In the previous experiments described in the preceeding sections, it becomes to be evident that PANI is electroactive and show redox reactivity
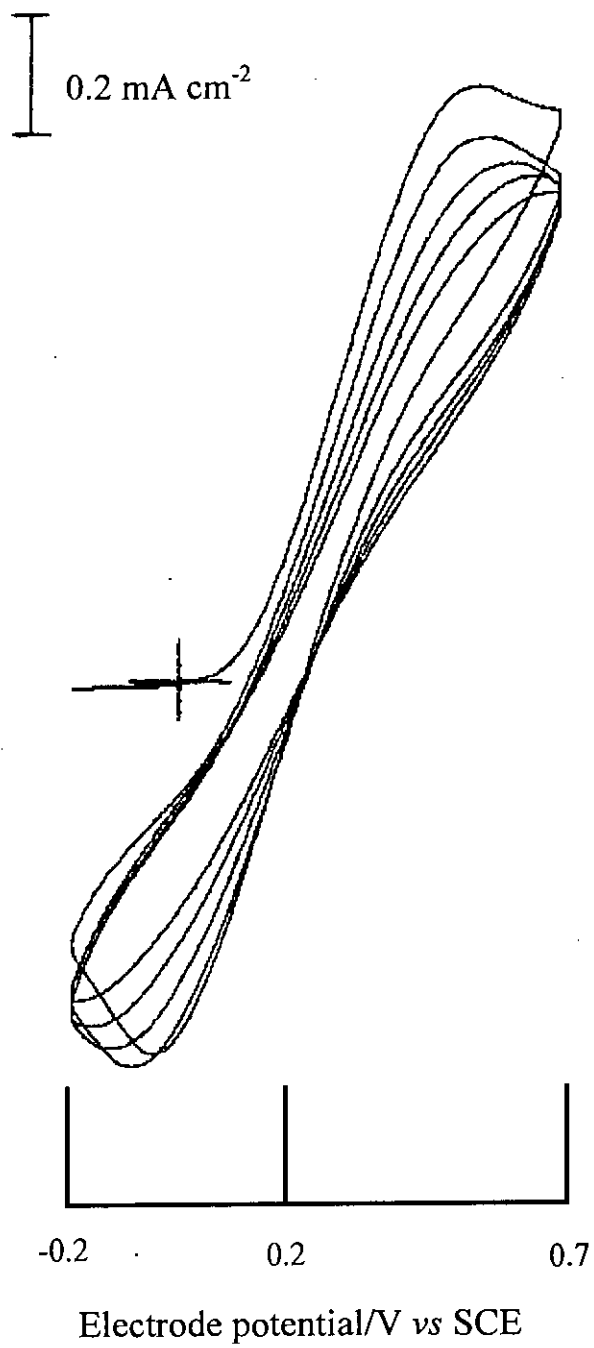
0.2 mA cm^{-2}

-0.2   0.2   0.7

Electrode potential/V *vs* SCE

Fig. 3.4.3: CV for PANI/Ni in aqueous K$_4$Fe(CN)$_6$ solution.

both in aqueous and non-aqueous solutions. Thus, PANI can be switched electrochemically between its oxidized (doped) and reducted (dedoped) states. However, its stability and durability in repeated oxidation and reduction cycles or at high positive potential should be examined in order to understand its stability in the electrochemical process. Figure 3.5.1 shows the CV of a PANI film (10 cycle thick) in 0.1M LiClO$_4$ aqueous solution at different scan cycles. The CV was recorded from 1st cycle to 30th one. From the CV it can be seen the excellent redox response in the 1st scan. That is, oxidation and reduction processes are taking place efficiently. However as the scan progress, the peaks, both anodic and cathodic, seem to be smaller, i.e. the redox activity tends to be lower. As the cycles reached to 30th one, both the anodic and cathodic peaks seem to be disappeared. The result thus indicates that the PANI film electrode lost it activity to perform the electrochemical process. This result indicates the instability of the PANI film toward the redox process for a longer period. The stability of the PANI film was further studied by applying high positive potential to the electrode. The result is shown in Fig. 3.5.2. The result shows that when the potential was switched to +1.0V, the PANI film electrode can perform the usual redox process (curve-a) when the potential was switched to +2.0V, the electrode gives nearly identical response (curve-b) indicating that the PANI film electrode is stable even at positive potential as high as +2.0V.

B.   PANI/Ni electrode

The Ni-modified PANI electrode was also tested for its stability in the repeated oxidation/reduction cycle and at the high positive potentials.

0.1 mA cm^{-2}

-0.2   0.2   0.6   0.8

Electrode potential/V *vs* SCE
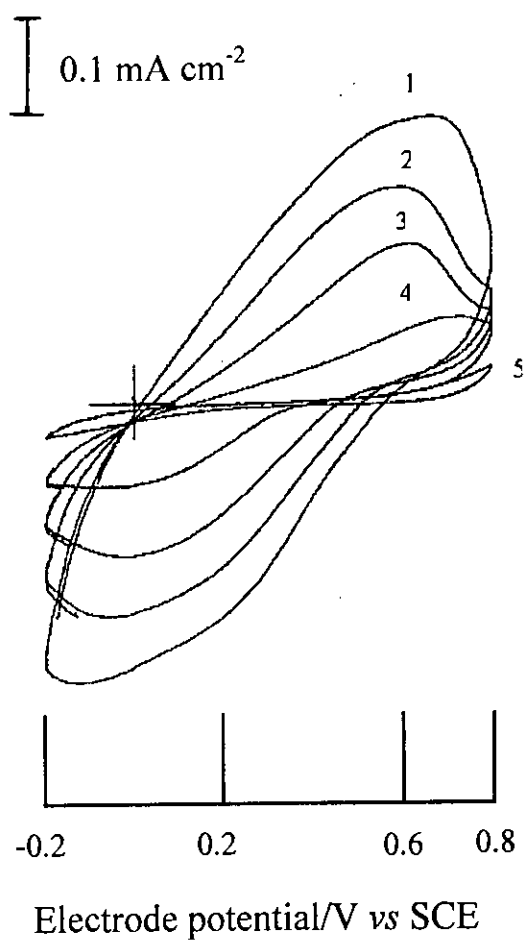
Fig. 3.5.1: CV of PANI in aqueous 0.1M LiClO$_4$ solution at different no. of scan cycle: (1) 1st (2) 2nd (3) 5th (4) 10th and (5) 30th.
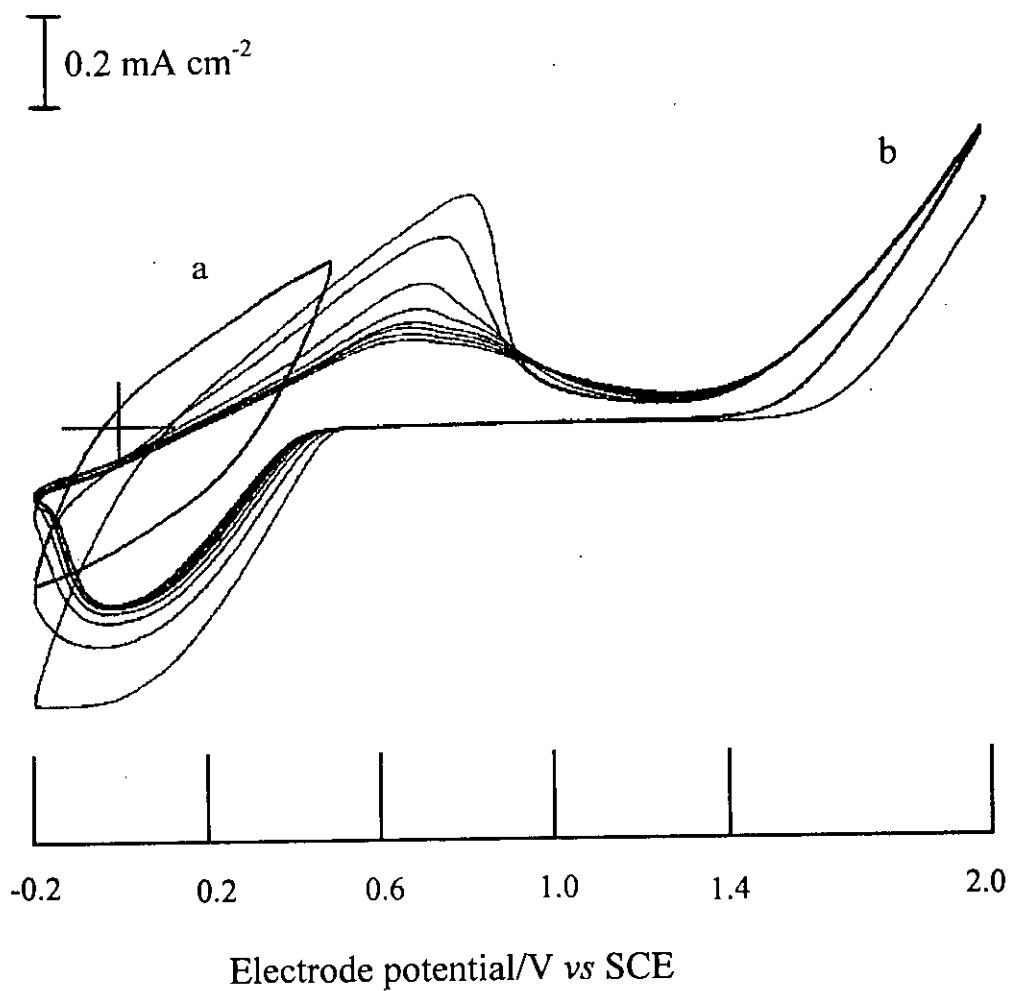
Fig. 3.5.2: CV of PANI film in aqueous 0.1M LiClO₄ solution: +0.5 V
(curve-a) and +2.0 V (curve-b).

The results are summarized in Figs. 3.5.3 and 3.5.4, respectively. The PANI film (synthesized by sweeping the potential ten times between −0.2 and +1.0V) was modified by Ni particles by the cathodic treatment of the film at −1.6V and allowing 50 mC charge in an electrolytic solution containing 0.1M Ni-II solution. Figure 3.5.3 shows the CV of a PANI/Ni film thus synthesized in a 0.1M LiClO$_4$ aqueous solution and the sweeping was allowed upto 30 cycles. Starting from the 1st to 10th cycle the redox response is very prominent. That is, oxidation and reduction processes are occuring efficiently on the PANI/Ni surface. In the 30th cycle, the redox response is still prominent. It is to be noted here that, the PANI film electrode appears to be inactive at the 30th cycle (Fig. 3.5.3). Thus, this result indicates the superior stability of the PANI/Ni than PANI film electrode. This may be due to the incorporation of Ni in its matrix which may harden the morphology to prevent any destruction of the surface during repeated sweeping process. Silica incorporated PANI film electrode also shows better electrochemical stability in the repeated oxidation/reduction cycle [50]. The PANI/Ni electrode was also investigated for its electrochemical stability at high positive potential. The result is shown is Fig. 3.5.4. The CV, as given in the figure was performed in 0.1M LiClO$_4$ solution. The film gave typical reversible redox response (Fig. 3.3.1) when +1.0V was applied. However, when the scan was reversed at more positive potential of +2.0V, redox phenomenon seems to be persisted but the reversibility found to be affected. This indicates that at high positive potential, although redox phenomenon is somewhat affected but its response is quite superior. It is to be noted here that when the PANI/Ni film was sweepted between −0.2 and +0.5V, the usual oxidation (doping) and reduction (dedoping) response is not prominent (Fig. 3.3.1) but when the sweeping is extended between − 0.2 and +2.0, the

$0.1 \ mA \ cm^{-2}$

Electrode potential/V *vs* SCE
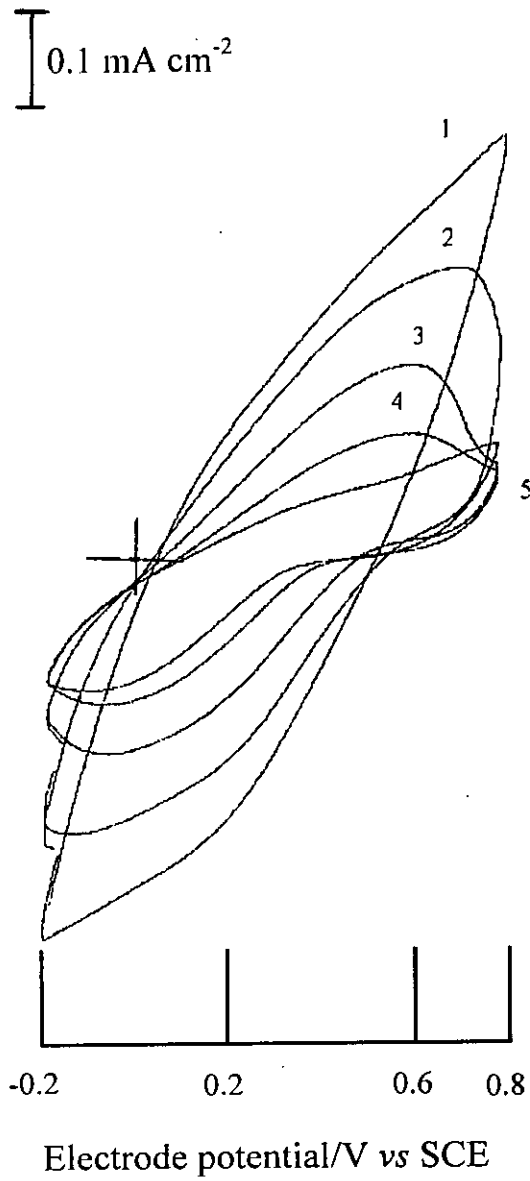
Fig. 3.5.3: CV of PANI/Ni in aqueous 0.1M LiClO$_4$ solution at different no. of scan cycle: (1) 1st (2) 2nd (3) 5th (4) 10th (5) 30th.

119

0.2 mA cm^{-2}

Electrode potential/V *vs* SCE.
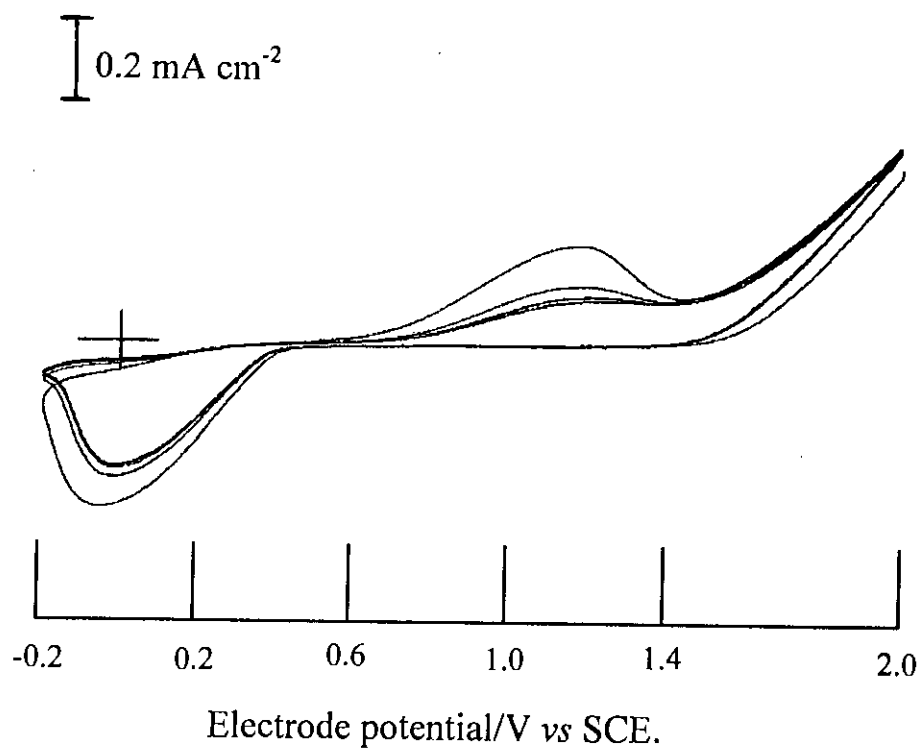
Fig. 3.5.4: CV for PANI/Ni film in aqueous 0.1M LiClO$_4$ solution at 2.0 V.

redox response become very prominent. This result also indicate the potential domin required for doping-dedoping of PANI/Ni film. In other words, activation of the film electrode occurs by treating it at high anodic potential. However, the present study clearly demonstrate that incorration of Ni particle into the PANI matrix produces a better stability of the electrode under applied potential of as high as +2.0V *vs* SCE.

References

1. D. M. Mohilner, R. N. Adams and W. J. Argersinger, *J. Am. Chem. Soc.*, **84** (1962) 3618.

2. J. Bacon and R. N. Adams, *J. Am. Chem. Soc.*, **90** (1968) 6596.

3. E. M. Genies and C. Tsintavis, *J. Electroanal. Chem.*, **195** (1985) 109.

4. E. M. Genies, C. Tsintavis and A. A. Syed, *Mol. Cryst., Liq. Cryst.*, **121** (1985) 181.

5. A. Volkov, G. Tourillon, P. C. Lacaze and J. E. Dubois, *J. Electroanal. Chem.*, **115** (1980) 279.

6. E. M. Genies and C. Tsintavis, *J. Electroanal Chem.*, **200** (1986) 127.

7. B. Wang, J. Tang and F. Wang, *Synth. Met.*, **13** (1986) 329.

8. E. W. Paul, A. J. Ricco and M. S. Wrighton, *J. Phys. Chem.*, **89** (1985) 1441.

9. A. G. MacDiarmid, J.-C. Chiang, M. Halpern, W.–S. Huang, S.-L. Mu, N. L. D. Somasiri, W. Wu, and S. I. Yaniger, *Mol. Cryst. Liq. Cryst.*, **121** (1985) 173.

10. W.–S. Huang, B. D. Humphery, and A. G. MacDiarmid, *J. Chem. Soc., Faraday Trans. 1*, **82** (1986) 2385.

11. W. W. Focke, G. E. Wnek, and Y. Wei., *J. Phys. Chem.*, **91** (1987) 5813.

12. D. M. Mohilner, R. N. Adams and W. J. Argersinger, *J. Am. Chem. Soc.*, **84** (1962) 3618.

13. E. M. Genies and C. Tsintavis, *J. Electroanal. Chem.*, **195** (1985) 109.

14. E. M. Genies and C. Tsintavis, *J. Electroanal. Chem.*, **200** (1986) 127.

15. A. F. Diaz and J. A. Logan, *J. Electroanal. Chem.*, **111** (1980) 111.

16. A. Kitani, I. Izumi, J. Yano, Y. Hiromoto and K. Sasaki, *Bull. Chem. Soc. Jpn.*, **57**(1984)2254.

17. R. Noufi, A. J. Nozik, J. White and L. F. Warren, *J. Electrochem. Soc.*, **129**(1982)226.

18. A Kitani, J. Yano and K. Sasaki, *J. Electroanal. Chem.*, **209** (1986) 227.

19. D. Orata and D. A. Buttry, *J. Am. Chem. Soc.*, **209** (1987) 3574.

20. J. Tanguy, N. Mermillod and M. Hoclet, *Synth. Met.*, **18**(1986)121.

21. N. Mermillod, J. Tanguy, M. Hoclet and A. A. Sted, *Synth. Met.*, **18** (1986)359.

22. J. Tanguy, N. Mermillod and M. Hoclet, *J. Electrochem. Soc.*, **134** (1987)795.

23. A. G. MacDiarmid, J. C. Chiang, M. Halpern, W. S. Huang, W. S. Huang, S. L. Mu, N. L. D. Somasiri, W. Wu and S. I. Yaniger, *Mol. Crys. Liq. Crys.*, **121**(1985)173.

24. A. G. MacDiarmid, N. L. D. Somasiri, W. R. Salaneck, I. Lundstrom, B. Liedberg, M. A. Hasan, R. Erlandsson and P. Konrasson, *Springer series in solid-state sciences.,* **63**(1985)218.

25. C. Chiang and A. G. MacDiarmid, *Synth. Met.*, **13**(1988)193.

26. W. S. Huang, B. D. Humphrey and A. G. MacDiarmid, *J. Chem. Soc., Faraday Trans*, **82**(1986)2385.

27. J. F. Wolf, S. Gould and L. W. Shacklette, Abstr, INOR 310, *192nd ACS Meet., Anaheim, CA. U.S.A.*, Sept. 7-12, 1986.

28. T. Kobayashi, H. Yoneyarna and H. Tamura, *J. Electrochem. Soc.*, **161**(1984) 419, **177**(1984) 281, 293.

29. A.-N. Chowdhury, Y. Harima, Y. Kunugi and K. Yamashita, *Electrochemical Acta*, **40**(3), (1996), 1993.

30. D. Landolt, *Electrochem. Acta,* **39**(8/9) (1994) 1075.

31. Y. Roichman, G. I. Titelman, M. S. Silverstein, A. Siegman and M. Narkis, *Synth. Met.*, **98**(1999)201.

32. Y. Cao, S. Li, Z. Xue and D. Guo, *Synth. Met.*, **16** (1986) 305.

33. F. Wang, J. Tang, X. Jing, S. Ni and B. Wang, *Acta Polym. Sinica.*, **5** (1987) 384.

34. G. Socrates, *Infrared Characteristic Group Frequecies*, Wiley, Chichester, 1980, p-53.

35. F. R. Dollish, W. G. Fateley and F. F. Bentley, *Characteristic Raman Frequencies of Organic Compounds*, Wiley, New York, 1974.

36. L. J. Bellamy, *The Infrared Spectra of Complex Molecules*, Chapman and Hall, London, 1975, p. 82, p. 277.

37. M. Angelopoulos, A. Ray and A-G. MacDiarmid, *Synth. Met.*, **21** (1987) 21

38. S. Ni, J. Tang and F. Wang, *Preprints of Symposium on Polymers*, Chinese Chemical Society Polymer Division, Wuhan, China, 1987, p. 638.

39. (a) D. Dolphine and A. Wick, *Tabulation of Infrared Spectral Data*, John Wiley & Sons, New York, London, Sydney, Toronto, 1977; (b) A. D. Cross and R. A. Jones, *An Introduction to Practical Infrared Spectroscopy, 3rd edn., Butterworth*, London, 1969.

40. R. H. Khan, "Influence of Doping Level on the Structure and Electrical Properties of Conducting Polymer". M. Phil. thesis, Dept. of Chemistry, BUET. Bangladesh, March 1999.

41. Y. Roichman, G. I. Titelman, M. S. Silverstein, A. Siegman and M Narkis, *Synth. Met.*, **98** (1999) 201.

42. S-A. Chen and W-G Fang, *Macromolecules*, **24** (1991) 1242.

43. K. K. Kanazawa, A. F. Diaz, R. H. Geiss and G. B. Street, *J. Chem. Soc. Chem. Commun.*, (1979) 854.

44. I. J. van der Pauw, *Philips Res. Repts.*, **13** (1958) 1.

45. J. Lange, *J. Appl. Phys.*, **35** (1964) 2659.

46. A.-N. Chowdhury, R. A. Khan and M. Hossain, *Indian J. Chem.*, 39A(2000), 501.

47. Z. Zhang and M. Wan, *Synth. Met.*, **132**(2003) 205.

48. N. U. Malik, G. D. Tuli and R. D. Madan, Selected Topics in Inorganic Chemistry, S. Chad and Company Ltd., New Delhi, (1983), p-261.

49. A.-N. Chowdhury, M. Atobe and T. Nonaka, Ultrason. Sonochem., 11(2004)77.

50. A.-N. Chowdhury and J. M. A. Rahman. *J. Chem. Soc.,* India, **51**(2) (2002) 66.

Conclusions

The one step electrochemical method provides a noble and facite route for the deposition of metallic particles onto the both bare Pt and PANI matrices. The Ni deposits adhere well to both the matrices and thus results a free-standing film and then can be peeled off for further use. The technique and the experimental conditions employed can yield 4.26% of Ni in the polymer matrix.

The electrolyte bath composition and scan speed have found to influence the Ni deposit. The acidic bath yielded larger size of the Ni whereas neutral bath composition gives the relatively smaller particles of Ni. The scan speed has also found to influence the particle size of Ni metal. The size of the metal particle reduces when scan rate switched from 50 to 200 mVsec^{-1}.

Analysis of the microstructures by an optical microscope confirmed that Ni particles as deposited on the substrates have definite size and shape with sharp edges. The deposits are uniformly distributed onto the substrate surfaces. The SEM analysis of the matrices also provides the presence of Ni in the PANI surface. The Ni particles as grown on the surface also show definite size and shape.

The solid state d.c conductance of PANI were lower by four order of magnitude when Ni was dispersed into its matrix. However, they can be easily made conductive as soon as it saturated with acidic media. By doing

this, PANI/Ni matrix can have both the electronic and magnetic properties and thus applicable to both as electronic and magnetic materials. Indeed, incorporation of Ni into the PANI bulk, results a paramagnetic property of the matrix. Magnetic susceptibility measurements confirm the paramagnetic property of the PANI/Ni sample. As evidenced by the XRD, the bulk PANI is completed amorphous in nature whereas insertion of Ni particles in it, yielded a crystalline structure. This will certainly help to improve the electronic property of this magnetic material.

The PANI/Ni matrix exhibited excellent electroactivity both in aqueous and non-aqueous electrolytic media. The potential can be reversible switch between its oxidized and reduced states. Thus, alike PANI, the PANI/Ni film can be doped and dedoped using electrolyte ions. Most of the applications of conducting polymer are result from their doping and dedoping characteristics. Thus, PANI/Ni material can play duel nature and finds wider applications to electronic and magnetic field. The electroactive materials should have appreciable electrochemical and environmental stability for their potential commercial uses. The PANI/Ni film electrode shows better durability and stability in the repeated potential scan and at the higher positive potential. In the electrochemical deactivation/degradation, PANI/Ni film electrode shows more stable voltammetric features compare to that of the bulk PANI film. Thus, incorporation of Ni in the PANI matrix improves its mechanical properties too. As a result, the critical electrochemical condition could not affects its surface morphology to results any deactivation or degradation.

126